ROZPRAWA DOKTORSKA

Institute of Physical Chemistry
Polish Academy of Sciences
Kasprzaka 44/52, 01-224 Warsaw

Microfluidic methods for creation of emulsions and new materials

by

Judyta Małgorzata Węgrzyn, M.Sc.

Under the supervision of Prof. nadzw. dr hab. Piotr Garstecki

Thesis submitted in fulfillment of the requirements
for the degree of Doctor of Philosophy

Within the International PhD Studies of the Institute of Physical Chemistry
of the Polish Academy of Sciences in Warsaw

July 2013, Warsaw

I. Abstract

Over the last few decades, miniaturization was one of the more important goals in the development of analytical techniques of both chemical and biological nature. The interest in this aspect roots in the prospects for benefits that come with minimization of the amount of reagents and therefore the reduction of the waste products. The ability of microfluidic systems to controllably handle small volumes of fluid, especially when combined with versatile vistas of precise detection of the outcomes of reactions, creates a potential for new sophisticated applications and for reduction of the cost of existing assays.

In the diversity of studies on microfluidic systems within the last 20 years, a considerable interest has been dedicated to the microfluidic techniques that rely on biphasic flow. This interest resulted in a wide range of applications of emulsion generators for both: i) screening analyses (where single droplets serve as individual micro reactors), what is particularly useful in microbiology, biochemistry as well as diagnostics, and ii) preparative purposes.

Production of polymeric capsules and gel microparticles of well defined size and content is pertinent when it comes to potential use in pharmaceutical, cosmetic or food industries. Droplets and particles might be successfully employed as carriers of active substances.

There is a variety of simple microfluidic generators of emulsions that have been introduced to systems devoted to high throughput production of polymeric particles. The state of the art, however, has not presented a construction capable of simultaneous formation of numerous streams of uniform droplets with strictly defined spectrum of their chemical content. The system presented in this thesis guaranties both high throughput and capability of generation of streams differing in content. This, in turn, might become useful in controlling the profile of slow release of entrapped active substances.

The present thesis is based on a set of experiments including design, fabrication and precise analysis of operation of microfluidic systems dedicated to simultaneous generation of a well defined number of streams of droplets. Each of the streams corresponds to a different predetermined concentration of miscible input sub-streams. The thesis also includes the description of the optimization of the procedure of bonding applied during fabrication of the microfluidic systems, and characterization of the working range of the systems dedicated to generation of micro-droplets with varied chemical content. An important aspect of the thesis is the characterization of the influence of viscosities of liquids and the order of delivery of these liquids to the microfluidic junction on the process of generation of droplets and on the reliability

of the system (preservation of the requested gradation of the content of the droplets). Additionally, the thesis contains an exemplary practical application of the proposed systems. The studied process consisted of a formation of microgels of polysaccharide blends, under strict control of the droplet size, enriched with a model active substance (gold nanoparticles) and secondly the investigation of the influence of the 'alginate to pectin' proportion on the rates of release of the nanoparticles.

The introduction part explains the fundamental concepts in microfluidics together with a brief description of microfabrication of the chips, the choice of material, the way of patterning the microfluidic networks, and binding particular elements of the system in order to obtain complete, ready-to-use, devices. The following sections demonstrate a typical division of microfluidic systems into two groups based on laminar and biphasic flow. This part describes both the variety and the versatility of microfluidic systems as well as examples of their numerous applications. Additionally, it introduces hydrogels as perfect materials for medical and pharmaceutical use, with particular reference to the alginate and pectin gels that were used in the experimental part of the thesis.

Then I proceed to presentation of a set of experiments dedicated to the development of tools for high throughput formation of monodisperse microdroplets of varied chemical content. The experiments comprise fabrication of the microfluidic systems, with the emphasis on the process of binding and characterization of microchips. Finally, I introduce the application of one of such systems to the production of hydrogel microparticles enabling modified release of the encapsulated model active substance.

II. Introduction

II.1. Microfluidic systems and their fabrication

Microfluidics is a discipline that covers designing, manufacturing and the use of devices that deal with the fluids of nano-, pico- or even femtoliter volumes inside microscale architectures. To consider the system as a microfluidic at least one of dimensions of the channels should be in the order of micrometer or tens of micrometers. A typical microfluidic system comprises a network of microchannels connected with the outside environment by means of a set of input and output ports. Depending on the application, the on-chip architectures might be modified with the presence of chambers, posts or other elements, essential in the project. The fluids are introduced to the chip through plastic tubings or steel capillaries connected with the input holes, and the flow is driven by applying external force by syringe pumps, gravity or pressurized containers).

For over twenty years the rapidly developing microfluidic technology has been used in numerous experiments dedicated to characterization of behavior of fluids at microscale[1-4] as well as for the development of assays applicable in chemistry[5], biology[6-10] or even medicine[11, 12]. This diversity of applications of microfluidic systems often sets specific requirements for the final characteristics of fabricated microchips, including parameters like the architecture of the microchannels or the selection of material. The process of fabrication of microfluidic systems might be in general divided into three stages: i) selection of proper material, ii) introduction of chosen pattern of microchannels to the surface of the material, and iii) assembly of particular elements.

The material used in chip fabrication should be durable, easily processable, and chemically resistant to the reagents used in the experiments. Moreover, in many applications the transparency of the material is highly desired as it allows for observation and monitoring of processes undergoing inside the network of microchannels. Among the materials typically used for fabrication of the microchips are: glass, PDMS (polydimethylsiloxane), PC (polycarbonate), PMMA (poly(methyl methacrylate)), COC (cyclic olefin copolymer), PEEK (polyetheretherketone) or PI (polyimide plastic resin)[13]. Each of these materials combines a set of specific features that make them useful in some applications and unpractical in others. The comparison of the characteristics of these materials can be found in the table below (**Table 1**).

Table 1. The comparison of features of materials most commonly used for fabrication of microfluidic systems: temperature of glass transition (Tg), permeability to UV-Vis radiation, chemical resistance, the easiness of processing and price. Used abbreviations: polydimethylsiloxane (PDMS)[14], polycarbonate (PC)[15], poly(methyl methacrylate) (PMMA)[16], cyclic olefin copolymer (COC)[17], polyetheretherketone (PEEK)[18], polyimide plastic resin (PI)[19].

	GLASS	PDMS	PC	PMMA	COC	PEEK	PI
Tg [ºC]	16-352	-125	145	105	70-177	143	210-433
VIS	+	+	+	+	+	+	+
UV	+	+	-	+	-	-	+
Chemical resistance	+++	+	+	+	++	+++	++
Processing	+	+++	++	+	++	+++	+
Price	+	+	++	++	++	+++	+++

Such a diversity of properties is well reflected in the variety of methods used for shaping the microstructures on the substrates and for bonding of slabs of material into liquid-tight chips. Among the most commonly used micro-structuring methods are: photolithography[20] (most suitable for soft polymers such as PDMS), molding[21], hot embossing[22], and milling[23] (favorable for stiff materials, as *e.g.* PC).

The chemical composition of the material (the presence of functional groups) as well as its physical properties such as stiffness or temperature of glass transition (T_g), play an important role in the process of bonding. The bonding itself is a critical step in the entire fabrication process because if executed incorrectly it may result in the destruction of the final structure or characteristics of microchannels, including deformation of the cross-sections as well as significant modification of their surface properties (*e.g.* wettability).

The most commonly used bonding techniques could be divided into three types: (i) thermal, (ii) chemical, and (iii) adhesive. Thermal bonding uses compressing the substrates against each other under elevated temperature, close to the temperature of glass transition (T_g). Such bonding is characteristic for joining slabs[24-28] made of stiff polymers (PC or PMMA), as well as thin foils (lamination)[21]. Additionally, the process may be assisted by modification of the selected material in an aqueous solution or an organic solvent. Thermal bonding is an easy and inexpensive method for obtaining durable connection, which does not involve sophisticated equipment. Nevertheless, despite the numerous advantages it is limited by the necessity of

application of high and aggressive temperatures that might considerably influence the structure of microchannels.

The temperature is not an issue in the case of the two other bonding methods. For instance, chemical bonding requires only chemically active surface of the material. Such a modification may be performed in two ways (i) by activation of the surface using physical agents (*e.g.* with UV/O_3 or plasma), and (ii) introduction of active groups that can bind to the substrate and modify the surface chemistry. The activation with UV/O_3 or plasma is primarily used for bonding of PDMS with PDMS, as well as for combinations of PDMS and glass, PMMA, polystyrene, *etc*.[29-31]. However, joining of the substrates needs to be performed shortly after the modification has been initiated as the activation of the surface diminishes very fast in contact with air. On the other hand introduction of chemically active groups results in a strong binding[32, 33], but at the same time it might affect the character of microchannel and cause undesirable effects such as wetting[34, 35].

Adhesive bonding includes a step of application of a layer of glue or resin[36-38] to the surface of the substrates. This method allows to bond together different types of materials, yet it might alter both the geometry of michrochannels and their surface chemistry. The development of new fabrication schemes dedicated to the known and new materials is a very active field of study of a growing industrial relevance.

II.2. Microfluidic techniques utilizing laminar flow

The laminar flow is characteristic for lower values of Reynolds number (Re< ~2000) and in microfluidic channels Re<<1[39]. Introduction of a number of streams of liquids to the system results in the presence of multiple stable equilibrium states between laminas of fluids[40] and sharp boundaries at their interfaces as their mixing is based only on very slow diffusion process[41].

Microfluidic techniques based on a single phase flow are applicable in a great number of experiments with particular relevance in chemistry, biology and biochemistry. Well developed techniques include electrokinetically driven separation of analytes present in the sample (*e.g.* microfluidic electrophoresis) or sorting of larger entities on the basis of their physical properties such as mass or polarizability. Additionally, laminar character of the flow allows for phenomenal control over the flow and diffusion of chemicals across lamelas of liquid, providing tools for *e.g*. serial dilutions, or studies on chemotaxis.

In the following subsections I present typical applications of single phase techniques with reference to separative purposes and bio-microreactors. Additionally, I focus my attention

on a systems dedicated to generation of gradients of concentration as they constitute an inspiration for a part of my research presented in this dissertation.

II.2.1. Systems dedicated to separation of samples

Microfluidic devices based on continuous flow are often used as a tool for separation of the sample components. Such systems allow for sorting entities present in the sample by using hydrodynamic forces but also by applying obstacles, or various sources of force field such as electric, magnetic, acoustic, optical, *etc.* or simply exploiting the gravity.

In general, the main difference between the conventional techniques of separation, such as chromatography or electrophoresis, and microfluidic systems is in the method of sample separation. In the first group the sample is separated on the basis of its interaction with the substrate (stationary phase filling of a chromatographic column). Microfluidic systems allow for continuous introduction of the sample to the microchannel, as well as for continuous collection of separated fractions. Additionally, no extra labeling before sorting is necessary as separation on microfluidic chip is often based on the differences in the size of particles, their charge or polarizability. This method is useful for separation of amino acids, larger molecules (*e.g*. DNA, proteins), cells or microparticles.

The simplest way of separation is hydrodynamic filtration. This method is based on the architecture of microchannels and the control of the flow rate. Hydrodynamic filtration is usually applied for separation of microparticles [42, 43] and it has been successfully used in the separation of red blood cells [44, 45].

More advanced procedure utilizes both hydrodynamic forces and the presence of solid obstacles in the system. Such method has been demonstrated by *Huang et al.*[46] and *Inglis et al.*[47] in the separation of DNA particles with 'deterministic lateral displacement', revealing high resolution of sizes, at high throughput. It is based on pumping of a solution of DNA through a microchannel equipped with a set of posts shifted from one row to another and aligning again after a number of rows. In this method particles much smaller than the gaps between the successive rows of posts follow the laminar flow while slightly smaller are forced to move across the array of the posts.

Another attempt of such separation – 'Brownian ratchet' – has been performed by several groups[48-50] and involved the flow of the sample through asymmetric array of obstacles. The separation depended on the value of diffusion coefficient of particular DNA macromolecules, what required application of low values of flow rates, which resulted in decrease of throughput.

Hydrodynamic separation may be assisted by the use of electric field in order to separate charged molecules and particles. For instance, *Huang et al*.[50] have been switching the value of electric field between two values E1 and E2 together with changing the direction of its application from parallel to diagonal forces to induce the movement of DNA molecules through an array of pillars. Obstacles might take the form of gaps as *Fu et al*.[51] have proposed. Combination of such obstacles with orthogonal electric field resulted in obtaining three separation regimes: i) Ongston sieving, ii) entropic trapping, and iii) electrostatic sieving corresponding to separation based on the thickness of the electric double layer, the size of molecules, and their charge, respectively. Such methods present both fine resolution of the sample ingredients and reasonable throughput.

A system devoid of physical obstacles can perform equally high quality separations and at the same time simplifies the architecture of the microfluidic chips. One of the methods based only on application of the electrical field is free-flow electrophoresis (FFE). In FFE, the sample is transported via a set of inflow channels to the main chamber of the chip where homogenous electric field is applied perpendicularly to the flow. The transport of molecules through the chamber is a resultant of the influence of the flow and electric field. During the separation process the components of the sample are oriented in particular charge-dependant manner and then collected by an array of outlet channels[52, 53].

Similar is the setup for free-flow isolectric focusing (FF-IEF). In FF-IEF, an additional gradient of pH is applied to the main chamber. It is done by placing (inside the chamber) a mixture of ampholytes forming a pH gradient right after the electric field is applied. The separation of sample components is based on the movement of amphoteric molecules (*e.g*. proteins) across the chamber until achieving pH corresponding to their isoelectric point (pI) and following the flow from that point[54-56].

An alternative to FF-IEF is dielectrophoresis (DEP). This technique requires application of heterogeneous electric field. In DEP particles or cells are polarized under the influence of electric field and move towards or away from the high intensity field[57, 58].

Despite many advantages resulting from using the electric field as a mean of separation, methods based on magnetic field may be regarded as superior due to their milder nature, a factor especially important in the case of dealing with biological samples. Additionally, the magnetic forces do not depend on the value of pH, surface charge or ionic strength. Such separation involves application of heterogeneous magnetic field perpendicular to the flow direction in order to provoke migration of particles susceptible to the influence of such field or magnetically labeled cells. Different level of magnetization eventually causes separation of components of the sample[59, 60].

Other way to perform a separation is the use of acoustic or optical forces. Both of them utilize differences in physical properties of sample ingredients for their separation. The first method involves generation of standing sound wave over the cross-section of the microchannel. The wave is selected in such a way that the nod is localized in the centre of the channel while two anti-nodes are situated near to the opposite walls. Particles or cells present in the sample move towards the node or anti-node under the influence of sound wave[61, 62]. Another method, relies on optical polarizability of sorted entities. The optical force is directed perpendicularly to the flow and the separation is dependent on the particles or cells size as well as on their refractive index[63, 64].

II.2.2. Continuous flow bioreactors

The term of 'bioreactor' may refer to a system that is a vessel designed to carry out biochemical processes[65], which involve the presence of live organisms or biochemically active substances (*e.g.* enzymes) derived from organisms. According to other definitions it can be described as a device for growing cells or tissues[66]. In both cases the volume of a bioreactor typically oscillates from a liter to cubic meters, what suggests high consumption of reagents and generation of large amounts of wastes. The exceptions are minibioreactors operating in microliters quantities.

The idea of progressive miniaturization of reaction systems considers the decrease of consumption of reagents as well as better control of the heat- and mass-transfer-limited processes. This tendency has influenced the technology dedicated to bioreactors. This in turn resulted in developing microreactors (including biomicroreactors), microseparators, and micro-heat exchangers. This trend focuses on fabrication of microchannel-based reactors made of stainless steel, ceramic, glass or polymeric materials, offering small dimensions at least one of which is smaller than 1 mm[67]. The character of continuous flow microreactors makes their usage beneficial in comparison to traditional methods, mostly because they enable operation in microfluidic environment, which results in minimization of material input as well as the wastes production, and reduction of energy consumption.

The use of microreactors for biocatalytic purposes usually is reduced to enzymatic reactions. In such cases enzymes could be present in the system either immobilized on a substrate[68] or in the form of solution. The immobilization of enzymes in a microchannel or a microchamber is one of the most challenging issues. The process should be characterized by reversibility, versatility and enable the retention of catalytic activity of utilized enzymes. Fulfillment of all of these requirements is not an easy task. There are however, numerous protocols dealing with this issue and some of them could be applied in microfluidic systems.

At the microscale the immobilization is implemented by packing the microchannels with modified beads[69] or 'monolithic structures', or by coating the walls of the microreactor with porous matrices[70] as well as covalently bound chemicals. Modern bioreactors with immobilized enzymes present many advantages such as reusability of biocatalysts, high stability, and the possibility to work in the large scale industrial systems in continuous operation for long periods of time without the decrease in the biocatalytic activity[71].

II.2.3. Architectures for generation of gradients in laminar flow

Considering chips for the generation of concentration gradients of chemical species in the continuous flow, one might categorize microfluidic systems into two groups: diffusion-based devices and gradient generators based on continuous flow. Microfluidic gradient generators completely based on diffusion, also called flow-free gradients, might be obtained in a microchannel or a chamber interconnecting two reservoirs, called 'source' and 'sink'. The main idea is to provide a link characterized by high resistance to flow in order to obtain stable gradients of concentration. Such characteristic involves application of narrow microchannels[72] or membranes[73] as well as gels (*e.g.* agarose)[41, 74]. However, this solution has a significant drawback namely the shape off gradient profile is limited by spontaneous diffusion as there is no possibility for active manipulation of the gradient.

In the case of continuous flow gradient generators the molecules are transported by a set of laminas to the region where the gradient is formed, and their concentration is determined by the flow in a precisely designed network of microchannels. As it is well known, low-to-moderate values of Reynolds numbers, typical for microfluidics, result in laminar flow and purely diffusional mixing[41]. The proper architecture of a chip involves the use of Kirchoff's equations results in a network of channels that take two or more input streams which iteratively split, combine, and mix their flows to create N outputs of predesigned combinations[75-82] (**Figure 1b-e**). The original design[83] (**Figure 1a**) has been improved[84] to reduce the number of operations (of splitting, combining, mixing) that need to be performed in order to obtain the desired number of outputs. This was achieved by adding a set of horizontal channels after each set of meanders.

All these techniques use a broad range of the network topologies, however, they all have one common feature: the sub-streams as well as their combinations are mixed within the network of channels generating the gradient at the outlet. Thus, the maximum throughput of these systems is limited by the rate of mixing, controlled in turn by the diffusional transport of molecules across the width of the channels. Nevertheless, if required, the application of high flow rates limits the extent of the diffusional mixing and produces sharp interfaces of the laminas

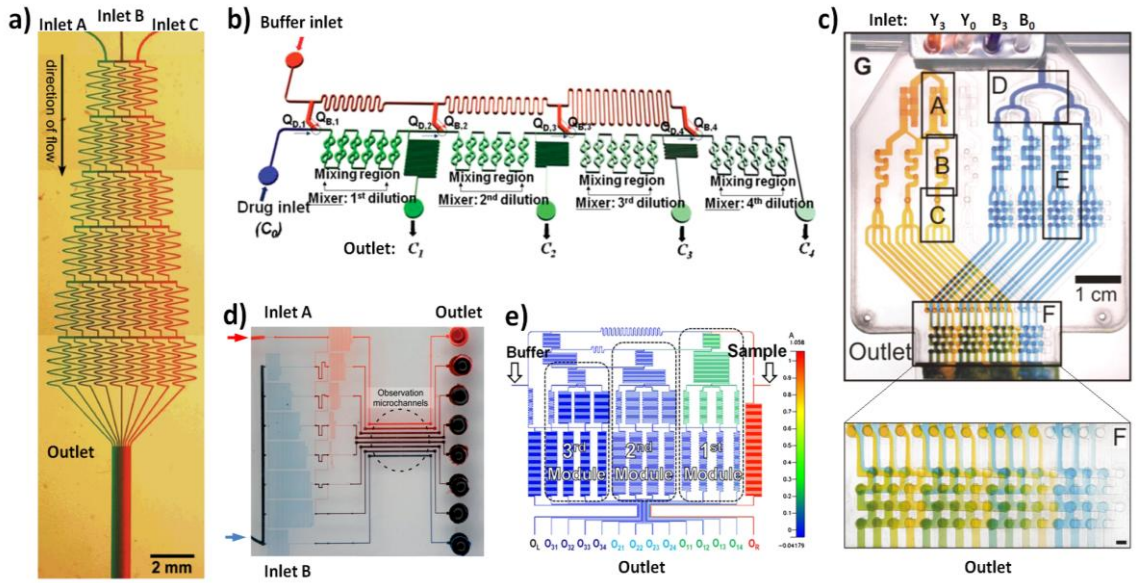

Figure 1. Exemplary photographs and schemes illustrating microfluidic systems dedicated to generation of gradients. (**a**) Photograph of a microfluidic device used for formation of gradient of green and red dyes in a solution. The three inlet channels (Inlet A, B, and C) provide fluids that are combined after series of operations and flow laminarly in a single, wide outlet channel[81]. (**b**) The concept of a chip for serial dilution, where each concentration is obtained in particular intersection by dilution of the drug solution with the buffer[78]. (**c**) Combinatorial mixer comprising characteristic sectors (marked A-F) performing subsequent operations necessary to obtain the gradient of concentration[75]. (**d**) Picture of a microfluidic network dedicated to generation of a linear gradient[80]. (**e**) Scheme of a microfluidic system based on a hybrid of serial and volumetric dilutions that allows obtaining linear gradient of concentration in each of three modules[79].

The microfluidic systems producing gradients of concentration may be applied in high throughput screening (HTS) as well as investigations on the chemotaxis phenomenon. The HTS is extremely useful in studies on dose-response in drug screening. While the standard procedure is expensive and time consuming, microfluidic systems provide the opportunity of simultaneous acquisition of data. This, in turn, reduces time necessary to perform the analysis. *Lee et al.* has proposed a microfluidic generator of concentration that exploited the combination of serial and volumetric dilutions[81]. Firstly, the sample was diluted with the buffer into a non-linear collection of concentrations, 2-fold or 10-fold logarithmic scales, and then splitted into parallel channels, which in turn were diluted linearly with separately delivered buffer. Such a system is capable of generating monotonic changes of concentrations in a wide range of logarithmic and linear scales what guaranties fast identification of a requested parameter (*e.g.* inhibitory concentration IC_{50}).

Chemotaxis is a relevant to processes observed *e.g.* in the organism, where cells migrate in a particular direction, attracted by the highest concentration of a signal molecule that may be produced by inflammation[85, 86] of cancer metastasis[87-89]. Conventional batch assays[90, 91]

do not allow for precise control of the gradient of concentration, degrading in time. Additionally, such methods are commonly performed in environment characterized with static buffer conditions or gradient of a single chemo-attractant[92, 93]. This, in turn, results in limited similarity to *in-vivo* conditions, which are much more complex and dynamic.

Microfluidic systems providing serial dilutions are claimed to be a perfect tool to simulate these conditions in a more reliable way. *Kim* and *Haynes*[94] have proposed the use of such a system to study all combinations of four chemo-attractants for the purposes of investigation of neutrophil chemotaxis. The method turned out to be a convenient way to study both the speed of response of the immune system as well as susceptibility to different combinations of stimuli. Another group has constructed a similar system to examine the impact of the concentration of particular chemicals on proliferation and differentiation of human stem cells[95]. At the same time such devices might be utilized to characterize the metastasis of breast cancer cells in the presence of different agents[96-98], which is essential for the basic, molecular-level understanding of the disease and developing a potential therapy.

Generators of concentration gradient could also be used in fabrication of substrate-bound gradients. This kind of application has been demonstrated by *Dertinger et al.* to investigate the influence of the substrate-bound poly-L-lysine on the neurons viability and orientation[75]. Featured examples reflect only partially the multiplicity of applications of gradient generators.

II.2.3.1. The influence of differences in viscosity on generation of gradient

Systems described in the former subsection are a convenient tool for obtaining gradient of concentration while mixing fluids characterized with similar viscosity. However, they are not capable of handling liquids of different viscosities.

Mixing of liquids of different viscosities produces a gradation of viscosity that influences the distribution of flow through a cascade of splitting and merging junctions in networks. In such a system, in order to preserve the designed concentration gradient at the outlet, it is necessary to apply additional linearization procedures[99] that are specific to the particular set of liquids.

II.3. Biphasic microfluidic systems

The biphasic microfluidic systems provide many possibilities that have not been available for continuous flow based devices. Application of geometries enabling to split one stream of fluid with another, immiscible one, is a very easy and convenient way to obtain well defined emulsions or more complex entities such as multiple emulsions. Generation of a set of independent droplets of nano- or even femtoliter volumes is favorable in a great number of studies. Such single microreactors of well described size and composition are deprived of the direct contact with each other and eliminate the problem cross-contamination. Additionally, a film of continuous phase present on the surface of michrochannels provides smooth transport of droplets across the system and guaranties the protection against deposition of solid products of polymerization (*e.g.* microbeads) or precipitation-based reactions (*e.g*. nanoparticles) on the walls.

Moreover, the nature of such systems promotes rapid mixing. Therefore, in comparison to continuous flow based devices, the mixing in biphasic devices is no longer diffusion dependant and relies only on the flow rates of continuous and droplet phases. This distinction has been found useful in studies on reaction kinetics[100, 101]. Further subsections describe in detail the strategies introduced in microfluidic systems dedicated to production of droplets and numerous application of such devices in the area of chemistry, biology, biochemistry, pharmacy and medicine.

II.3.1. Formation of droplets and types of droplet generators

Conventional systems dedicated to formation of emulsions, such as colloid mills, stirred vessels, toothed disc dispersing, *etc.*[102] produce emulsions of water in oil (W/O) or oil in water (O/W) by vigorous stirring or sonification. Obtaining emulsions in such a manner is fast but at the same time it provides poor control over the distribution of the drop size of the emulsion.

Microfluidic systems based on droplet formation are a convenient tool to obtain not only water-in-oil (W/O)[103] or oil-in-water (O/W) emulsions but even more complex configurations (e.g. W/OW, O/W/O, etc.)[11, 104]. Additionally, they assure high uniformity of volumes of obtained droplets[105] in terms of size and composition as well as reasonable throughput.

The main idea of generation of emulsions in microfluidic system is that the continuous phase is to wet the walls of the main microchannel of the chip. This can be achieved by

modifying the surface of the walls of microchannels. The character of the continuous phase imposes the type of modification, that should be introduced to make the surface either more hydrophilic[34] or hydrophobic[35]. It has also been shown that for the same junction the droplet and continuous phases may be switched if a proper surfactant is added[106]. An advantage of such systems is a precise control over the size of the droplets. It is achieved by manipulation of the flow rates of dispersed and continuous phases and of the geometry of the microchannels' network. Additionally, the wide range of materials used for fabrication of microfluidic systems enables proper adjustment to applied reagents which eliminates the problem of affecting microchannels by some solvents.

Generation of emulsions in microfluidic systems may be performed in several ways. Typical geometries used most often for this purpose include: T-junction, cross-junction, Y-junction, flow-focusing or three-dimensional axisimetric microfluidic devices, including capillary based systems. Further subsections contain thorough description of abovementioned geometries.

II.3.1.1. Cross-flow geometry (T-junction)

T-junction is the simplest module used for generation of droplets in microfluidic systems (**Figure 2**)[3, 107-110]. This element of architecture is formed by joining two microchannels perpendicularly, so that it resembles letter T. Furthermore, this kind of junctions might be placed on the chip in parallel in order to increase its general throughput[111]. In general, the microchips incorporating T-junctions as a droplet generator display characteristic regimes of operation: squeezing, dripping and jetting[112-114]. In the first stage the dispersed phase fills almost whole section of the main channel, while the continuous phase appears as a thin film on its walls. This leads to the increase of the pressure in continuous phase up stream which causes transition to squeezing of the droplet phase[115] until its neck breaks up. Within this regime the droplet size is dependent on the ration of the flow rates of the droplet and continuous phases. There is a critical value of capillary number (*Ca*) that promotes the transition from one regime to another. It has been observed[113] that for the values above $Ca \sim 10^{-2}$ the shear stresses start to play crucial role in the process of break-up, and the system enters a mode similar to the dripping regime in an unbounded, co-flowing liquid. In the case of further increase of the *Ca* above $Ca \sim 0.3$, the system switches from stable dripping to jetting[114].

T-junctions not only allow for producing droplets. This particular geometry is often used to merge droplets or splitting them into smaller ones[116]. It could also be modified in such a way that more than one side channel connects to the main channel at the same point. This results in production of droplet out of two[117] or three[118] fluids co-creating the dispersed phase.

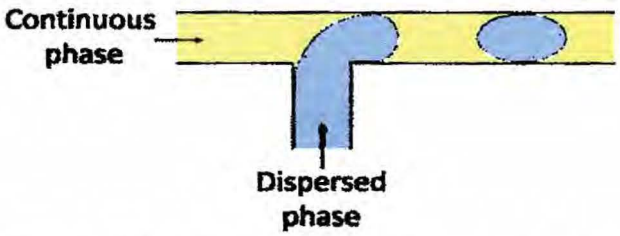

Figure 2. Schematic illustration of T-junction droplet generator. Continuous and droplet phases correspond to yellow and blue colors, respectively.

The architecture of a cross junction enables two different ways of droplet formation (**Figure 3a** and **b**). The first one involves introduction of the continuous phase to the side channels (arms of the cross) and droplet phase to the perpendicular one. The stream of the droplet phase surrounded by continuous fluid is thinned from both sides till the moment its neck is thin enough to pinch off as a droplet[119]. Combination of such junction on one microchip enables formulation of multiple emulsions, which could be easily turned into *e.g.* core-shell entities[120, 121].

If the system supplying the chip is reversed (continuous phase flows through perpendicular channel, while droplet phase feeds the side channels), the cross junction works as a double T-junction, producing droplets from each of them, alternately[122] (**Figure 3b**).

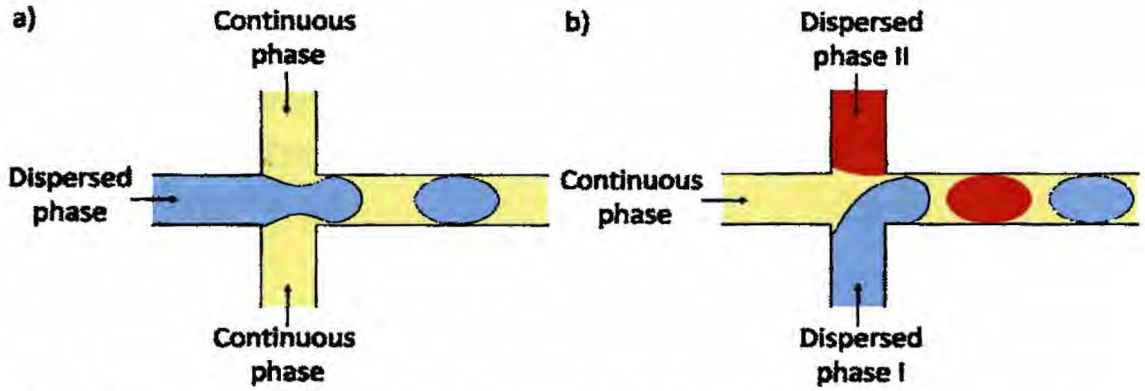

Figure 3. Schematic illustration of two different ways of droplet formation in cross-junction: (**a**) resulting from squeezing the stream of droplet phase symmetrically by continuous phase flowing out of channels forming arms of the cross and (**b**) produced the same way as in the case of classical T-junction. Continuous and droplet phases correspond to yellow and blue colors, respectively. Red color is used to mark the other dispersed phase.

II.3.1.2. Flow focusing geometry

Standard microfluidic flow-focusing device (MFFD) was developed by *Anna et al.*[123]. In the most classical example of such a system, the dispersed phase flows through the middle channel while continuous phase, through two outer channels (**Figure 4a**). The two streams of continuous phase pass through a small orifice implemented downstream. The droplet phase is squeezed from both sides into a thin filament while passing the orifice and eventually breaks up in the orifice itself or downstream from it[124].

In general, there are four distinct regimes of droplets generation in the MFF devices: squeezing, dripping, jetting, and tip-streaming[125]. The squeezing regime is characterized by droplets size that is approximately equal to the orifice diameter and the mechanism of breakup is similar to the one observed in T-junction. In dripping regime the dispersed phase jet gets narrower what results in considerably smaller droplets while for jetting the elongation of the jet continues downstream from the orifice and volume of produced droplets is less controllable. The tip-streaming regime is observed in the presence of a surfactant at a very high rates of flow[125]. The most characteristic for this regime is even longer jet breaking up into very small droplets away from the orifice.

If the fluid residing in the middle channel reveals higher affinity to the surface it acts as a continuous phase, while the outer channels carry the dispersed phase, that is breaks into droplets at the orifice alternatively (**Figure 4b** and **d**). Additionally, exploitation of flow focusing systems results in deriving more sophisticated configurations[126]. For instance, the implementation of a sequence of flow-focusing generators leads to fabrication of multiple emulsions (**Figure 4c**). This type of entities could be further used in fabrication of polymeric particles of *e.g.* core-shell type.

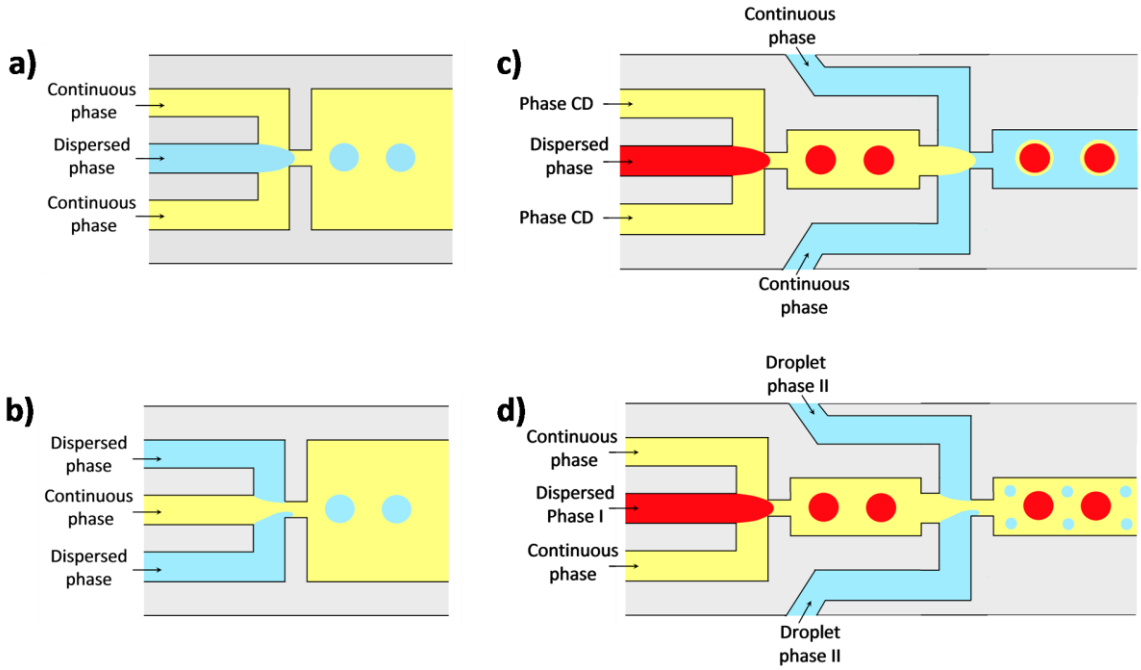

Figure 4. Schemes (**a**) and (**b**) show microfluidic flow-focusing devices designed to form a single emulsion but presenting different surface energy. (**a**) droplets are formed by periodic breakup of the stream of droplet phase supplied by central channel. (**b**) dispersed phase shows higher affinity to the wall in comparison to the continuous phase, what results in production of droplets by shearing off the side streams by continuous phase. (**c**) an exemplary system for production of double emulsions in FFD arrangement. (**d**) a method for obtaining two populations of droplets. Continuous and droplet phases correspond to yellow and blue, respectively. Red color is used to mark the other dispersed phase (illustration based on exemplary schemes presented by *Seo et al.*[126]).

II.3.1.3. Co-flow geometry

Axisymmetric microfluidic devices offer several advantages in comparison to other droplet-based systems. However, the most relevant is the elimination of the problem of wetting. In the junction-based and planar flow focusing techniques the contact of the droplet phase with the walls of microchannel is limited only by a thin film of continuous phase. If the surface of the channel is not definitely hydrophilic or hydrophobic, an extra modification might be necessary to avoid wetting. In axisymmetric systems the dispersed phase is surrounded by continuous fluid what eliminates the aforesaid problem (**Figure 5**). Many materials have been implemented in fabrication of axisymmetric systems in order to obtain a device that would work reproducibly under different conditions. To obtain the axisymmetric systems *Takeuchi et al*. [127] have proposed a system made of PDMS, while *Xu et al.* [128] has placed a needle inside PMMA microchip, and *Morimoto et al*. [129] has fabricated a device by combining photolithography and stereolithography. Nevertheless, the most attractive, so far, is fabrication of axisimmetric systems out of glass capillaries, initiated by *Utada et al.*[130] and continued by others[131, 132]. They

comprise of inner, circular and outer, square, capillaries placed one within the other and glued to the glass slab for immobilization. Such system characterizes by high level of resistance to most of chemicals – in contrary to PDMS, swelling under influence of some solvents – and could be fabricated in a reproducible manner.

The dispersed phase could be focused in the capillary-based axisymmetric devices in two different ways, using: i) co-flow or ii) counter flow.

The axisymmetric system operates in a co-flow manner if both the droplet phase, implemented as an inner fluid, and continuous phase, used as the outer one, flow in the same direction (**Figure 5a**). The outer fluid surrounds the tip of the inner capillary and leads to the droplet pinch off. Emulsions produced in such a way present high level of uniformity of droplets and are often used as a template for polymeric particles[133].

The counter flow approach uses the inner capillary as a reservoir for the emulsion and both droplet and continuous phases supply the device from opposite directions (**Figure 5b**). The main advantage of such configuration is that it allows for production of droplets smaller than the orifice of inner capillary in contrary to co-flow systems[133].

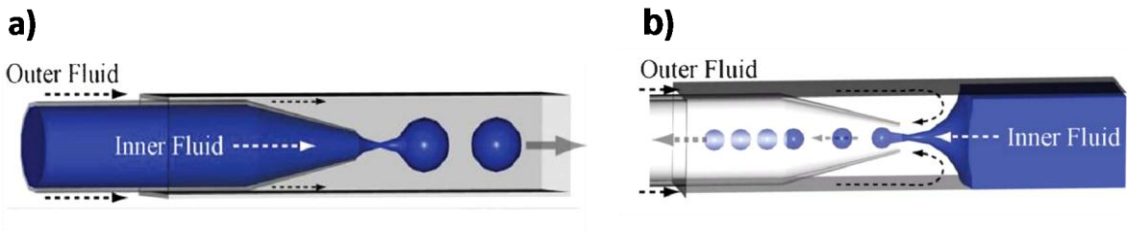

Figure 5 Schemes of glass capillary devices designed for making single emulsion droplets in co-flow (**a**) and counter-flow (**b**) manner. Arrows indicate the flow direction of fluids and drops[133].

II.3.2. Influence of viscosity on formation of droplets

It is well known that the viscosity of the droplet phase influences both the operational range of flow rates, and the volume distribution of the droplets[4, 126, 134-137]. For example, *Berthier et al.* [136] has shown that the use of fluids with higher viscosities results in production of smaller droplets. Also *Tice et al* has demonstrated that, in a T-junction, the range of applicable rates of flow becomes narrower for increasing viscosity of the input droplet phase. According to the data, the higher the viscosity of the inner phase, the sooner (*i.e.* at progressively smaller flow rates) the system shifts to the co-flow regime. It seems however, that the problem of droplet formation out of a droplet phase comprising of two liquids differing in viscosities has not been investigated so far.

II.3.3. Control of droplet's composition

The control of composition of the droplets is relevant when it comes to reactions, when the results depend not only on specificity of applied reagents but also on their concentration. There are several methods dedicated to production of arrays of droplets differing in content, creating a great potential for analyses devoted to screening for most preferable reaction conditions.

II.3.3.1. Control of droplet content by changes of flow rates of input streams

The content of a single droplet might be controlled in several ways: i) batch dilution, ii) zone dilution, iii) the control of the flow rate of droplet's components and iv) merging droplets on demand (DOD).

The batch dilution method was introduced in 2010. A group of authors proposed an automated microfluidic platform (DropLab) for programming droplet based reactions[138]. They achieved dissimilarity of droplet content by aspirating different volumes of sample, reagents, as well as diluent (**Figure 6a**), and confirmed the utility of the device by performing enzyme inhibition assays, protein crystallization screening, and identification of trace reducible carbohydrates.

The zone dilution system was made as a hybrid of well characterized analytical techniques – electrophoresis (CE), high-performance liquid chromatography (HPLC) or flow injection analysis (FIA) – and microfluidic droplet generator. *Edgar et al.*[139] and *Niu et al.*[140] have taken advantage of separative abilities of CE and HPLC, respectively, and have turned discrete zones in the process of separation, into droplets-by-droplet generating module (**Figure 6b**). Similar approach has been undertaken by *Cai el al*. [141], who developed a microfluidic chip for large scale concentration gradient by coupling FIA module with a droplet generator to perform an enzyme inhibition assay.

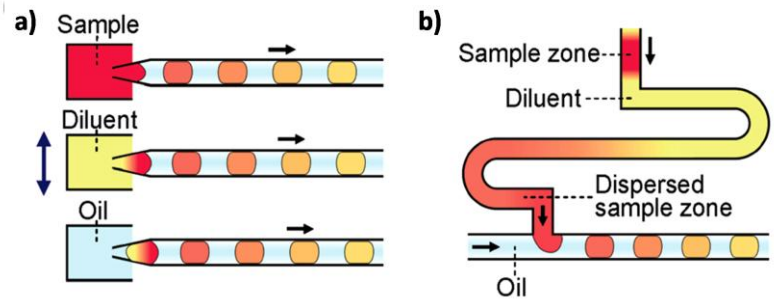

Figure 6. Various generation modes of concentration gradients in droplet-based microfluidic systems using the batch dilution (**a**), and zone dispersion (**b**)[141].

Another way of differentiation of particular droplet content involves the manipulation of rates of flow of the components of the droplet phase. The simplest architecture destined for this purpose is a modified T-junction. In such a geometry the microchannel supplying the droplet phase, splits into two or more microchannels each providing a solution that is to be mixed with the other ones in a required ratio and then turned into a droplet at the junction (**Figure 7c**). The proportion of reagents may be tuned by providing strict control of the flow of droplet phase sub-streams. This is usually done by implementation of computer software dedicated to operation of syringe pumps. Such a set up enables programming a sequence of desired rates of flow that correspond with the final content of the droplet. Ismagilov's group has used such systems in their experiments dedicated to protein crystallization[142] and successfully determined the kinetics of the process.

The combination of fine control over the flow rates of droplet phase components with the idea of merging droplets with each other or with a stream of fluid offered by microfluidic systems has provided some of other means of achieving gradation of concentrations, namely post- (**Figure 7a**) and premixing (**Figure 7b**). The idea of postmixing is based on a coalescence of two droplets moving at a different speed[143]. It also involves joining a droplet with a stream of other substance co-forming droplet phase[10].

The last technique uses electric field to force the coalescence – so called electrocoalescence of previously produced droplets (**Figure 7d**). *Churski et al.*[144] has introduced a technique suitable to produce droplets of a well defined volume by applying a set of magnetic valves together with a computer program providing control over the volume of droplets, the time of formation of droplets and their merging in electric field.

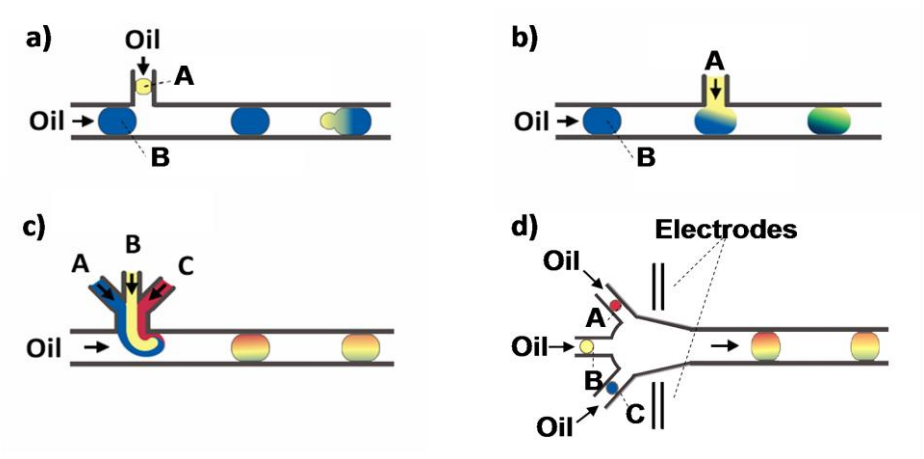

Figure 7. Schematic illustration of forming arrays of droplets characterized with different content. Premixing (**a**) and postmixing (**b**); Modified T-junction equipped with three microchannels joined into one at the entrance to the main channel (**c**); System designed for production of droplets on demand (DOD) and their further fusion in the process of coalescence (**d**). Letters A, B and C stand for three different reagents co-forming the droplet phase. Oil refers to continuous phase (illustrations partially copied from *Du et al.*[138]).

II.3.3.2. Simultaneous production of droplets differing in composition

Several systems offering a combination of gradient and droplet generators have been introduced enabling simultaneous formation of streams of droplets exhibiting a gradation of concentrations of chemistry (**Figure 8**). For example, *Lorenz et al.*[145] used the original gradient generator[83] to provide five dilutions of a fluorescent dye into five droplet generating modules. *Damean et al.*[146] has used the outlets of a gradient generating device[84] as the base for the dispersed phase supplying parallel droplet generators to form a linear gradient of fluorescein diphosphate in order to screen the activity of an enzyme (alkaline phosphatase).

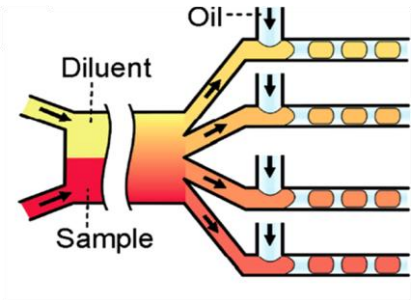

Figure 8. Scheme illustrating a combination of gradient generator based on continuous flow (diffusive gradient) and modules for droplet formation[141].

II.3.4. Potential applications

The variety of materials dedicated to fabrication of microfluidic systems together with available geometries and diverse technical solutions, such as automation, gives a wide range of possible applications. Additionally, features such as low consumption of reagents, compartmentalization and limitation of vaporization, that eliminates the cross-contamination, promote applications of analytical and biochemical nature. On the other hand, high throughput as well as considerably narrow size distribution makes the systems a perfect tool for preparatory purposes. The next two subsections present an overview of numerous applications of droplet based systems in various fields.

II.3.4.1. Analytical and biochemical studies

Droplet-based microfluidics has defined a new generation of systems suitable for a great number of applications. They guarantee high efficiency and control of the processes. Moreover, localizing the reagents inside discreet droplets eliminates some undesired phenomena (*e.g*. evaporation) and provides for fine-tuning and maintaining reaction conditions.

This type of systems are suitable for performing chemical syntheses, including nitration of benzene[147-149], halogenation of alkenes[5] (**Figure 9a**) and aromatics[150], as well as more complex syntheses as in the case of obtaining azo dyes[151]. Additionally, in the past several years, the applications in the area of chemical synthesis has extended to formation of nanoparticles[152]. Microfluidic devices turned out to be very convenient mostly due to the enhanced mixing, what results in obtaining low size distribution of these entities. The chaotic mixing was also found to be a relevant factor deciding on the size of crystals obtained in the process of protein crystallization[10] (**Figure 9b**).

Droplet-based microfluidic systems are equally useful from the analytical point of view, *e.g*. as a tool for microextraction[153]. Due to emulsification the interfacial area increases significantly what promotes better mass transfer. Compartmentalization allows also occurrence of so called rapid mixing[3] providing a homogenous environment inside particular droplets. This, in turn, guaranties reliable determination of kinetics of numerous processes, including of enzymatic assays[100, 101].

Even more sophisticated applications concerning DNA sequencing[154] or evolution of proteins[155, 156] profit from compartmentalization. Moreover, droplets might be used as vessels for carrying cell organelle[8] (**Figure9d**), entire cells[8, 9, 157, 158] (**Figure9c**) or more complex organisms such as nematode[159] (**Figure9e**). Interior of the droplet secures stability of the environment and the interface between droplet and the continuous phase protects the content of such a micro-container from cross-contamination as well as leaking.

Compartmentalization together with the possibility of handling the content of particular droplet (by *e.g.* fission or fusion), creates a fine base for screening tests of both chemical as well as biochemical nature. Multiple systems dedicated to optimization of conditions for protein crystallization[122, 142, 160, 161] or to investigation of the influence of antibiotic cocktails on the growth of bacteria[162], have been reported.

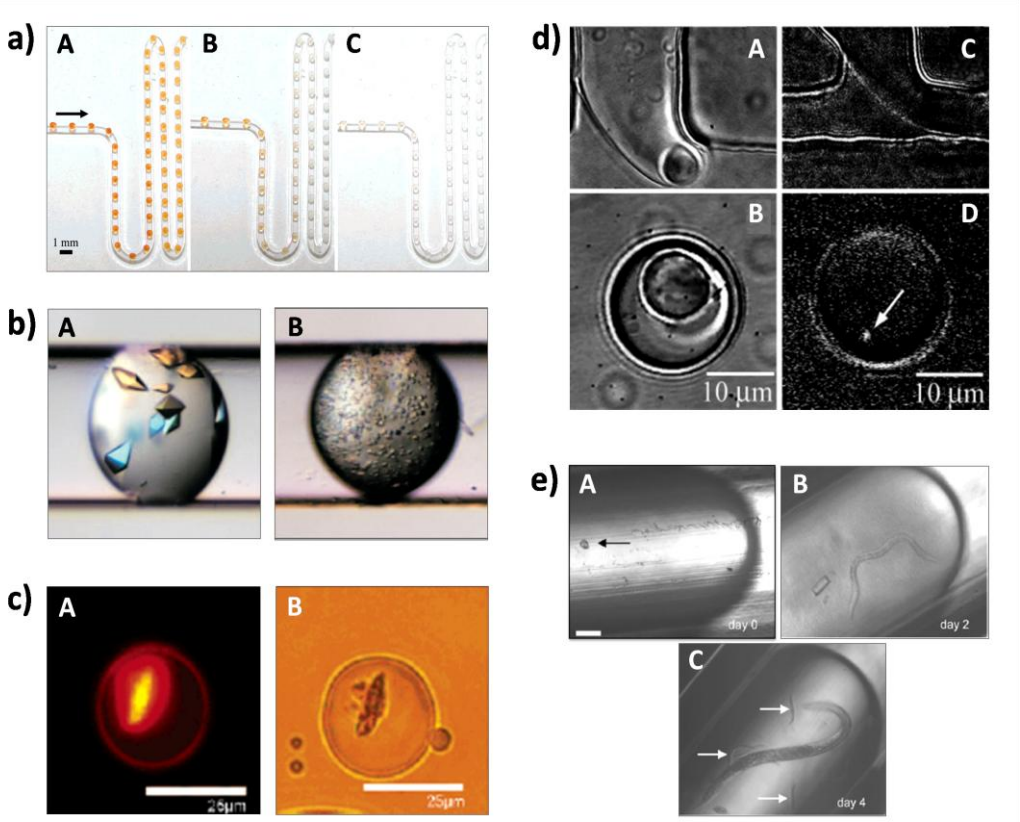

Figure 9. Illustration of exemplary applications of droplet-based microfluidic systems. (**a**) Visualization of reaction of bromination of styrene inside droplets of organic solvent. The photographs A-C show the same experiment performed at three different sets of flow rate of organic phase[5]. (**b**) Microphotographs demonstrating an effect of fast chaotic mixing (A) and slow chaotic mixing (B) on protein crystallization under identical conditions[10]. (**c**) Encapsulated MCF7 breast cancer cell recorded by fluorescent microscopy (A) and light microscopy (B)[9]. (**d**) Process of entrapping a cell (A) and a mitochondrion (C) inside of a droplet. Microphotographs B and D show encapsulated cell and mitochondrion, respectively[8]. (**e**) A-C photographs present the growth stages of a nematode trapped in a droplet[159].

II.3.4.2. Preparatory purposes

There are plenty of protocols describing the use of microfluidic chips as a mean to obtain hollow[163-166] (**Figure 10c**), porous[163, 167] or solid particles[164], as well as more complex systems such as entities build up of multiple emulsions coated with a polymer[11] (**Figure 10b**). Additionally, due to the strong dependency of the character of polymeric microparticles not only from the composition or size but also shape, the possibility of manipulation with their form is also relevant. Apart from that, microfluidic systems allow for fabrication of particles characterizing with more elaborate structure, *e.g*. Janus, multilayer or even donut-shaped particles, plugs and discs.

The anisotropic particles might be useful in new materials technologies due to their unique scattering and packing properties[168]. Moreover, as they represent a group of such a diversity of shapes, they could be successfully used as models of complex systems *e.g.* bacteria or red blood cells (RBC)[169]. Specific form of particles might affect their transport through membranes, targeting capabilities, ability to attach to other structures, undergo the internalization by the cell as well as sorting after successful incorporation. Such particles may be also used as carriers of active substances due to thinner and thicker areas in the structure influencing their decomposition under certain conditions[170, 171].

The simplest way of fabrication of anisotrtopic particles in microfluidic systems is a combination of a droplet generator (*e.g.* T-junction or flow focusing) and an output channel or a chamber imposing certain shape of produced emulsion. This has been used by *Xu et al.*[172] (**Figure 10a**), who employed a flow focusing device for production of emulsion. Manipulating with the width and depth of the outlet channel, or chamber, they obtained desired shape of the droplet before its UV or thermal solidification occurring downstream.

Nie el al., has applied similar strategy to solidify highly monodiperse Janus particles (JPs) and ternary polymer particles synthesized in a flow focusing microfluidic device[173] (**Figure 10d**). Production of two-phase and three-phase monomer droplets relied mostly on rapid polymerization, turning the droplet structure solid. Additionally, they performed selective functionalization of JPs by introduction of active moieties in one part of the particle or in the process of bio-conjugation of albumine and JPs after their polymerization.

Another approach to fabrication of polymeric microparticles uses supraparticle synthesis based on application of nano or microparticles (max several micrometers in diameter) called Pickering particles, which stabilize the supraparticle. Such a particle-stabilization supports phenomenon, called 'arrested coalescence', is controllable[174, 175] and has been found very useful in both production of more advanced structures, like anisotropic emulsions or particles[176], as

well as triggered release of trapped substances [177], creating a great potential for medical applications.

Furthermore, microfluidic systems are a practical tool for controlled synthesis of polymeric particles of micrometer size. The variety of available shapes and materials that may be employed in the process of their production creates the foundation for a great number of applications. Microparticles of the same kind can be successfully used in studies on self-assembly. Due to their ability of self organization they can form the structures of closely packed crystals displaying potentially usable optical characteristics (light diffraction or photonic band gaps)[178, 179]. The same feature may be used also to obtain better packed column packing[168] or porous materials[175].

Another area of microfluidics' application is food[180-182] and cosmetic[183] industries, where well-defined entities could provide the color or be used for stabilization of the products. Finally they might be used as carriers of substances exhibiting particular properties such as aromas. The same feature makes polymeric particles suitable for medical applications. Such particles could be loaded with active substances[133, 184], what in combination with triggered release[185, 186] could result in obtaining a powerful tool dedicated to drug delivery and targeted therapy.

Equally pertinent is the possibility of encapsulation of microorganisms such as bacteria[8, 187, 188]. Encapsulation of live organisms in polymeric envelopes creates not only the environment for their growth but at the same time provides additional protection from external conditions. Such entities may be used for carrying *e.g*. probiotic cells through the gastro-intestinal tract[6, 189] or for transplantation as encapsulated animal cells[7, 190] are well protected against immune response.

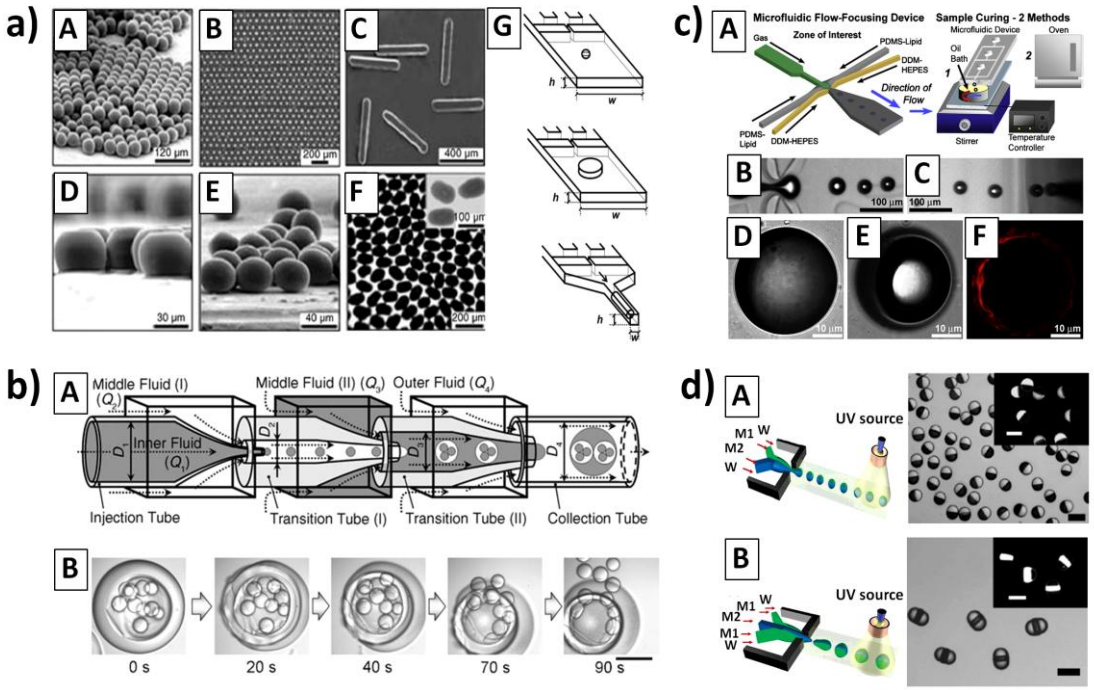

Figure 10. Examples of application of microfluidic devices for preparatory purposes. (**a**) A set of flow focusing architectures[126] (G) dedicated to produce polymeric particles of different shapes[172] (A-F). (**b**) The axisymetric system for formation of multiple emulsions (A) together with an exemplary application of produced entities for the gradual release of their content[11] (B). (**c**) A setup (A) for production (B,C) of hollow particles (D-F)[165]. (**d**) The schemes of the systems for formation of Janus droplets and droplets with ternary structure (on the left) together with microphotographs of obtained particles (on the right)[173] presented in section A and B, respectively.

II.4. Hydrogels – structure and applications

According to the IUPAC definition, the hydrogels (also known as aquagels) are a kind of gel materials containing water as a swelling agent[191]. The characteristic structure of hydrogels is formed out of chains of strongly hydrophilic polymers, which enable retention of considerable quantities of water (even >20%) in their network but at the same time don't undergo dissolution in accumulated solvent.

One of the most relevant consequences resulting from entrapping such an amount of water in the polymeric network is its rubbery, soft consistence, strongly reducing the value of interfacial tension between hydrogel surface and a surrounding aqueous solution. The phenomenon limits adsorption and unfolding of proteins on the surface of the hydrogel. Moreover, the soft consistency prevents from irritating surrounding cells and tissues. This feature strongly enhances, unfortunately does not ensure, the biocompatible character of the material. Furthermore, higher amount of absorbed water causes softness and low durability of the polymer that results in problems with its technical processing[192].

Additionally, presence of pores makes the hydrogel permeable to ions or low molecular weight molecules of biological significance. This could be found both useful and problematic, depending on the application. Controlled release of active substances arrested in the polymeric network as well as diffusion of important molecules through an implant to surrounding tissue seems very advantageous. However, uncontrollable leakage of substances used during fabrication of hydrogel might result in an inflammation or even rejection of applied implant.

It seems that the high content of water makes hydrogels similar to living tissue. This, in turn, together with porous nature of hydrogels provides a great potential of applications of such materials especially in medicine and pharmaceutical industry. All the biomimetic properties of hydrogels make them an advanced material for fabrication of contact lenses, adsorbents, biosensors, burn dressings, artificial organs for implantation, bone ingrowth sponges, coatings for catheters, and many others. Additionally, the discovery of contractible polymers (*e.g.* polyacrylonitrile) has a great potential in development of artificial muscles [193].

Moreover, the sensitivity of some hydrogels to pH[194] or temperature[195] makes them perfect materials for triggering release of active substances. There are four typical ways how medical product is administrated: orally, rectally, vaginally or directly to the skin (in the form of polymerized multiple emulsions). A hydrogel loaded with an active substance has to be well-defined in terms of release criteria in order to ensure the delivery of the drug in a controllable manner.

Hydrogels are usually obtained as a result of conversion of already existing polymers, by forming polyelectrolyte complexes[196] or in the process of cross-linking[197] occurring after introduction of additional agent (*e.g*. metal ions). Applied conditions (volume of water present during polymerization, pH of the solution or concentration of cross-linking agents) affect the properties of fabricated material. The abundance of possible hydrogel properties, deriving from various conditions of polymerization, creates a wide spectrum of potential applications.

Hydrogels cover a wide group of compounds of both natural and synthetic origin. Among synthetic polymers one can find cross-linked dextrans or cross-linked and enzymatically treated collagens, *etc.* while the natural ones include agarose, methylcellulose, hyaluronan, gelatin or even whole group of polysaccharides.

The following subsections focus on two representatives of polysaccharides – alginate and pectins – as due to their character as well as former experience with the materials they were selected as model polymers in the final experiment discussed in the part V. The information included below contains detailed description of these hydrogels and their exemplary applications.

II.4.1. Alginate

The term 'alginate' is usually used for salts of alginic acid (*e.g.* sodium alginate, ammonium alginate, *etc.*) as well as its derivatives or the alginic acid itself. Alginate is a negatively charged polymer that belongs to the group of polysaccharides and is quite abundant in the natural environment. It occurs in the body of brown algae (*Phaeophyceae*, mainly *Laminaria*), constituting up to 40 % of the dry residue. It has been also identified as one of the capsular polysaccharides present on the surface of soil bacteria, *Pseudomonas aeruginosa* and *Azetobacter vinelandi*[198, 199].

Alginate is regarded as a linear binary copolymer composed of so called M and G residues corresponding to (1→4)-linked β-D-mannuronic (pKa 3.38) and α-L-guluronic acids (pKa 3.65), respectively (**Figure 11a**). Such residues may be distributed in the structure of alginate in various ways. They can form covalent bonds between monomers of the same type (M-M or G-G) as well as of different types (M-G) (**Figure 11b**). Additionally, they are present in the polymeric structure as both single insets and whole groups of individual monomer (blocks), creating M-blocs, G-blocks or mixed, MG-blocks (**Figure 11c**).

Moreover, it has been revealed that the ratio of mannuronic to guluronic acids depends on the source of alginate and is frequently correlated with the seasonality as well as geographical region[200, 201]. For instance, the increased amount of G-blocks has been identified in *e.g*. *Laminaria hyperborea*, while the dominance of M-blocks has been observed in *e.g*. *Macrocystis pyrifera*. There has been even isolated a bacterial strain containing alginate composed in 100% out of mannuronic acid[202]. Such a structural diversity may be inconvenient in experiments requiring application of materials of well defined properties.

This is mostly because the ratio of M to G strongly influences the process of gelation. Preparation of hydrogels out of polymers richer in M or G residues results in formation of weaker or stronger gels, respectively[203]. Additionally, light and short molecular chains could reveal poor engagement in formation of gels therefore the tightness of mass dispersion is highly recommended.

The sequence of M and G residues could be determined by high-field NMR-spectroscopy. However, in the commercial alginates, where the structural uniformity is reqired, the tailoring of chains is done by application of mannuronan C-5 epimerase (from bacteria *Azobacter vinelandi*), an enzyme carrying out the reaction of epimerization of M-units into G-units[198, 199]. Alginate is a polyanion therefore its solubility depends on the ionic strength of the solution and its pH.

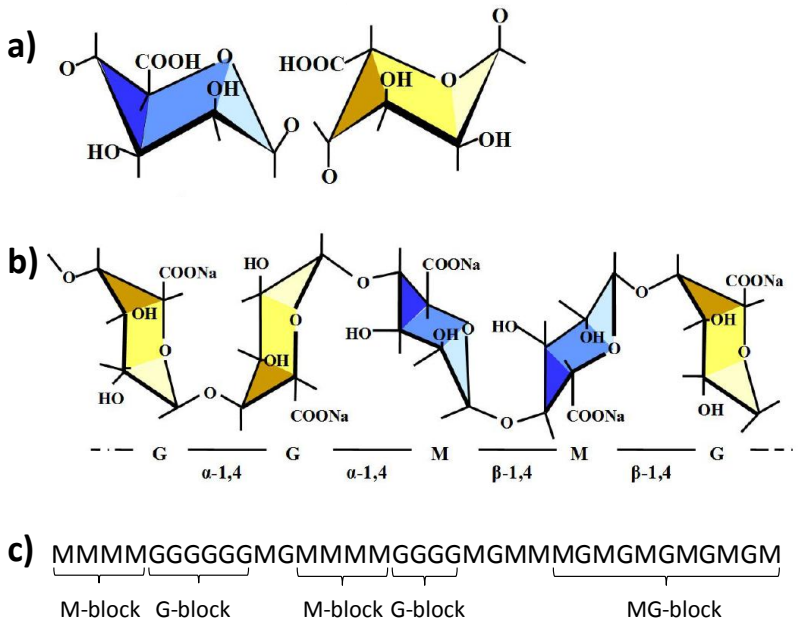

Figure 11. Structure of alginate. **a**) units of alginates structure (β-D-mannuronic acid - blue - and α-L-guluronic acid - yellow), **b**) possibilities of covalent bonding of individual residues, **c**) alginate chain presenting various combinations of monomers linking, including M-M, G-G, M-G, blocks[197].

II.4.1.1. The process of gelation

The formation of gel is one of the most useful features of alginates. This process occurs either at low pH or under influence of polyvalent metal ions such as calcium ions (Ca^{2+}) (**Figure 12**). The low pH promotes formation of hydrogen bonds and results in obtaining of an acidic gel, whereas the addition of a cross-linking agent (metal ion), promotes gelification by capturing the linker by guluronic residues in a specific coordinate bonds (**Figure 12**). The structure and specificity of formed complex was described in 1973 by *Grant et al.* with an 'egg-box model'[204], which has been confirmed by X-ray diffraction by Stokke's group in 2007[205]. There are three most relevant factors that strongly influence the process of gel formulation: i) the geometry of the ligand (length of the chain and the amount of G-blocks in its structure), ii) the separation of the unit charges on the chain, and iii) ability of association of chains. As the subunit G is directly responsible for formation of the ligand-ion complex, the longer the G-sequence (>20xG), the more stable is the cavity for interaction with the linker ion. Under the influence of multivalent ions the polymeric chain adopts zigzag shape in the areas rich in G-block sections and creates characteristic 'pockets' for ion coordination. Such cavities might be formed by both – two separate polymeric chains or one long chain. The kinetics of this process is very fast, resulting in non-uniform gel if direct mixing of polymer and cross-linker is performed.

There are, however, two controllable ways that could be used in order to obtain homogeneous gel material: i) diffusion and ii) internal setting methods. The first method involves applying a water bath enriched with multivalent ions, diffusing through the structure of alginate and subsequently cross-linking the polymeric chains located deeper in alginate solution. The other one is based on mixing the solution of alginate with a poorly soluble salt of multivalent ions (such as $CaCO_3$) dispersed in the solution. The process of gelation is initiated by decreasing the pH, what leads to the release of metal ions from their salt, and formation of complexes with alginic chains.

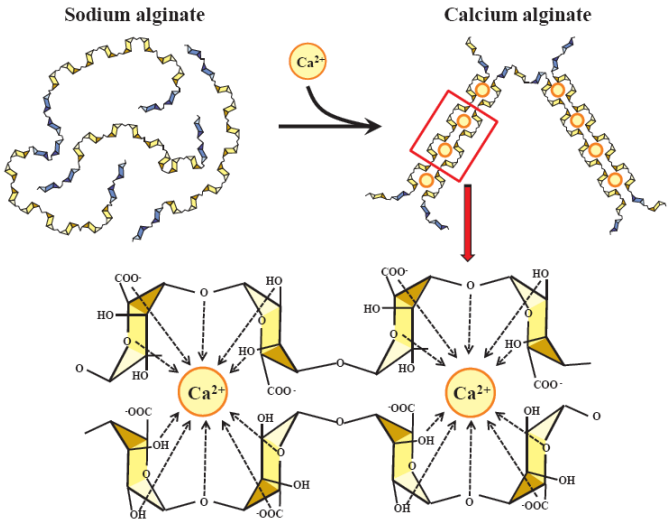

Figure 12. Gelation of alginates. Interaction of chains of sodium alginate with calcium ions and formation of egg-box structure of calcium alginate[197].

II.4.1.2. Alginates in microfluidics

Formulation of alginate gels by means of microfluidic chips gives a great potential for fabrication of entities characterized by high level of uniformity of volumes of droplets at a reasonable throughput. Additionally, such systems provide wide range of options in manipulation with streams of particular ingredients what guaranties even better control over composition of formulated microbeads.

Production of microgels in microchips may be performed in several ways. All of them produce alginate microdroplets inside the system of microchannels but differ in the way of their solidification. The process of gelation might be performed outside or inside microfluidic system.

Gelation outside microfluidic systems is the most basic and thoroughly described method. The procedure is very simple and involves transfer of polymeric droplets formed in the microfluidic network directly into an aqueous solution of salt containing polyvalent metal ions.

This kind of gelation allows avoiding the problem of the gel adhering to the walls of microchannels which may lead to clogging of the system. However, the method causes deformation of microgels shape. Transition of alginate droplets from continuous phase to water bath corresponds to changing surrounding environment from less to more viscous one[206] ('viscosity effect'). In order to improve receiving spherical shape of microgels obtained by this particular method *Capretto et al.*[206] has studied the addition of glycerol into the solution of ions as well as placing a film of continuous phase on the surface of water bath to mitigate the crossing from one environment to another. These attempts resulted in minimization of occurrence of defects in the gels morphology.

At the same time *Hu et al.*[207] have used the 'viscosity effect' to produce different shapes of microgels (**Figure 13**). Additionally, the authors have studied how the 'collecting height effect' affects the final shape of gels and optimized the conditions promoting the formation of particular microgels. According to their observations, spherical gels could be obtained if cross-linking was initiated in the continuous phase. In the series of experiments the authors obtained well specified spectrum of microgels forms. Anisotropic particles present a great potential based on the unique scattering and packing properties[131], as carriers of active substances or as models of some objects they're similar to *e.g.* bacteria or red blood cells (RBC)[169].

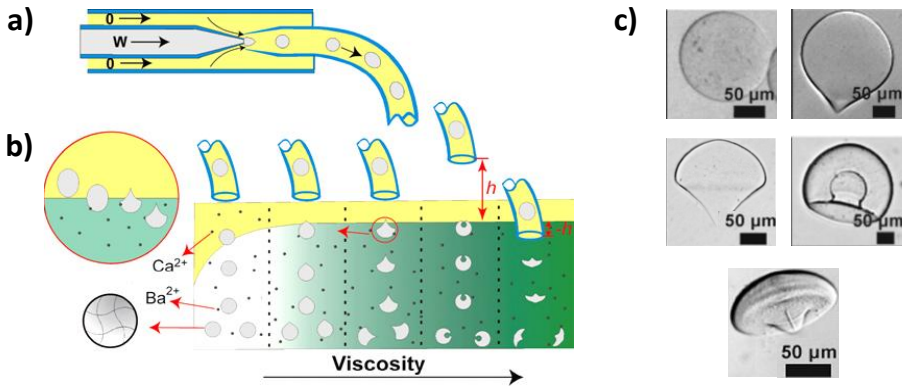

Figure 13. Scheme of microdroplets formation in a co-flow system (a) as well as the influence of viscosity and the 'collecting height effect' on the final shape of microgels (b), and micrographs of gels formed under different conditions (c)[207].

There are two main ways of performing gelation inside microfluidic chips. The process of gelation might have external or internal character. In the first case it occurs by diffusion of metal ions suspended in the continuous phase into the polymeric structure. The process is comparable with the gelation outside microfluidic systems (**Figure 14**). In such method the dispersive phase consisting of alginate interacts with metal ions as early as in the process of

droplet formation and stays in contact with them while flowing through the channel and outlet tubing. This type of gelation does eliminate the problem of obtaining deformed gels but at the same time it is the source of other complications. First of all the external gelation performed inside microfluidic systems involves dissolution of inorganic salts in a non polar continuous phase. *Zhang et al.*[208] have exploited sonification in order to disperse organic salt of calcium (calcium acetate) in the soybean oil (**Figure 14**). The contact of the salt with the aqueous droplet of alginate resulted in dissociation and diffusion of calcium ions into the droplet causing its solidification. In addition, the longer the contact of droplets with the continuous phase, the deeper the ions penetrate the droplet. Therefore the process of gelation can be controlled in time regime. Specific duration of cross-linking may result in gels with only partially solidified core.

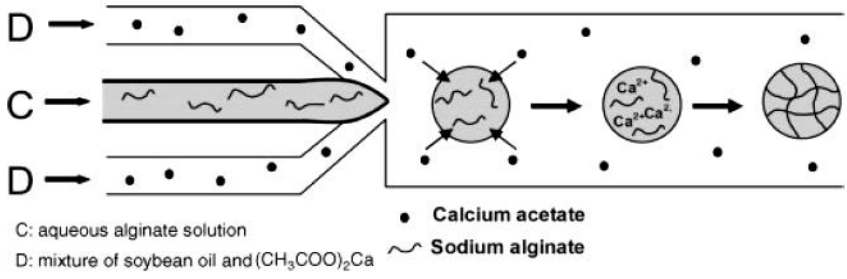

Figure 14. Schematic illustration of formation of droplets by means of flow focusing system and the process of external gelation inside a microfluidic network [208]. The cross-linking agent (Ca^{2+} ions in the form of calcium acetate) is dispersed in the continuous phase (D) and diffuses to the interior of polymeric droplets turning them into gel structures.

The other method of gelation inside a microfluidic system is called internal setting method (**Figure 15**). The method involves dispersion of the cross-linker in the alginate droplet phase in the form of inactive, inorganic salt poorly soluble in water. The metal ions are 'activated' by the diffusion of an activating agent present in the continuous phase to the interior of formed droplet. The triggered release of cross-linker initiates gelation and it proceeds as the droplet moves through the microchannel. *Zhang et al*. [208] have used calcium carbonate as the bounded version of cross-linking agent and soybean oil with acetate acid as the continuous phase. The contact with aqueous phase initiates the diffusion of hydrogen ions into the droplets therefore changing the pH of the inner environment of the droplet and in consequence releasing calcium ions of the salt.

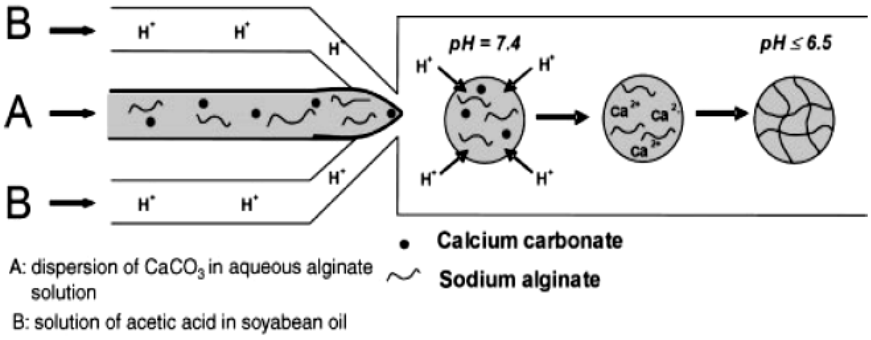

Figure 15. Schematic illustration of formation of droplets by means of flow focusing system and the process of internal gelation inside a microfluidic network [208]. The process of solidification occurs under influence of cross-linking agent (Ca^{2+} ions in the form of calcium carbonate) suspended in the droplet phase (A) and is activated by diffusing hydrogen ions (dispersed in the continuous phase) into the polymeric droplets.

The main problem with the techniques involving gelation inside microfluidic systems is the possibility of gels aggregation resulting in blocking of the microchannels. However, fine tuning the rates of flow of the continuous and the droplet phases can minimize this issue.

In order to increase the effectiveness of formation of alginate gels a combination of internal and external gelation can be performed. The initial gelation is carried out inside microchannels and the cross-linking is then continued in a water bath enriched in multivalent ions. As the surface of polymeric droplets is partially solidified their susceptibility to deformations resulting from transition from continuous phase to water solution where their complete transformation into gels has place[206, 209], and, in turn, allows to avoid the limitation characteristic for typical inside gelation.

II.4.1.3. Applications

Alginates are non toxic and present high biocompatibility. These features predestinate them to be used in food and pharmaceutical industries as well as in medicine. Moreover, their ability to bind multivalent ions, makes them a useful tool to remove heavy metal ions from industrial wastes in the process of biosorption[210].

In the food industry alginates are marked with symbol ‘E’ in accordance with the international codes of food additives (E400 – alginic acid, E401 – sodium alginate, E402 – potassium alginate, E403 – ammonium alginate, E404 – calcium alginate, E405 – propylene glycol alginate) and due to the absence of taste and color they are perfect as additives to the food as emulsifiers, stabilizers, and thickeners.

The ability of alginates to undergo gelation creates a great potential in the area of drug delivery. Additional features of alginates are their susceptibility to swelling under different pH

conditions[194] as well as decomposition in the presence of enzymes digesting uronic acids. Both of the properties might be exploited in the applications involving controlled release. Alginic gels have been also found as a perfect material for encapsulation of enzymes[211], microorganisms[6], and cells[7] or as coating elements of medical equipment. Protection of entrapped entities from the influence of the environment could be particularly useful in transplantation[7]. Moreover, thanks to their ability to absorb moisture alginates are utilized in dressings, creating optimal conditions for healing processes.

II.4.2. Pectin

The name 'pectin' comes from Greek 'pektikos' meaning 'to congeal' or 'solidify' which corresponds with their gelling properties. Pectins are polysaccharides present in the cellular wall of all land plants[212]. They are composed out of sequences partially methyl-esterified (1→4)-linked α-D-galacturonate residues (called 'smooth' regions) responsible for gelation and other sugars as D-xylose, D-glucose, L-rhamnose, L-arabinose, and D-galactose (called 'hairy' regions) deprived of gelling properties (**Figure 16**). While the strength of alginate gels is characterized by M/G ratio, the pectins are described with the degree of estrification (DE) or amidation (DA). Thus pectins are often categorized as low- or high-ester (DE of <50% or >50%, respectively).

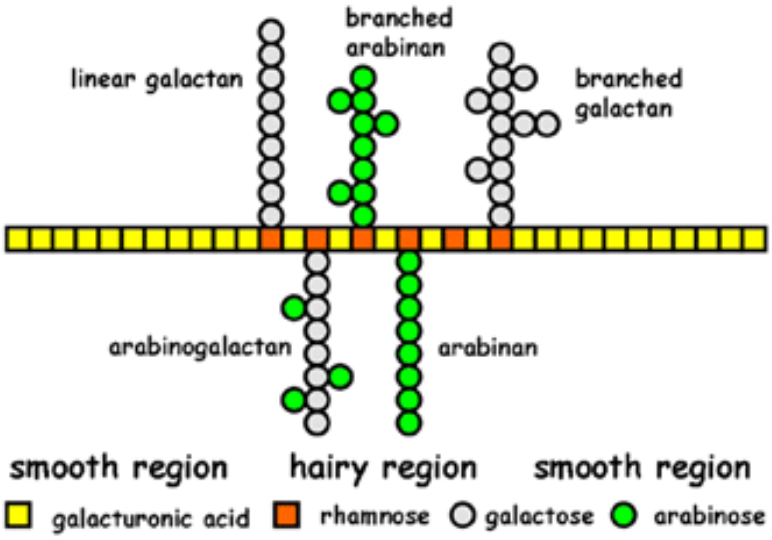

Figure 16. Scheme of a typical structure of pectin built up of 'smooth' regions built up out of methyl-esterified (1→4)-linked α-D-galacturonate residues (yellow squares) and 'hairy' regions consisting of other sugars such as L-hamnose (red squares), D-galactose (white circles) and L-arabinose (green circles)[213].

II.4.2.1. The process of gelation

Gelation of pectins depends on the type of the pectin (its DE and DA), pH, temperature and the concentration of cross-linker. It occurs when (1→4)-linked α-D-galacturonate residues are cross-linked in order to form three dimensional network suitable for entrapment of water and other entities. The mechanism of gelation might proceed in two ways depending on the level of methylation. In high-ester pectins junction zones are formed by cross-linking homogalacturonate chains by hydrogen bridges and hydrophobic forces between metoxyl groups while in low-ester pectins such junctions are produced by calcium ions cross-linking between free carboxyl groups of different chains in accordance to previously described 'egg-box' model[214, 215]

II.4.2.2. Pectins in microfluidic

Despite the fact that pectins are well characterized and their properties are noteworthy, there are very few reports considering their use in microfluidic systems. Fang and Cathala have presented formation of pectin hydrogels carrying out gelation inside a microfluidic chip. The stream of the pectin droplet phase was merged with an additional stream containing cross-linking agent (Ca^{2+}). The process of gelation occurred in winding channels while mixing the components of the droplet, what resulted in reasonably monodisperse gels[216].

Internal gelation has been performed by another group, which has proposed a flow focusing microfluidic device dedicated to formation of Janus particles, further subjected to enzymatic hydrolysis[217]. The first stage of preparation involved formation of droplets out of two streams of aqueous solutions of pectin combined at the junction in such a way that the interface between them could be preserved. Additionally, both streams contained cross-linker suspended in their volume in the form of calcium carbonate. Calcium ions were released in contact with the continuous phase containing acetic acid supplied to the system through two extra microchannels located downstream.

There has also been an attempt to combine the external gelation inside a microchannel with a solidification outside the system. The authors have thoroughly investigated the influence of various factors (concentration of calcium ions, concentration of acid or time of gelation) on the process of gelation and slow release of gold nanoparticles from pectin microgels[218]. The application of the continuous phase enriched in acetic acid and suspension of calcium carbonate created the source of cross-linking agent and initiated on-chip gelation, which was continued in the same solution outside the system. The three cited reports are the only examples describing the process of gel formation with the use of pure pectin. The remaining studies are based on blends of polymers.

II.4.2.3. Applications

The capacity for gelation, in combination with non-toxicity and biodegradability make them – similarly to alginates –applicable as food additives, that are marked with E440 (E440a (i): pectin, E440a (ii) – sodium pectinate, E440a (iii) – potassium pectinate, E440a (iv) – ammonium pectinate, E440b – amidated pectin). Their ubiquity in natural products and non toxicity put them on the list of compounds of unlimited consumption.

Moreover, pectins are a vital element of the diet as they are known for their beneficial influence on human's health. They reduce the level of cholesterol, perform regulatory functions in small intestine, and even present an anticancer effect. Furthermore, pectins reveal high resistance to proteases as well as amylases – enzymes present in the upper part of human's digestive tract. It means that they are not digested until intestine, where pectidases are present. This feature together with their gelling properties makes them a very attractive material for encapsulation. Very promising is the enclosing of medicines[12] in particular the ones designed for treatment of colon cancer[219]. Pectin gels could also be used in gene delivery[220] or as carriers of probiotics, protecting them from the external environment on their way to intestine[6]

II.4.3. Pectin-alginate blends

Miscellaneous members of polysaccharides' family might be mixed together in order to form synergistic gels. The properties of such arrangements strongly depend on the character of the compounds they originate from. However, the blends often reveal features that are neither sum nor exclusion of individual properties of the components. They are rather specific[221] and do not have unequivocal explanation. This type of mixtures might present different size of pores[222] or undergo gelation under conditions that are not specific for the solution of particular polymers.

This phenomenon is observed also in alginate-pectin blends. Both polymers originally demonstrate differences in the water permeability, stiffness, conditions that promote their degradation, *etc.*, while their combinations exhibit yet another character. Behavior of mixed gels has been examined under variety of values of pH, temperature, *etc*.[221]. The characterization of films formed of alginate-pectin blends has been performed mainly by TEM or SEM[221] and the kinetics of gel formation as well as gel characteristics has been studied by oscillatory measurements.

According to the literature, the strongest alginate-pectin gels are formed of alginate rich in G-block regions and high-methylated pectin, at low values of pH. This feature indicates strong interactions between hydroxy groups of guluronic acid present in alginate and methoxy groups located in pectin chain[223]. Due to the specific properties of the synergistic compositions

they are often exploited for production of membranes or films (potentially useful in food and pharmaceutical industries) and gel beads that might be applied in drug delivery or entrapment of microorganisms.

For instance, *Sandoval-Castilla et al*. have investigated the influence of the composition of synergistic gels on the survival of probiotics and have proven that the alginate to pectin ratio in binary blends affects the shape as well as textural properties of microbeads, thus it can provide variable level of protection for microorganisms against unfavorable environmental factors *e.g.* gastric acids or bile salts[224]. Similar observations has been made by another group, which additionally studied the impact of chitosan coating on mass transfer and reproduction of poultry probiotic cells[6].

The influence of alginate to pectin ratio is relevant when it comes to investigation concerning entrapment of drugs. In the conditions typical for *in-vivo* experiments, the degradation time of alginate-pectin gel is strongly dependant on its composition. *Pillay et al*.[225] have produced several sets of pellets, each at different alginate to pectin ratios, and investigated the process of release of model active substance from the structure of the gel particles. The pellets were produced in reproducible manner, however with variable physical properties, geometry, swelling and release behavior.

Jaya et al. have introduced a method of microgels production using solutions of different alginate to pectin ratio. In the developed protocol a stream of mixed polysaccharides with additional amount of drug is divided into droplets by gaseous phase after going through an encapsulation nozzle and then undergoes gelation based on the internal method[226]. Formulated gels containing pharmaceuticals exhibit different profile of drug release depending on the composition of the bead. Their observations have confirmed the former reports on the relationship between the gel properties and its composition. This knowledge is potentially useful when searching for a natural material with specific parameters applicable in medicine or pharmacy.

III. The aim of the work

The main idea of presented thesis was the development of inexpensive and easy to operate microfluidic system suitable for simultaneous formation of streams of droplets with variable content. Moreover, the obtained chip, ought to be not only well defined by design but also unaffected by the viscosity of used fluids, in contrast to other gradient generating systems described in detail in the **Introduction** part (see subsection **II.2.3.**). This involved elimination of parts of architecture based on laminar flow typically applied for gradient formation[75-82].

First of all, my project involved the development of the most convenient and least invasive methodology of obtaining the device and then the optimization of its operation parameters. The low invasiveness of the method was specified on the basis of investigation of its influence on the shape of cross-section and level of wettability. Additionally, the applicability of the obtained device was demonstrated, by using it for production of microgels carrying model active substance (nanoparticles of gold).

According to the literature, production of polymeric microparticles and microgels is of great interest when it comes to practical applications in numerous fields. The variety of shapes and properties of such entities have made them an attractive material for *e.g.* experiments dedicated to self assembly. Their ability of self organization results in formation of structures of closely packed crystals displaying potentially usable optical characteristics (light diffraction or photonic band gaps)[178, 179]. Moreover, the anisotropic particles might be useful in new materials technologies due to their unique scattering and packing properties[168]. The diversity of shapes of microparticles and their similarity to some objects make them applicable as models of *e.g.* bacteria or red blood cells (RBC)[169]. Furthermore, the specific shape of particles influences their transport through membranes and their decomposition under certain conditions[170, 171]. High biocompatibility and biodegradability of microparticles additionally extends the scope of their potential applications. The hydrogels studied in the thesis have been found so far as a perfect material for encapsulation of drugs[211], enzymes[211], microorganisms[6] or even cells[7]. Protection of entrapped entities from the influence of environment could be particularly useful in transplantation[7].

Applications of pharmaceutical and medical nature usually require high throughput techniques in order to produce particles with satisfying rate. Although, there is a great number of microfluidic chips devoted to high throughput production of polymeric particles[111], a system that would allow for simultaneous formation of numerous streams of monodisperse droplets with well defined spectrum of their content may be very useful. Additionally, production of

microparticles in a reproducible manner, independently of the viscosity of mixed fluids would be even more profitable.

The systems I was interested in combine all aforesaid features, that is: low cost, high throughput production of parallel streams of uniform polymeric particles, and their well defined content. Such systems can become particularly useful for profiling the slow release processes, which in turn will make them an important tool in pharmaceutical, cosmetic or food industries.

IV. Materials and methods

IV.1. Chemicals

- 2-Propanol, 99,7 % p.a. (Chempur, Poland)
- Acetic acid (CH_3COOH), 99,5-99,9 % p.a. (Chempur, Poland)
- Acetone (CH_3COCH_3) (**MMK**), 99,5 % p.a. (Chempur, Poland)
- Alginate sodium salt (Danisco, Poland)
- Calcium Carbonate ($CaCO_3$), p.a. (Chempur, Poland)
- Calcium Chloride ($CaCl_2$), p.a. (Chempur, Poland)
- Dichloromethane (CH_2Cl_2) (**DCM**), 99,8 % p.a. (Chempur, Poland)
- Deionized water (H_2O) (Milipore)
- Dodecylamine (**DDA**), 99 % p.a. (Sigma-Aldrich, Germany)
- Glycerol, 99,5 % p.a. (Chempur, Poland)
- Gold nanoparticles (3 mg/mL) (prepared in accordance with the methodology introduced by *Jana et al.*[227])
- Hydrochloric acid (HCl), 35-38% p.a. (Chempur, Poland)
- Ink (Quink, Parker Washable Blue)
- Ink (Encre Rouge, Waterman, France)
- Methyl ethyl ketone (**MEK**), 99,8 % p.a. (Loba Chemie, Austria)
- n-Hexadecane, 95 % (Alfa Aesar, Germany)
- Pectin (NECJ A2 'Medium sensitivity to calcium ions', Pektowin, Poland)
- Sorbitan oleate (**Span80**) (Sigma-Aldrich, Germany)
- Rapeseed oil, Kujawski (ZT Kruszwica, Poland)

IV.2. Fabrication of microfluidic systems

Fabrication of microfluidic devices begins with preparation of the design in a graphic software (**Figure 17**). All of my devices comprised three layers. Two of the layers were equipped with separate networks of microchannels dedicated to delivery of fluids, while the third one contained a set of through-holes to connect the channels of the outer layers with each other.

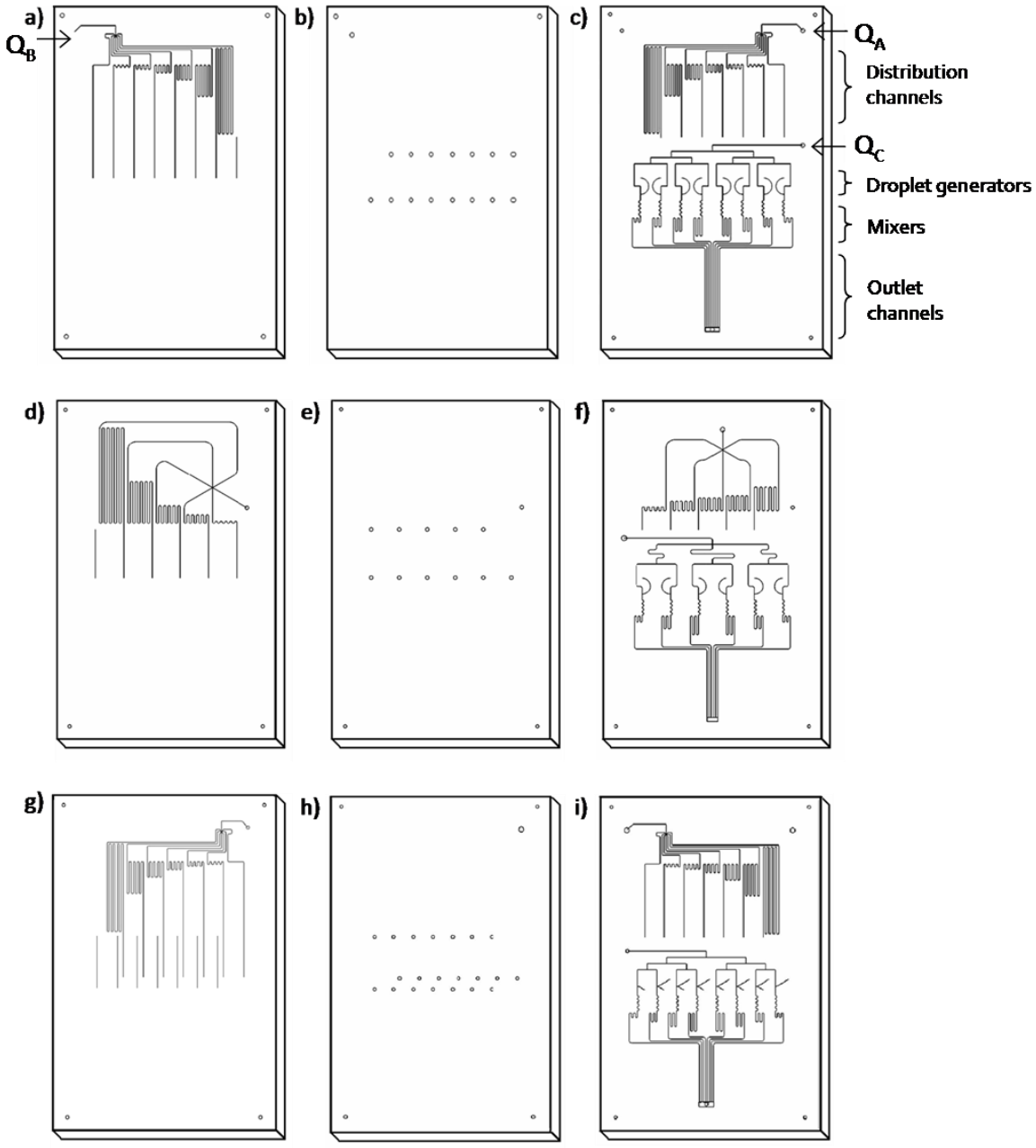

Figure 17 The layouts of the elements of linear (upper set of schematics – (a), (b), (c)), logarithmic (middle set – (d), (e), (f)) gradient generators and system dedicated to application of fluids of different viscosity (lower set – (g), (h), (i)). Top layer (a, d, g) as well as bottom layer (c, f, i) comprise network of channels while the inner layer (b, e, h) is equipped with through-holes to provide connection of the top layer with the bottom one. Each system incorporates three input streams – two for the droplet phase and one for the continuous phase – as well as set of microchannels responsible for gradient generation, a network for propagation of the continuous phase, a series of droplet generators, followed by the meanders facilitating mixing, and outlet channels at the end.

IV.2.1. Process of milling

The chips were fabricated via CNC micro milling (MSG4025, ErgWind, Poland) on the basis of formerly prepared design (**Figure 17**). Each of my microchips comprised three layers of

polycarbonate (Macrolon®, Bayer), two of which (2 mm thick) contained networks of microchannels (of uniform cross section 200 x 200 μm (±10 μm)), while the third one (1 mm thick) – through-holes for connection of the other two.

The milling machine was also used to remove 100 μm deep layer of the polymer from the polycarbonate substrates in order to compare behavior of the both external and bulk material in the presence of the solvent vapors (see subsection **V.1.1.2.**).

IV.2.2. Bonding

The elaborated procedure of bonding involved: cleaning the milled slabs, swelling the surface layer of PC with vapors of dichloromethane (DCM) [228] and bonding the three layers together using registering pins after and compression (0.2 MPa) of the plates at 130 ^{o}C for half an hour.

All procedures involving application of stable temperature while swelling the PC slabs, were performed with the use of a water bath, stabilized on the magnetic stirrer with the hotplate (IKA® RCT Basic) and monitored with the thermocouple (CZAKI® Thermo-Product).

IV.2.3. Modification of microchannels' surface

The devices used for the formation of a gradient of concentration with liquids of different viscosities were additionally modified with dodecylamine to minimize wetting effect. In the modification process I used syringe pumps and a thermostat (ED3, Julabo, Germany). The surface of microchannels was flushed with 5 % solution of DDA in ethanol (at flow rate of2 mL h^{-1} per each microchannel). During the operation the chip was placed in the thermostat (60 ^{0}C). The solution was removed from the channels by means of compressed air. Next, the channels were washed using isopropanol (at flow rate of 4 mL h^{-1}) at room temperature for 0.5 h. Finally, the microchannels were dried using air[35].

IV.2.4. Solution of glycerol

I used deionized water (Milipore) to prepare 62 % w/w solution of glycerol (Chempur, Poland) that was further applied as an input stream of the droplet phase. The viscosity of the applied solution of glycerol was 10 times higher than of water.

IV.2.5. Solution of ink

I used deionized water (Milipore) to prepare 15 % w/w solution of ink (Quink, Parker Washable Blue or Encre Rouge, Waterman, France). I dissolved proper amount of the ink in deionized water and applied the mixture as an input stream of the droplet phase.

IV.2.6. Solutions of hydrogels with and without gold nanoparticles

I prepared 1 % w/w solution of sodium alginate by dissolution of suitable amount in deionized water (Milipore), mixed it until obtaining homogenious solution, and applied it as the droplet phase. In order to obtain 1 % solution of sodium alginate containing gold nanoparticles I prepared 1.5 % solution of sodium alginate in deionized water analogically and then I added appropriate amount of gold nanoparticles suspension to dilute 1.5 % solution of sodium alginate to 1 %. I used the obtained solution as the droplet phase.

I order to obtain 1 % w/w solution of pectin I dissolve appropriate amount of the pectin powder in deionized water (Milipore). I prepared the 1 % solution of pectin with gold nanoparticles by diluting 1.5 % solution of pectin in deionized water with gold nanoparticles suspension.

IV.2.7. Fluids used as a continuous phase

I prepared the solution of the continuous phase by dissolution of 2% w/w of sorbitan oleate (Span80) (Sigma-Aldrich, Germany) in hexadecane (Alpha Aesar, Germany) and filtered with polyethylene terephthalate syringe filters with 45 µm sized pores (PET 45/25, CHROMAFIL Xtra). In the experiment dedicated to production of microparticles I used rapeseed oil (Kujawski, ZT Kruszwica, Poland) without any additives.

IV.2.8. Biphasic bath for the external gelation

In order to turn alginate-pectin emulsions into microgels I prepared biphasic bath. The bottom layer consisted of aqueous solution of calcium chloride (1 M, $CaCl_2$). The top layer comprised 0.5 % w/w calcium carbonate ($CaCO_3$) and 5 % w/w of acetic acid (CH_3COOH). In the first stage I dissolved certain amount of calcium carbonate in adequate volume of acetic acid and then the mixture was suspended in rapeseed oil using ultrasounds. I chose the procedure as the most efficient, on basis of the studies conducted by *Ogończyk et al.*[218] on the optimal conditions for gelation of pectins.

IV.2.9. Purification of microparticles

The procedure of purification of microparticles involved: i) removing of both oil and aqueous layers from above the microgels, ii) transfering of the microgels to a clean reservoir, iii) washing 5 times with fresh, 10 mL portion of deionized water. After the last rinsing I transferred the microgels to a funnel with a filter to remove the excess of water. However, at no time the microgels were allowed do dry and I used them in that form to conduct the release studies.

IV.2.10. Experimental set up

The experimental set up consisted of three parts: the first one responsible for supplying the system with fluids, another essential for the image recording and processing, and finally - the device itself. In the experiments engaging fluids of the same viscosity, I used syringe pumps (Harvard Apparatus, PHD2000) to provide all liquids, whereas in the experiments with liquids of different viscosities, I used a set of reducing valves and capillaries to control the the flow rates of the infused fluids (Q) by adjusting the values of the applied pressure (p). I established the relationship between Q and p during a calibration process, what allowed me to determine Q from the value of applied p. I changed the length of the capillaries to preserve a constant ratio (1:1) of the infused fluids creating the droplet phase[229]. To acquire videos that I subsequently analyzed with a MatLab routine, I used a stereoscope (Nikon SMZ1500) equipped with a fast camera (Photron 1024).

V. Results

The first part of the following section presents fabrication of microfluidic systems made of polycarbonate, where the particular emphasis is put on the process of bonding as a crucial stage of preparation of the chip. Subsequent sections are focused on: i) the mathematical fundamentals of generation of gradients by fabricated devices, that guaranties maintaining the gradient of concentrations regardless to the differences in viscosity of applied fluids, ii) the characterization of their working range, iii) the correlation between the designed and experimentally determined gradient of concentration, and iv) the quality of produced emulsions, most importantly the level of the volume distribution. The last issue raised in this part concerns the practical application of the designed devices. It describes simultaneous formation of hydrogel droplets consisting of different at variable ratio of pectin to alginate, followed by solidification in the bath containing the cross-linker (Ca^{2+}) and the slow release of gold nanoparticles entrapped in their structure.

V.1. Chemical bonding of microfluidic devices

In the next subsections I describe the process of developing the methodology for bonding microfluidic systems made of polycarbonate (PC). The choice of material was a result of compromise between its price, resistance to chemistry and its processability. Moreover, due to the complexity of target system, application of stiff polymer was required. The availability of milling machine and the perspective of development of methodologies referred to surface modification of PC made this material suitable to my experiment.

V.1.1. Optimization of parameters of chemical bonding

I developed the procedure of bonding of polycarbonate slabs directly for dichloromethane (DCM), a substance used in the industry as an excellent PC solvent. Additionally, some supplementary experiments were performed in order to show the applicability of the established methodology to two other solvents: methyl ethyl ketone (MEK) and acetone (MMK).Both of the substances are often considered as non-solvent of PC as they are responsible only for swelling the top layer of the polymer.

All of the applied substances exhibit reasonable stability in the examined temperatures (20-30 ^{o}C) and neither of them come into chemical reaction with the PCs. These are most desired properties, allowing for reproducible interactions with the PCs and avoidance of side effects. In the process of optimization of bonding, I performed the characterization of swelling

the surface layer of PC with DCM as well as the influence of pressure and temperature applied while press-welding. The other optimized factors were the volume of the solvent, time of exposure to the solvent vapors, the temperature and the thickness of modified layer.

In order to provide reproducibility of the procedure I proposed a setup that guaranties uniform distribution of vapors around modified slabs and fine control of other conditions such as vacuum or volume of the solvent. The setup consisted of: a round bottom flask (50 mL) as a container for the solvent, a glass desiccator (263 D K^{-1}, Simax, Czech Republic, of internal volume of approximately 5.5 L) as a chamber for modification and a vacuum pump (V-700, Buchi, Switzerland) (**Figure 18**). The procedure comprised three stages: i) placing PC slabs in the desiccator, ii) evacuating the air from the desiccator to 10 mbar and iii) connecting the desiccator to the flask filled with fiven amount of the solvent. The homogenous distribution of vapors is achieved by introducing a magnetic stirrer to the desiccator.

According to the observations the pressure inside the desiccator, after the evaporation of the solvent, seems to be roughly proportional to the volume of the solvent. For instance, 1 mL of DCM produces the pressure of 90 mbar, while 2 mL of DCM – 160 mbar.

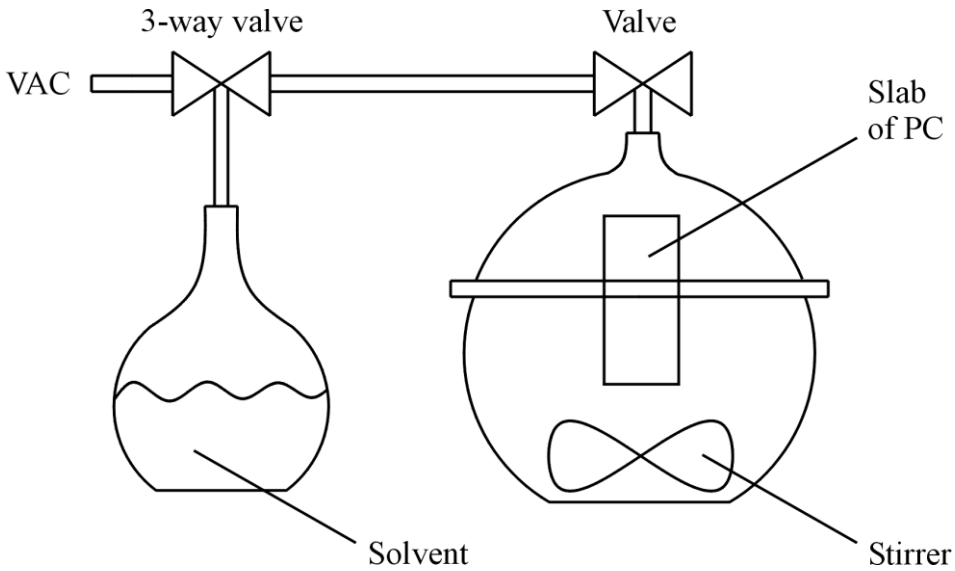

Figure 18. The experimental setup dedicated to swelling PC surface in the vapors of different solvents. It comprises a vacuum pump (VAC), a desiccator (where PC slab is placed), a flask with the solvent and a stirrer for better distribution of vapors inside the desiccator.

V.1.1.1. Volume of the solvent

During the search for optimal conditions of bonding PC by its modification in the vapors of the solvent, I noticed that the thickness (*d*) of the layer of swollen polymer was of the crucial meaning when it came to bonding. For the thin layer (*d* ≤15 μm) the bonding is either

ineffective or weak enough to be easily broken with bear hands. On the other hand the layer thicker than ~30 µm promotes deformation of the geometry of microchannels due to much softer and elastic structure of swollen. Application of high pressure required for press welding leads to substantial damage of the microfluidic architecture.

The layer of swollen PC turned out to be strongly dependent on the volume of used solvent. In order to provide more specific information on the process of penetration of PC by the solvent I designed a series of tests using PC plates of different thicknesses (0.75, 2, 5 mm.) and sizes. The material was exposed for 30 minutes to different volumes of the solvent (1, 2, 4, 6, 8, and 10 mL). As the modified region might be successfully visualized with an optical microscopy the test resulted in a set of micrographs, which provided profiles of the swollen layer (*d*) that were dependent on the volume of used solvent. The **Figure 19** presents a set of micrographs that illustrate the influence of the volume of DCM on the penetration of the PC. On the basis of a collection of such micrographs I measured the thickness of the swollen layer twice for all outer edges, recording 16 values for each plate. I calculated parameter *d* as a mean value of the 16 measurements.

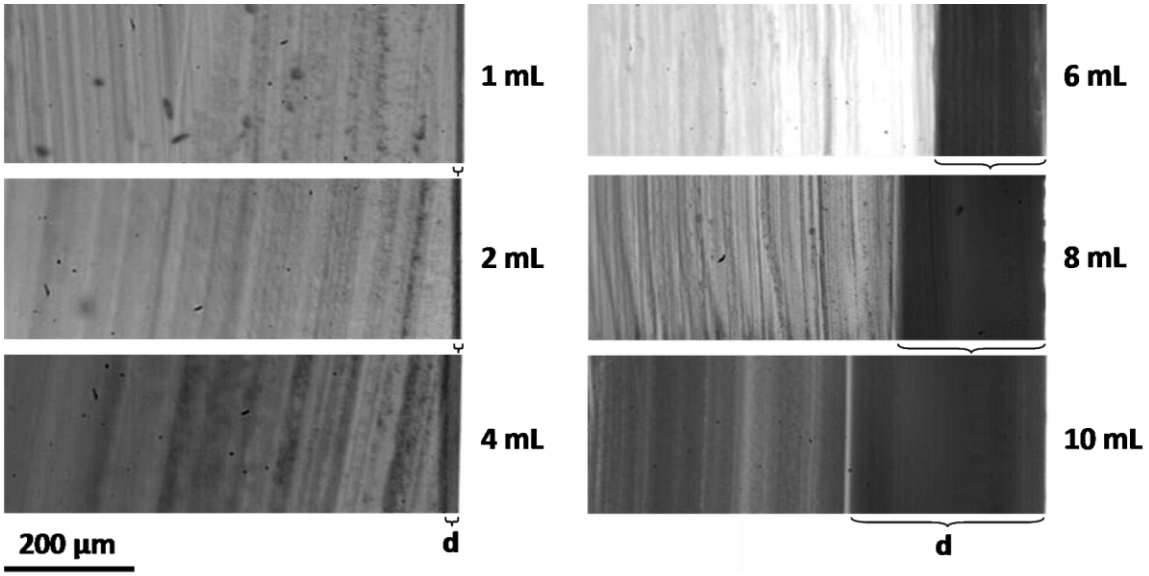

Figure 19. A set of micrographs illustrating the thickness of swollen layer of PC slabs exposed to different volumes of the solvent (*V*: 1, 2, 4, 6, 8, 10 mL). The depth of penetration of PC by the solvent is marked as *d*.

Collected results are presented in the form of a graph illustrating dependency of the mean thickness of modified layer from the volume of applied solvent (**Figure 20**). According to the graph the penetration of the polymer initially is not affected by the volume of the solvent as *e.g.* the volumes from 1 to 4 mL yield reproducibly *d* ~ 20 µm. However, after exceeding the volume of 4 mL, a drastic increase of the size of swollen layer is observed. Furthermore, I

discovered that *d* did not depend on the surface area of the slabs subjected to modification. A slight effect of the plates thickness on the size of swollen layer was observed, however no accurate explanation of the phenomenon could be presented.

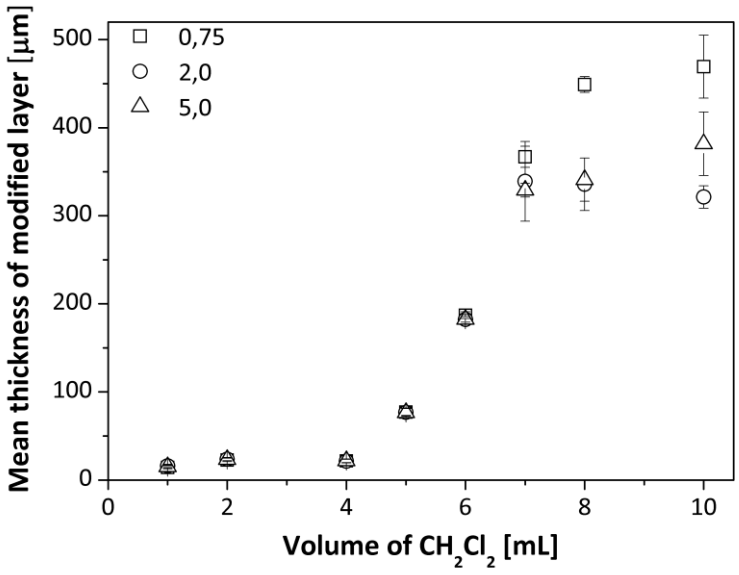

Figure 20. Effect of the volume of dichloromethane on the observed size of the swollen layer of the polymer of plate thickness: 0.75 mm (squares), 2 mm (circles) and 5 mm (triangles). The time of exposure was fixed at 30 min. The depth of penetration was measured at sixteen different points on each slab.

In general, the main reason for observed effects might be associated with slight differences in the composition of polycarbonate that concern both the surface and the bulk. Nevertheless, according to the results the influence of the volume of DCM on d is significant, and thus it is critical to choose the correct amount of the solvent for the procedure. Considering the minimal effective bonding was obtained for $d \sim 20$ µm, further experiments concerning characterization of the bonding procedure were performed for the solvent volume equal 1 mL.

V.1.1.2. Temperature

The process of evaporation of the solvent is rapid as well as strongly endothermic, and it causes sudden drop of temperature of the flask containing evaporating liquid. I conducted a set of experiments in order to investigate whether the temperature of water bath destined for stabilization of the solvent's temperature while evaporation has any influence on the swelling process on the thickness of modified layer. Regarding possible differences in the composition between the surface of PC slabs and the bulk material I carried out a test for both the outer surface of the plates as well as at 100 µm below the surface. The experiment was conducted at several temperature points (22, 25, 28, and 30 ^{o}C) with the set described in the subsection **IV.2.2.**, and at constant volume of the solvent (1mL).

The inner surface was obtained by milling off 100 µm layer of the PC. The thickness of the removed layer was chosen on the basis of previously determine*d* profile of the swollen polymer. The depth of swollen layer (*d*) is approximately constant in the range of 1-4 mL of solvent (*d* ~ 20 µm). This might suggest the presence of additional layer that inhibits the penetration of the material if smaller volumes of the solvent are used. The removal of 100 µm deep layer was assumed to be sufficient to reach the bulk material as it exceeded the 'critical' value of *d* five times.

Obtained results reveal lack of any specific influence of the temperature of the water bath on *d*, what is illustrated in the **Figure 21**. Nevertheless, they clearly indicate differences of up to 15 µm in the obtained value of *d*, between the material bulk and its surface.

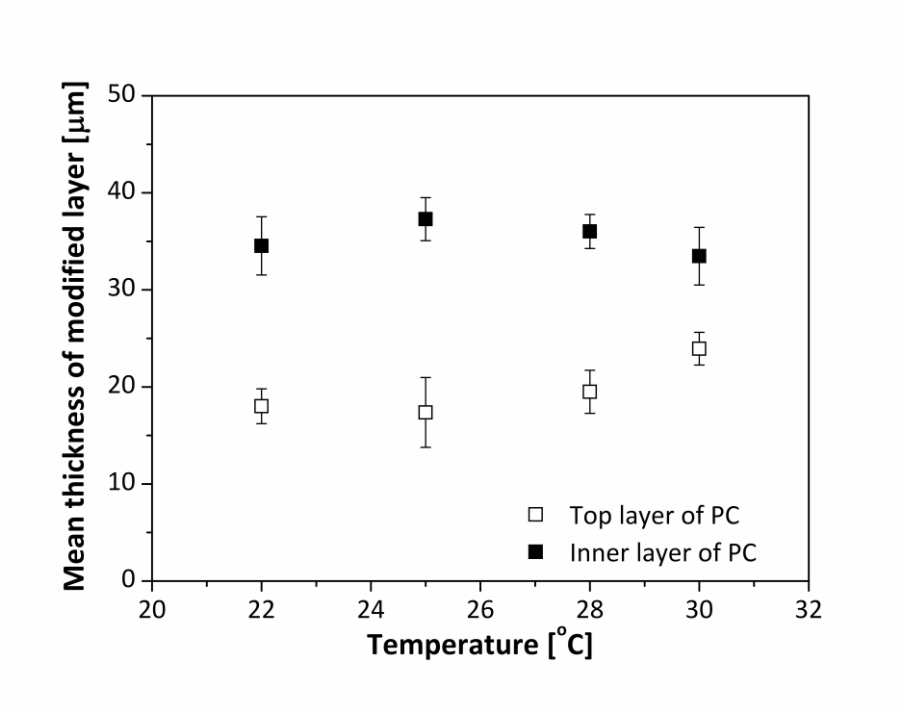

Figure 21. The dependence of the mean thickness of modified layer (*d*) from the temperature of water bath applied during evaporation 1mL of the solvent, in the case of both top layer (empty squares) and bulk material (solid squares).

V.1.1.3. Time of exposure to the vapors

I employed the thickness of swollen layer (*d*) as a parameter for characterization of kinetics of diffusion as a function of time of exposure to the vapors of DCM, MEK and MKK. I analyzed the images obtained in the same manner as in the section **V.1.1.1.** for different times of exposure (up to 250 minutes for DCM and 40 minutes for MEK and MKK). The PC plates were in contact with vapors produced out of 1 mL of swelling agent.

According to the specification of the material, the surface of the used PC sheets should be deprived of any protective layers. However, the analysis of the results from the former section might suggest the presence of protection of some kind. In order to compare the behavior of 'inner' and 'outer' PC in vapors of the swelling agents, plates in dimensions of 20 x 10 x 2 mm were prepared and partially devoid of a layer of ~100 μm from the surface.

The results obtained for DCM revealed the same relationship between the time of exposure and the thickness of modified layer for both external and bulk material. Nevertheless, the values of *d* obtained for the bulk PC were ~15 μm deeper in comparison to the external material (**Figure 22**).

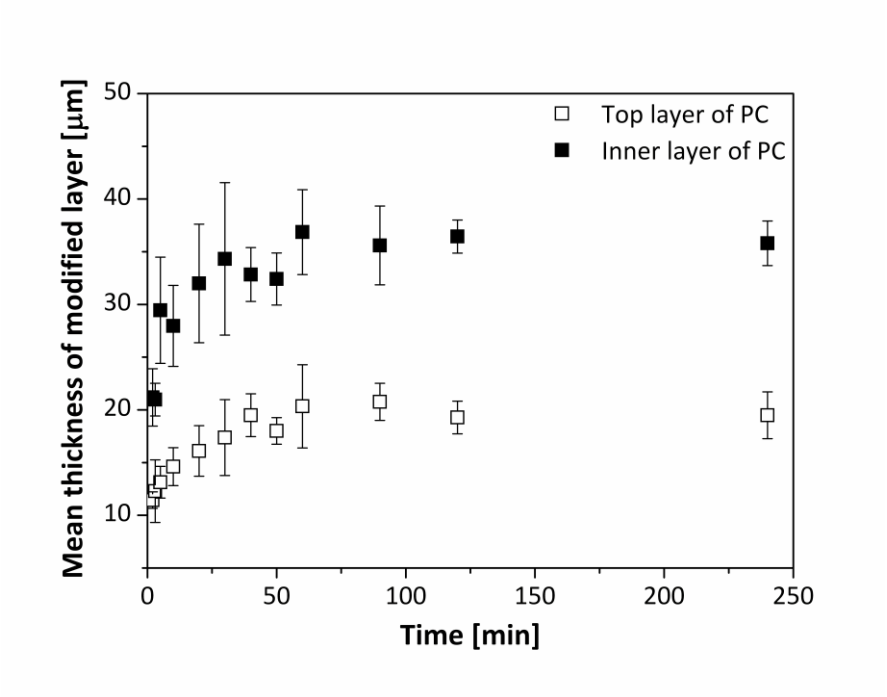

Figure 22. Plots obtained for the thickness of modified layer vs. time of exposure to the solvent vapors in the case of both top layer (empty squares) and bulk material (solid squares). Exposure of slabs with a layer of ~100 µm milled off results in a qualitatively similar profile yet the depth of penetration was by ~15 µm higher than for the unmodified slabs exposed to the vapors.

In accordance with obtained results, the first 30-40 minutes are crucial for the swelling process and for longer times of exposure, the penetrations reaches plateau. On the basis of this observation I exposed the PC slabs without external layer removed to the vapors of the other two swelling agents – MEK and MKK – for 40 minutes. Analyzed data suggest that the control of the *d* value is possible by adjusting the time of exposure (**Figure 23**). Additionally, the profile *d*(t) for MEK and MKK roughly corresponds to the one obtained for DCM. The only difference is intensity of interaction of the solvents with the material. Both MEK and MKK reveal more invasive character than DCM as they present higher capability to penetrate the PC (*e.g.* at t = 20 min., *d* produced by MEK or MKK is ~10 µm deeper than the one obtained with DCM). Moreover, the results of the experiment imply that the changes of thickness of modified layer over time [*d*(t)] cannot derive from simple diffusion and point to a more complicated process characterized by an exponentially saturating function[230].

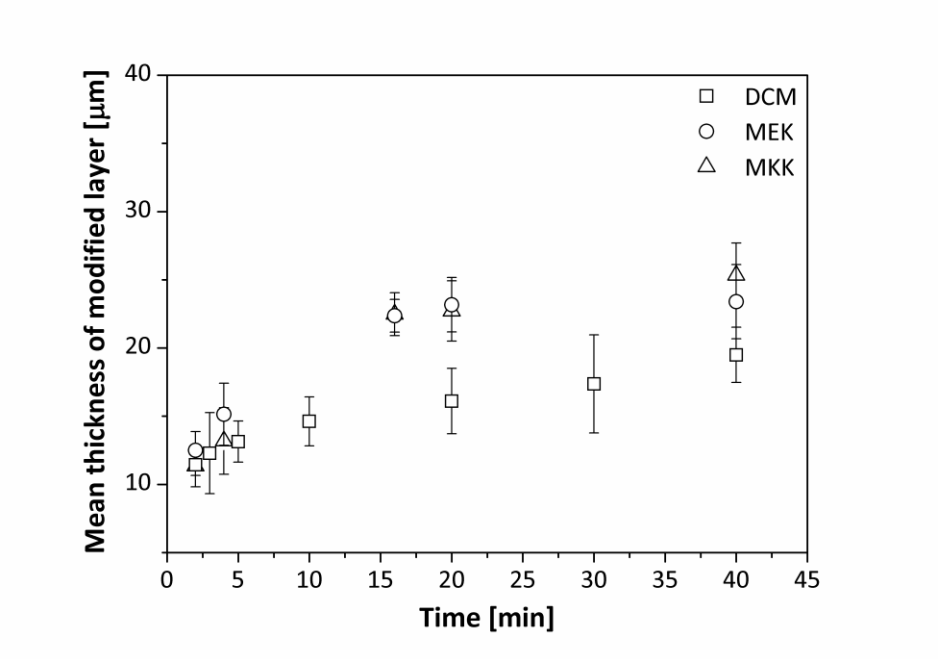

Figure 23. Presentation of the dependence of *d* on time of exposure of the slabs to vapors of DCM, MEK and MMK.

In order to verify the presence of a protective coating on the surface of PC I used X-ray Photoelectron Spectroscopy (XPS) dedicated to the determination of elemental composition of the surface and the bulk material (where the top layer of ~100 μm was milled off as in previous experiments). The measurements were performed with the use of VG Scientific photoelectron spectrometer ESCALAB-210 and A1 Ka radiation (1486.6 eV) from X-ray source operating at 15 kV and 20 mA. The spectra show slight differences in the percentage of all elements present in the PC, particularly silicone (Si) (**Figure 24**). The measurements revealed that the amount of silicone is almost six times higher in the bulk material than in the surface layer. This, in turn, might influence the process of penetration of the material by the swelling agent, observed as deeper penetration of the slabs deprived of outer layer.

As the composition of PC slabs from different manufacturers may vary, I note that application of my procedure to material of different type or origin might require a recalibration of *d*(t).

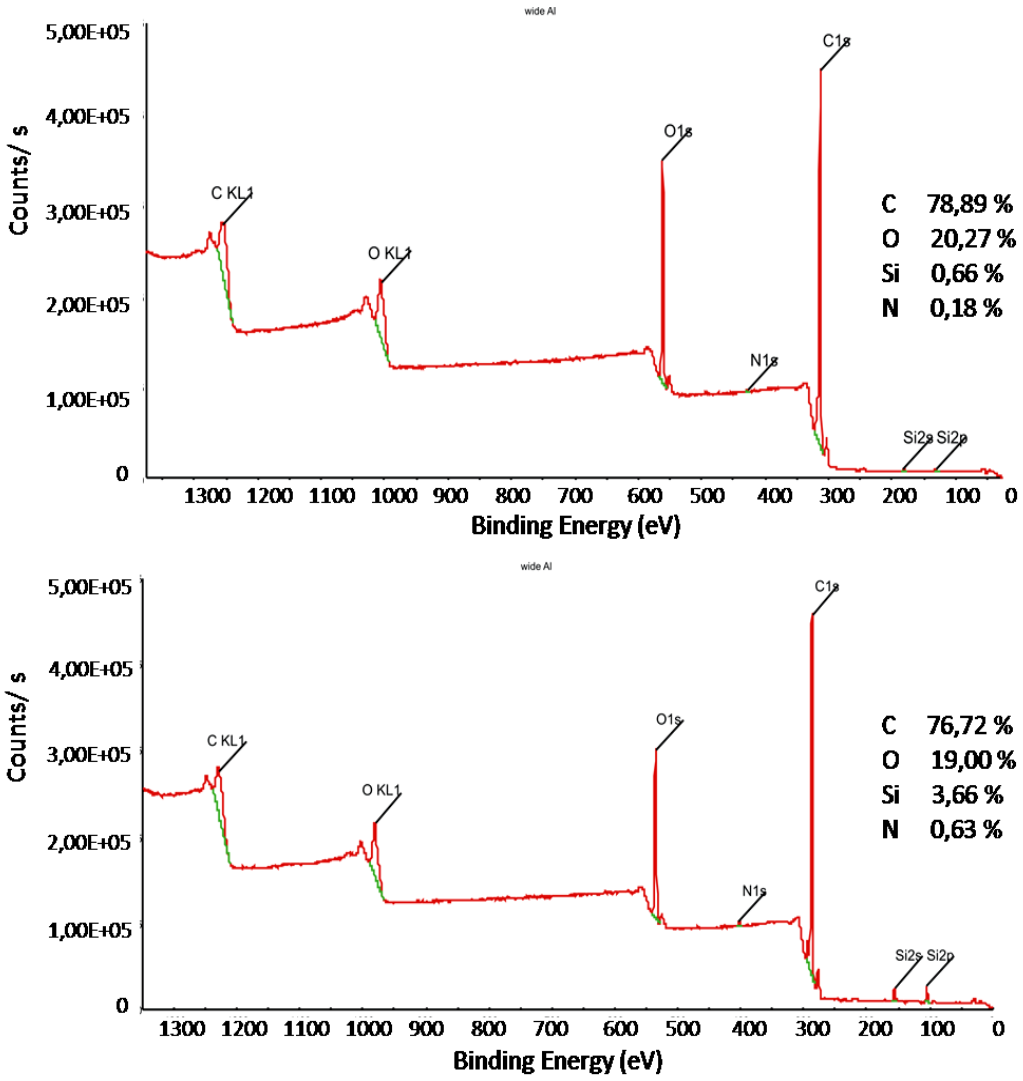

Figure 24. XPS spectra of PC: externl layer (at the top) and inside layer (at the bottom).

V.1.2. Characterization of the bonding

I completed the bonding procedure by press welding the PC slabs formerly modified in the vapors of the solvent, using a thermal press. The available press offers stable heating up to 200 ^{o}C and allows for application of pressure (up to 5 MPa) by compressing the object between two flat metallic plates. The last stage of bonding was preceded by heating the press to selected temperature. To ensure uniform pressure distribution I put the bonded elements between two additional PDMS sheets.

During the optimization of the process of bonding I took into account parameters such as temperature (*T*), pressure (*p*), and time (*t*). On the basis of the previous experiences with thermal bonding, I set the sealing time of 30 minutes. Then I investigated three values of

temperature: 125 °C, 130 C, 135 °C. All of them were much lower than the temperature of glass transition (T_g = 145 °C). For each temperature point I tested the pressure in the range of 0.05 and 0.4 MPa. The optimization was done for the plates pre-exposed to DCM and two other swelling agents using the already established procedure.

In case of DCM all the conditions yielded reproducibly solid bonding without significant deformation of the channels (**Figure 25**). Only the extreme conditions (T = 135 °C and p = 0.4 MPa) produced minimal deformation.

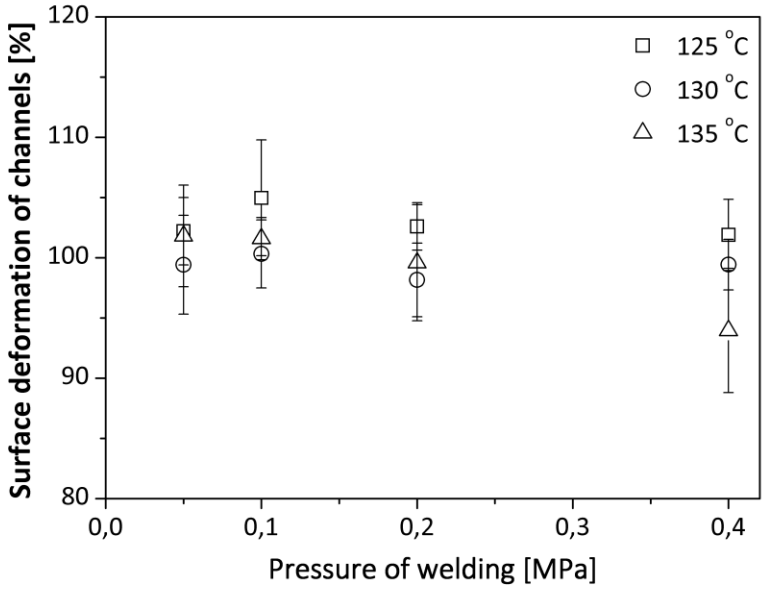

Figure 25. Quantitative characterization of bonding process as a function of pressure and temperature (squares, 125 °C; circles, 130 °C; triangles, 135 °C). The values of deformation of channels surfaces were evaluated on the basis of formula $S\ S_0^{-1}$ x 100%, where S is the area of channels cross section after bonding [mm^2], and S_0 is the area of channels cross section before bonding [mm^2]. The areas of four channels were measured for each sheet.

V.1.2.1. Strength of the bonding

I determined the strength of obtained seal using two methods. The first method included fabrication of a simple polycarbonate chip made of 20x20 mm plates of different thickness (0.75 and 5 mm) with a round chamber milled inside and then pressurizing the system (**Figure 26**). The diameter of the chamber was 10.4 mm and its height equaled 1 mm. The chamber comprised a through-hole (of diameter of 1.2 mm) enabling its connection with the source of pressure. **Figure 26** presents the chip before bonding.

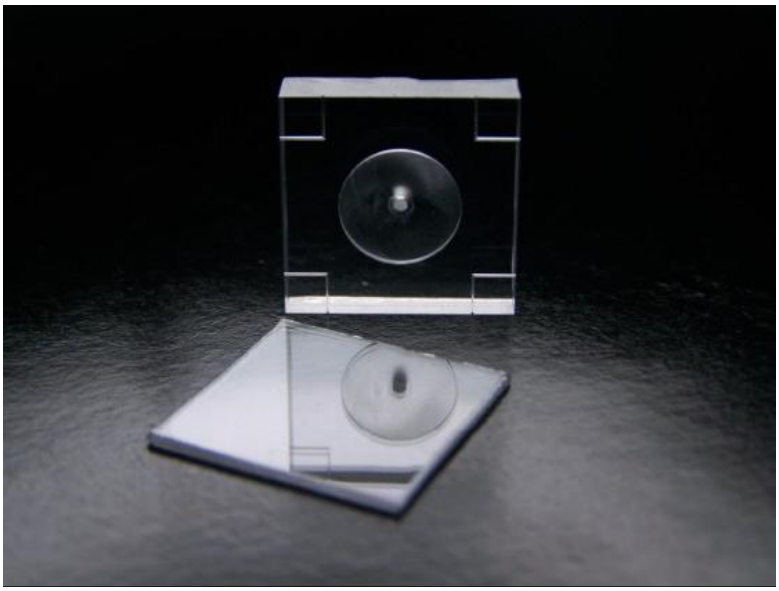

Figure 26. Polycarbonate slabs used in the experiment for verification of the strength of the bonding.

After bonding the two PC slabs I glued in the tubing and the system was subjected to the test of resistance to the pressure. I connected the device via tubing to the source of nitrogen and placed the chip in a water bath. Then, I applied the pressure of the gas and gradually increased it till the moment the bubbles appeared. Occurrence of the bubbles was assumed to be a result of the first stage of delamination, leading to a burst. The destruction of the seal typically occurred above 0.4 MPa, depending on the temperature applied in the process of press welding. I observed the highest resistance of the system to pressure when bonding was performed under temperature of 135 ^{o}C. The chip obtained in such conditions did not undergo lamination until the value of pressure exceeded 0.6 MPa.

The other method was based on verification of the critical normal stress. To perform this test I used chips that were made of two 5 mm thick PC slabs bonded together. Each slab was deprived of any extra channels or chambers on the contact area. However, they both were equipped with through-holes milled parallel to the bonding surface to assess directly the critical normal stress. I used the through-holes to attach wires to both sides of the device in order to conduct stretching test. After bonding two plates together the chip was hanged up using the fishing line and the through-holes drilled in the top plate. The through-holes present in the bottom part were used to attach a bottle. During the test I successively filled the bottle with water till the rapture of the seal of PC slabs. The influence of the size of bonded plates was also tested. I examined the chips prepared out of slabs in dimensions of 5 x 5 mm (area of bonding – 25 mm^2) and 10 x 10 mm (area of bonding – 100 mm^2).

It turned out that the connection was broken at about 1.7 kg and 4.2 kg for smaller and larger chips, respectively. This indicates that the average critical normal stress is~ 0.55 MPa and this value corresponds to the results obtained in the previous test.

V.1.2.2. Influence of chemical modification on the characterization of microchannel's surface

Exposing the material to the influence of chemical substances may result in alteration of its properties such as transparency or wettability[34, 35]. Additionally, mat surfaces in microfluidic systems drastically hinder observation of the processes, taking place inside the channels, and may make optical detection ineffective. Furthermore, well characterized surface of microchannels is crucial to the quality of the flow, which could be easily disturbed by undesirable wetting effects.

Application of surface modification in vapors of a solvent might result in irreversible changes in the character of the surface. In order to eliminate such a possibility, I investigated how the procedure of surface modification affects the behavior of the system.

I tested the transparency of modified slabs by the use of a Multi-Spec-1501 Shimadzu spectrophotometer (Japan). The acquired UV-Vis transmitance spectra confirmed that the proposed procedure of bonding does not affect the transparency (**Figure 27**).

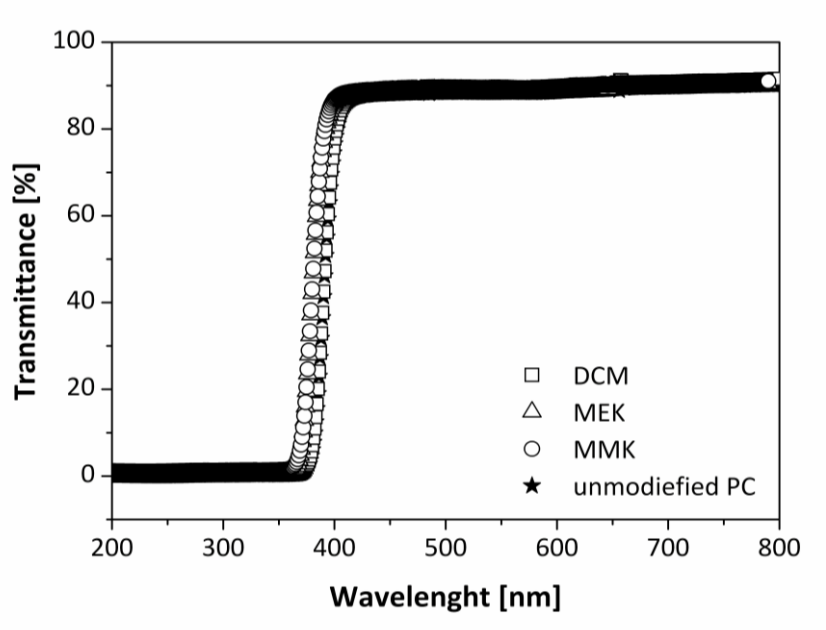

Figure 27. UV-VIS transmission spectra of the native (unmodified) PC and of three plates modified via exposure to the vapors of the three different solvents (1 mL each) that I used: DCM (squares), MEK (triangles) and MMK (circles). The temperature of exposition was T=25 ^{o}C and the time of exposure was t=30 minutes. The thickness of the modified layer was between 15 and 20 µm.

Additionally, the contact angle measured before and after the modification does not change, what clearly shows the lack of influence of the solvent vapors on the wettability.

V.1.2.3. Comparison of chemical and thermal bonding

The optimized method covers a fully controlled exposure of slabs of polycarbonate to the vapors of solvents. Press welding employs a pressure proportional to the surface of fabricated system and an elevated temperature, which – in contrast to thermal bonding – does not exceed temperature of glass transition (T_g). The developed method provides strong bonding of the polycarbonate elements, without affecting their internal structure either chemically or physically. In comparison to other methods, especially traditional thermal bonding, the procedure I developed is less invasive while maintaining high quality of bonding of elements (**Figure 28**).

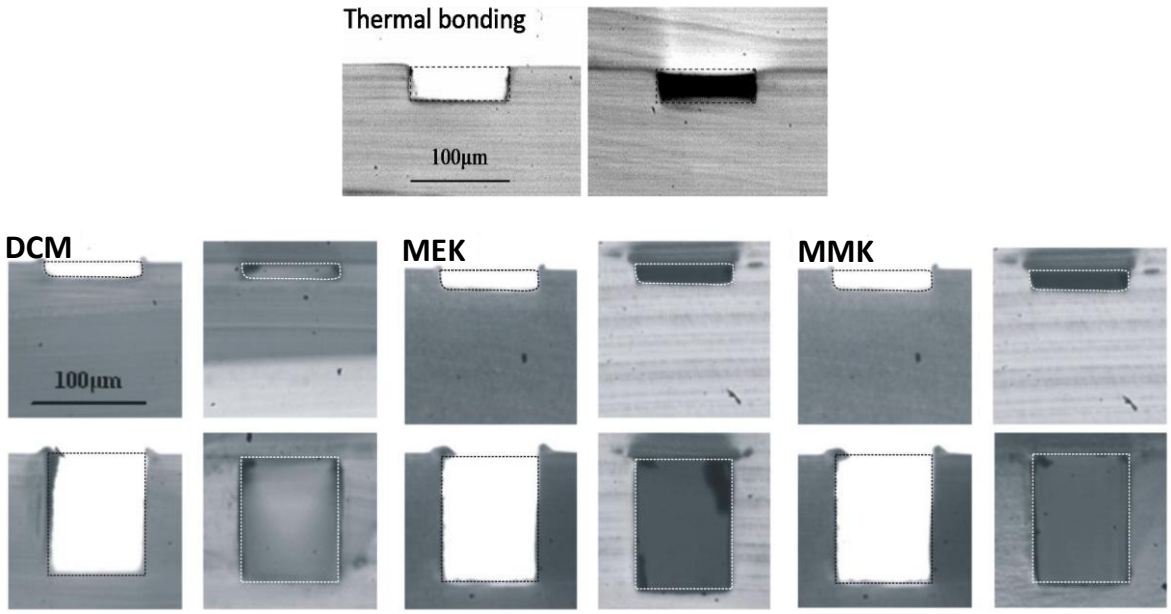

Figure 28. Micrographs of the cross-sections of microchannels performed before and after pressure welding of slabs. Top micrograph presents the results of thermal bonding. A set of micrographs at the bottom demonstrates bonding after modification in vapors of DCM, MEK and MMK, respectively. The dotted line rectangles mark rectangles visualize the fit of the shape of the channel before and after bonding. The top illustration reveals noticeable deformations of the structure of microchannel, caused during thermal bonding while bottom cross-sections are not affected.

V.2. Formation of gradient of concentration in droplets

Presented systems comprise three polycarbonate (PC) plates. Two of them (the top and the bottom plates) enclose a system of microchannels while the third, middle one, contains a set of holes providing contact we the other two. The architecture of the microchannels milled on the surface of outer plates includes the part responsible for generation of gradient of content, a set of parallel junctions dedicated to droplet formation, meanders for increasing efficiency of mixing, and output channels for observation of the gradient (**Figure 17**).

Described chips are supplied with two miscible fluids (A and B), co-forming one stream – a droplet phase – which is then turned into a set of streams of droplets by liquid C, a continuous phase not miscible with the other two.

Due to the precisely designed system of the channels, each stream of droplets is characterized by a different and well defined composition of A in B. Furthermore, providing slight differences in applied architecture (minimization of the contact between fluids co-forming the droplet phase by removing part responsible for co-flow **Figure 17g**) allows for supplying the systems with fluids of different viscosity without influencing the obtained gradient.

In further subsections I introduce the theoretical model that explains how the gradient of concentrations is generated inside the networks of microchannels. Moreover, I determine the quality of fabricated systems by specifying the operating range, establishing the level of size distribution as a function of flow rates, and comparison of the designed profile of concentration with the one obtained from measurements. Additionally, I investigate the influence of viscosity of input fluids as well as modification of the surface on the working range of the systems.

V.2.1. Theoretical model

Each channel in the microfluidic network can be described with a combination of parameters, such as length (l), area of cross-section (s), hydraulic resistance (r) and pressure (p). In microchannels of the same cross-section the resistance is proportional to their length. Moreover, according to the Ohm's law, the flow rate (q) of the fluid in a single microchannel is inversely proportional to the resistance. These dependencies are crucial in designing more complex networks, in order to provide the highest possible control of the flow while minimizing the sources of supply.

A system driven only hydrodynamicly is less expensive in comparison to *e.g.* automated devices as it does not involve an application of additional elements such as valves or extra software to control its operation. The further sections discus in detail the assumptions and

calculations essential in designing a microfluidic systems capable of simultaneous formation of gradient of concentration by mixing two miscible fluids in various, but well defined rations.

In the situation when the inlet chennels – dedicated to delivery of liquids A and B – split into *N* channels $\{A_i\}$ and $\{B_i\}$, each of new-formed channels is characterized by hydraulic resistances $\{r_{Ai}\}$ and $\{r_{Bi}\}$. Furthermore, fluids A and B flow through particular channels with the flow rate q_{Ai} and q_{Bi}, respectively. The network is designed in such way, that the channels A_i and B_i join into one stream of a droplet phase at certain points (called confluent points), situated at the entrance to the collective channels and terminated with droplet generators. In accordance to characteristics of channels I assumed that droplet generators are supplied with a droplet phase at total flow rate (sum of rates of flow of streams A and B) which is $q = q_{Ai} + q_{Bi}$, where q_{Ai} and q_{Bi}, define the flow rate of the streams of substances A and B, respectively, in particular channel. At the same time $q = (Q_A + Q_B) / N$, where Q_A and Q_B refer to the flow rate of fluid A and B, respectively. It means that the total flow rate of the two droplet liquids through each droplet generator is the same. Additionally, concentration $\hat{C}_i$ of B in the *i*-th inlet is $\hat{C}_i = q_{Bi} / q$.

When designing the microfluidic network of channels, I first select the desired combination of concentrations $\{\hat{C}_i\}$, and then calculate i) the adequate values of resistances ($\{r_{Ai}\}$ and $\{r_{Bi}\}$), as well as ii) the required ratio of the input flow rates of the two liquids Q_A/Q_B. I first establish Q_X as a sum of q_{Xi} ($Q_X = \sum_{i=1}^{N} q_{Xi}$), where $X = A$ or B. Then I define each $q_{Xi} = \Delta p / r_{Xi}$, where Δp is the difference of pressures at the inlet and at the end of the distribution channel (the *i*-th confluent point). On the basis of $\hat{C}_i$ definition, I know that $q_{Ai} = q\ (1 - \hat{C}_i)$ and $q_{Bi} = q\ \hat{C}_i$. This, in turn, results in proportion $Q_A / Q_B = (\sum_{i=1}^{N} \hat{C}_i) / (N - \sum_{i=1}^{N} \hat{C}_i)$ yieldig the required ratio of inflow rates of the fluids co-forming the droplet phase. Considering the Hagen Poiseuille law $Q = \Delta p / r$, I determined the ratios $r_{Ai} / r_{Ak} = (1 - \hat{C}_k) / (1 - \hat{C}_i)$ as well as $r_{Bi} / r_{Bk} = \hat{C}_k / \hat{C}_i$, and in combination with the fact that the hydraulic resistance is linearly proportional to the length of channels of the same cross-section, I could rewrite these in such way that: $l_{Ai} / l_{Ak} = (1 - \hat{C}_k) / (1 - \hat{C}_i)$ and $l_{Bi} / l_{Bk} = \hat{C}_k / \hat{C}_i$. This means that by setting an arbitrary length of one channel in each set $\{l_{Ai}\}$ and $\{l_{Bi}\}$ I can calculate the lengths of other channels.

By implementing the procedure described above I designed and fabricated three devices to examine their compliance with the theory. Two of them were dedicated to produce emulsion out of fluids of similar viscosities, while the other one to liquids differing

in the value of viscosity. In the first case I designed a system dedicated for generation of a linear gradation of $\hat{C}_i$, where I set eight outlet channels for generation $\{\hat{C}_i\}$ = {1, 6/7, 5/7, 4/7, 3/7, 2/7, 1/7, 0}. Choosing an arbitrary reference length l_{A1} = 26.28 mm a set of $\{l_{Ai}\}$ = {26.28, 30.68, 36.76, 45.96, 61.32, 91.96, 183.96, infinity} [mm] and (setting l_{B8} = 26.26 mm) $\{l_{Bi}\}$ = {infinity, 183.96, 91.96, 61.32, 45.96, 36.76, 30.68, 26.28} [mm] was obtained. The second device was designed to produce a logarithmic variation of $\hat{C}_i$, what resulted in six outlet channels enabling production of $\{\hat{C}_i\}$ = {1, 1/2, 1/4, 1/8, 1/16, 0} with corresponding lengths of the distribution channels $\{l_{Ai}\}$ = {50, 53.33, 57.14, 66.67, 100.00, infinity} [mm] and $\{l_{Bi}\}$ = {infinity, 320, 160, 80, 40, 20} [mm]. The last chip characterized by the same parameters as the first one but with minimized length referring to the part of device responsible for co-flow of streams A and B. The channels of 'infinite' length require zero flow, therefore simply do not incorporate them into the design. The layouts of the channel networks on each layer are given in Fig. IV1. I also denote the pressures (p) at confluent points, as marked on the diagram.

V.2.1.1. Justification of the model

To prove the correctness of following assumptions I determined the equality of the pressure drops Δp in the distribution channels. **Figure 29** demonstrates a simplified architecture of a gradient generator. The diagram includes only two outlet channels. Each out of the three inlets supplying the network with fluids – A and B co-forming droplet phase and C, feeding chip with the continuous phase – splits into two microchannels. Each microchannel in the network is described by its hydraulic resistance (*r*) and flow rate (*q*), in the figure they are marked with an appropriate index referring to the transported substance. I also introduced the pressures (*p*) at confluent points, as marked on the diagram (**Figure 29**).

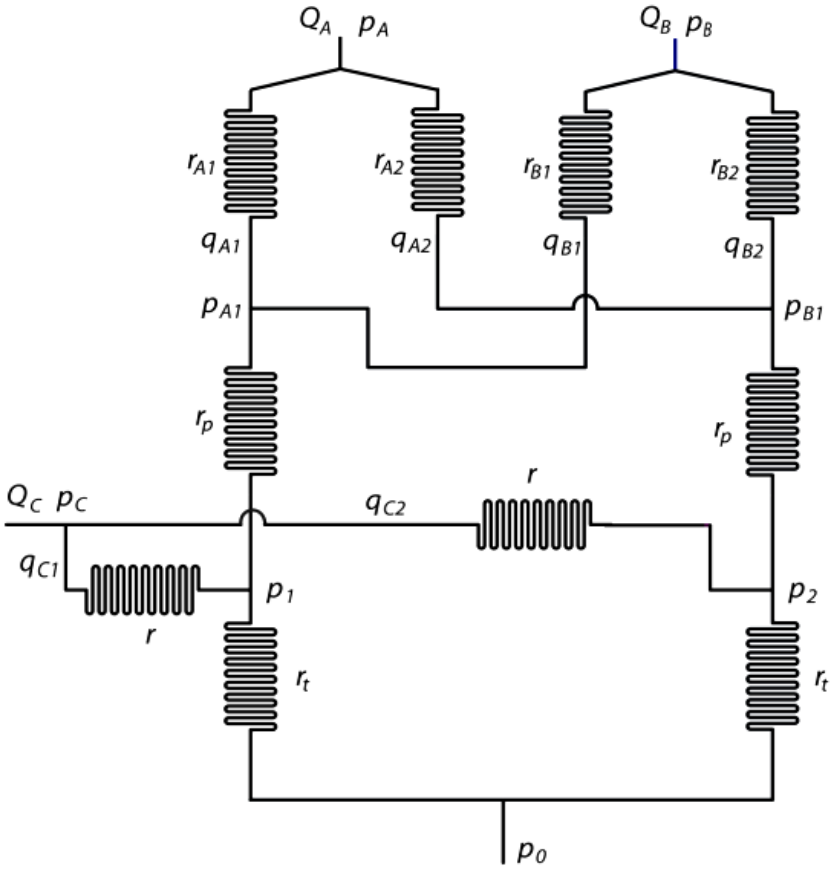

Figure 29. V12 Diagram of the microfluidic system dedicated to distribution of two miscible streams A and B splited into droplets by non-miscible fluid C. Hydraulic resistance (r) and flow rate (q) are marked with an appropriate index referring to the transported substance. The pressures (p) are marked with indexes corresponding to particular channels.

I calculated the pressure (*p*) and flow rate (*q*) in each microchannel by applying the Kirchhoff's circuit laws[231, 232].

$$(p_A - p_{B1}) + (p_{B1} - p_2) - (p_C - p_2) + (p_C - p_1) - (p_{A1} - p_1) - (p_A - p_{A1}) = 0 \quad [1]$$

$$(p_B - p_{A1}) + (p_{A1} - p_1) - (p_C - p_1) + (p_C - p_2) - (p_{B1} - p_2) - (p_B - p_{B1}) = 0 \quad [2]$$

$$(p_C - p_1) + (p_1 - p_0) - (p_2 - p_0) - (p_C - p_2) = 0 \quad [3]$$

According to the Ohm's law:

$$q = \Delta p / r \quad [4]$$

where r_{Xi} – the hydrodynamic resistance of the *i*-th channel,

q_{Xi} – the volumetric flux of X solution in the *i*-th channel,

Δp – the pressure difference between two points in the same channel

I obtained

$$r_{Xi} = \Delta p / q_{Xi} \quad [5]$$

Then I applied equation [5] in equations [1]-[3]:

$$r_{A2}\, q_{A2} + r_p\,(q_{A2} + q_{B2}) - r\, q_{C2} + r\, q_{C1} - r_p\,(q_{A1} + q_{B1}) - r_{A1}\, q_{A1} = 0 \quad [6]$$

$$r_{B1}\, q_{B1} + r_p\,(q_{A1} + q_{B1}) - r\, q_{C1} + r\, q_{C2} - r_p\,(q_{A2} + q_{B2}) - r_{B2}\, q_{B2} = 0 \quad [7]$$

$$r\, q_{C1} + r_t\,(q_{A1} + q_{B1} + q_{C1}) - r_t\,(q_{A2} + q_{B2} + q_{C2}) - r\, q_{C2} = 0 \quad [8]$$

This eventually lead to:

$$q_{A1} = (qr + Q_A r_{A2} - Q_B r_{B2}) / (r_{A1} + r_{A2} + r_{B1} + r_{B2}) \quad [9]$$

$$q_{B1} = (q(r_{A1} + r_{A2} + r_{B1} + r_{B2} - r) - Q_A r_{A2} + Q_B r_{B2}) / (r_{A1} + r_{A2} + r_{B1} + r_{B2}) \quad [10]$$

$$q_{C1} = q_{C2} = Q_C/2 \quad [11]$$

where $q = q_{Ai} + q_{Bi}$ and $Q_X = \sum_{i=1}^{N} q_{Xi}$.

Calculation of Δp_1 and Δp_2 resulted in equality of the two terms, Δp_1 and Δp_2

$$\Delta p_1 = p_1 - p_0 = r_t\,(q_{A1} + q_{B1} + q_{C1}) = p_0 + r_t\,(q + Q_C/2) \quad [12]$$

$$\Delta p_2 = p_2 - p_0 = r_t\,(q_{A2} + q_{B2} + q_{C2}) = p_0 + r_t\,(q + Q_C/2) \quad [13]$$

For the streams A and B splitting into *N* channels the following relationships could be described:

$$r_{A(i+1)}\, q_{A(i+1)} + r_p\,(q_{A(i+1)} + q_{B(i+1)}) - r\, q_{C(i+1)} + r q_{Ci} - r_p\,(q_{Ai} + q_{Bi}) - r_{Ai}\, q_{Ai} = 0 \quad [14]$$

$$r_{Bi}\, q_{Bi} + r_p\,(q_{Ai} + q_{Bi}) - r\, q_{Ci} + r\, q_{C(i+1)} - r_p\,(q_{A(i+1)} + q_{B(i+1)}) - r_{B(i+1)}\, q_{B\,(i+1)} = 0 \quad [15]$$

$$r\, q_{Ci} + r_t\,(q_{Ai} + q_{Bi} + q_{Ci}) - r_t\,(q_{A(i+1)} + q_{B(i+1)} + q_{C(i+1)}) - r\, q_{C(i+1)} = 0 \quad [16]$$

Where $n \in [1, n]$

The combination of [14] – [16] resulted in:

$$q_{Ai} = (q\, r + Q_A\, r_{A(i+1)} - Q_B\, r_{B(i+1)}) / (r_{Ai} + r_{A(i+1)} + r_{Bi} + r_{B(i+1)}) \quad [17]$$

$$q_{Bi} = q - q_{Ai} \quad [18]$$

Finally, the flow rate of continuous phase, $Q_C = \sum_{i=1}^{N} q$, can be transformed to $q_{Ci} = q_{C(i+1)} = Q_C/n$ to obtain:

$$\Delta p_i = p_i - p_0 = r_t\,(q_{Ai} + q_{Bi} + q_{Ci}) = p_0 + r_t\,(q + Q_C/n) \quad [19]$$

$$\Delta p_{(i+1)} = p_{(i+1)} - p_0 = r_t\,(q_{A(i+1)} + q_{B(i+1)} + q_{C(i+1)}) = p_0 + r_t\,(q + Q_C/n) \quad [20]$$

What confirms the expected equality $\Delta p_i = \Delta p_{(i+1)}$

V.2.2. Microfluidic devices taking input from fluids of equal viscosities

Below, I present photographs of the microfluidic systems used for generation of different concentration profiles (linear and logarithmic) using fluids characterized by similar values of viscosity. The chips incorporate common elements marked on the photographs (**Figure 30**):

- inlets,

- distribution channels for A and B concerning generation of gradient

- a set of channels between the confluent points and the T-junctions where liquids A and B flow together,

- a network responsible for transporting the continuous phase C, to a set of T-junctions through a symmetric cascade of microchannels presenting equal hydraulic resistance for all *N* lines,

- a set of T-junction droplet generators,

- a set of meanders for accelerating mixing of the droplets content,

- a set of outlet channels that allow for simultaneous visualization of the streams of droplets.

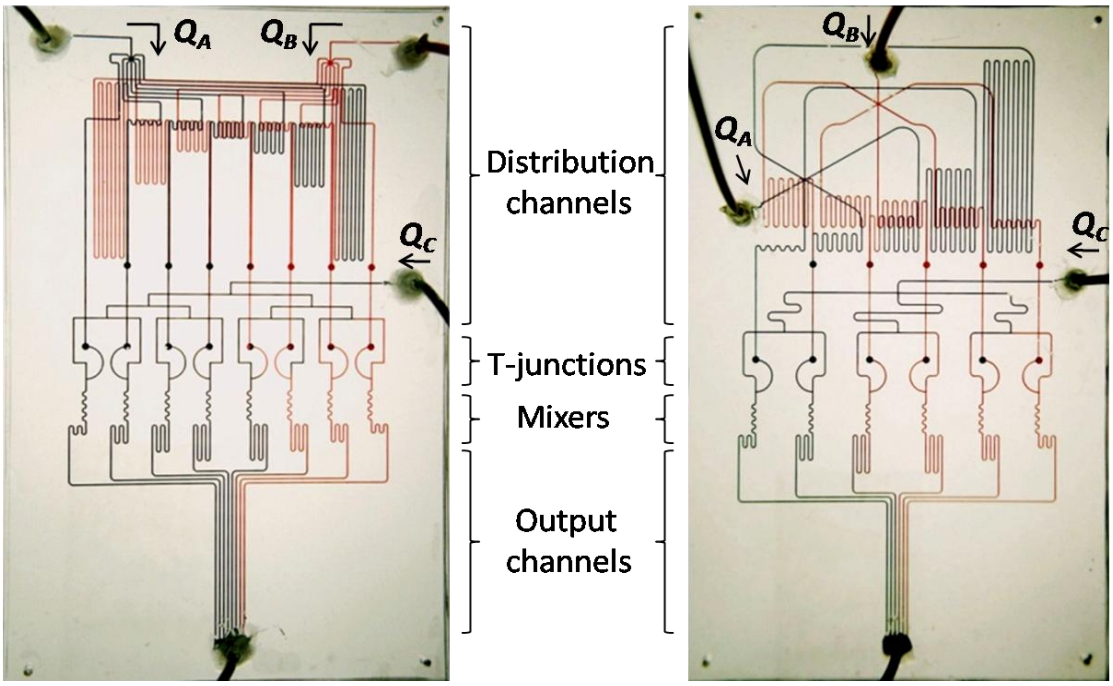

Figure 30. The photographs illustrate two microfluidic systems that I used for generation of a linear (left) and logarithmic (right) variation of the concentration of a dye across the output channels. Sections responsible for distribution of fluids, formation of droplets, mixing and the output are marked in the photograph with wavy brackets. For better visualization of microchannels, I pumped red ink into the inlet for liquid A, blue ink into the inlet for liquid B and green ink into the inlet for the continuous liquid

V.2.2.1. Characterization of throughput: comparison of single junction with gradient generator

I determined the operating range and volume of droplets formed in the parallel junctions by varying the flow rate of the droplet ($Q_D = Q_A + Q_B$) and the continuous (Q_C) phases. I used a single droplet generator in order to compare its throughput and the operating range with the junctions included on my chip. Both systems were described by the same dimensions of cross-section (200 x 200 µm) and the same architecture (side channel joining the main one at the right angle). I applied water as the dispersed droplet phase, and a 2% (w/w) solution of Span80 in hexadecane as the continuous phase. The single T-junction displays the scaling relation characteristic to low values of capillary numbers[113, 233, 234] where the volume (V) of the droplets depends on the ratio of the flow rates of the droplet (Q_d), and of the continuous (Q_c) phases (**Figure 31a**). **Figure 31b** presents the range of flow rates, within which the system produces droplets. Outside this range the device shifts either to a laminar co-flow[235, 236], or jetting[237] regimes. The maximum throughput of the droplet phase in a single junction is *ca.* 6 mL/h and corresponds to the frequency of droplet production – 174.33 [drop/s].

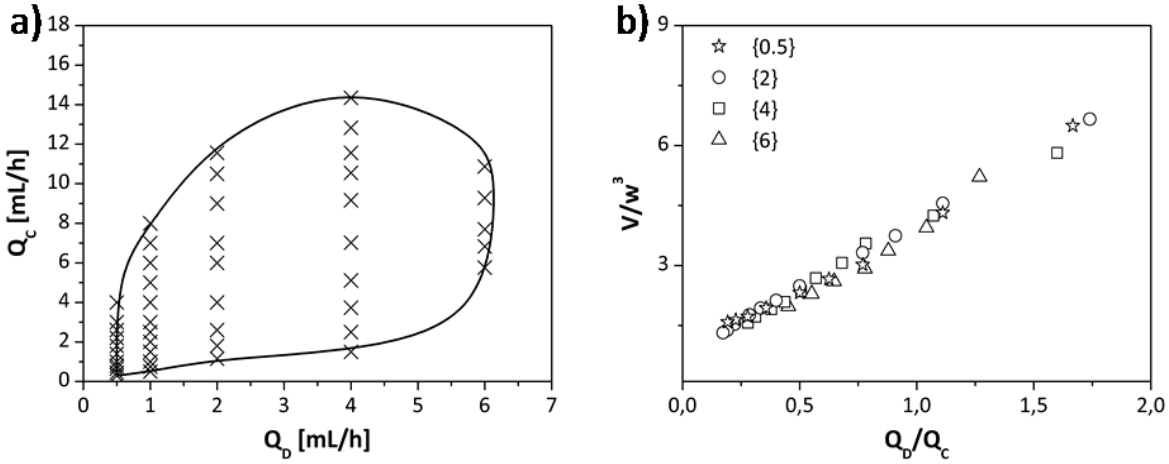

Figure 31. Characteristics of the single T-junction. a) Illustration of the scope of droplets volumes as a function of the ratio of flow rates, b) The operating range of the T-junction in the dripping regime determined by the rates of flow (the numbers in curly brackets refer to Q_D in [mL/h]).

In order to widely describe the (Q_D, Q_C) space, I first varied Q_C for three constant values of Q_D={6, 16, 30} [mL/h], and then varied Q_D for Q_C={2, 5, 10} [mL/h]. This allowed me to determine the values of flow rates that promote the dripping regime (**Figure 32**). The working range determined for microchips dedicated to simultaneous formation of droplets revealed similar trend to the one presented by single T-junction. However, I observed a noticeable reduction in the operating range of the T-junction comprised in gradient generating systems. In my opinion that might be a result of slight differences between the junctions, resulting from imperfections during their fabrication.

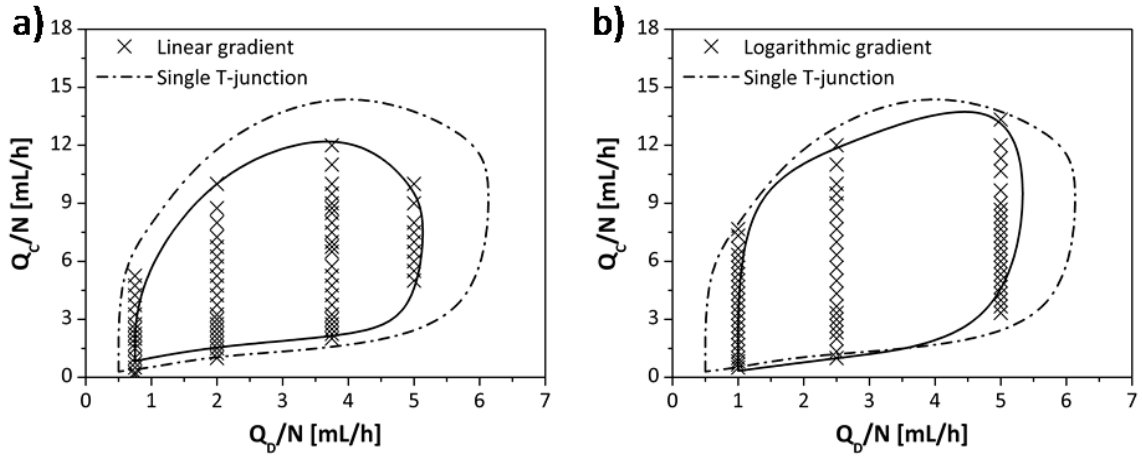

Figure 32. The solid lines show the ranges of operation of the linear (a) and logarithmic (b) systems within the dripping regime. The crosses refer to the experimental points from the parallel devices, and display values obtained per single T-junction. The dashed lines, presented for the comparison, show the working range of a single T-junction.

I also determined the volume of the droplets for particular configurations o Q_D and Q_C. **Figure 33** demonstrates these trends, together with micrographs of the droplets of different volumes resulting from various flow rates of the droplet and the continuous phases. The obtained results revealed that the volume of droplets varies with applied Q_D and Q_C, in similar manner as the single T-junction.

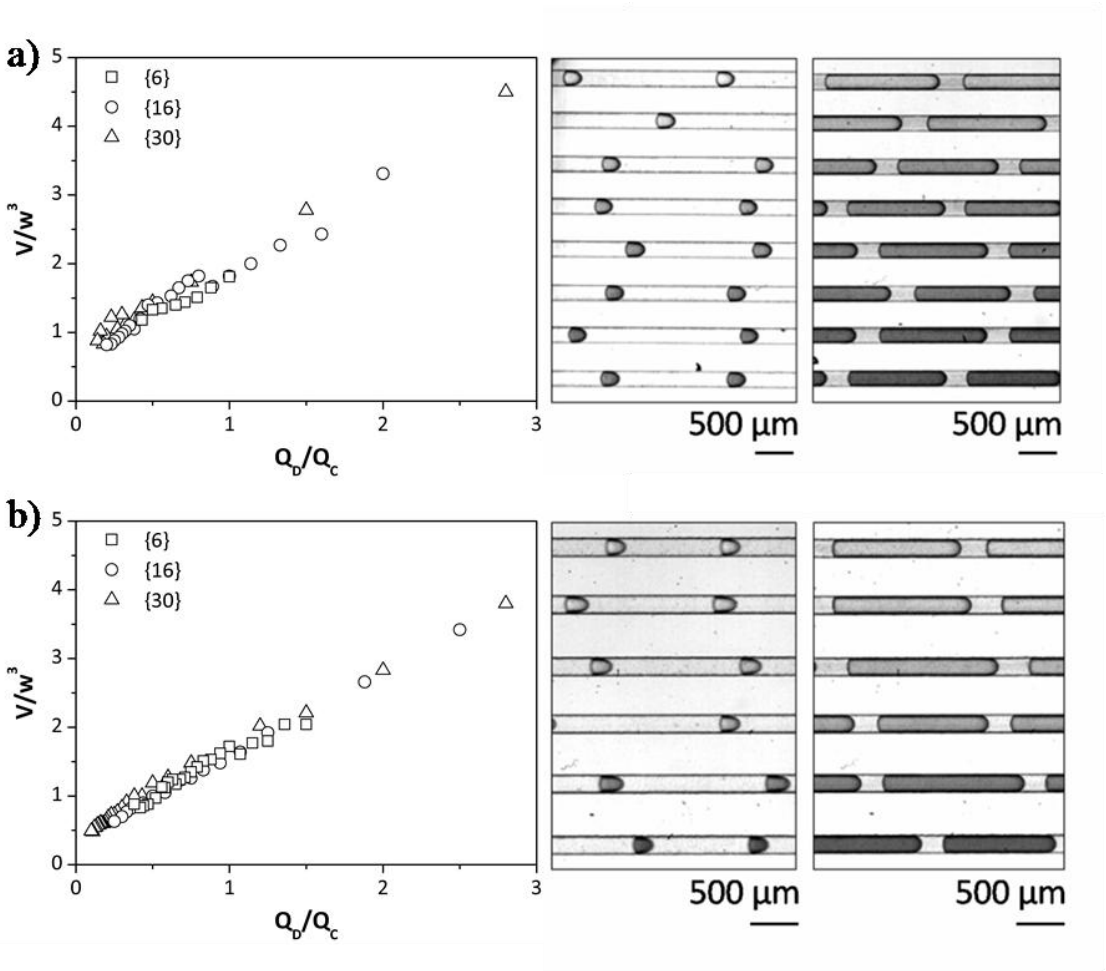

Figure 33 The influence of the ratio of flow rates of the droplet and continuous phases on the volume of the microdroplets for linear (a) and logarithmic (b) gradients. The numbers in curly brackets refer to Q_D in [mL/h]. Micrographs illustrating the microdroplets differing in size, represent the dependence of the volume on the applied rates of flow (left micrographs: Q_D=6 mL/h , Q_C=55 mL/h, right micrographs: Q_D=6 mL/h , Q_C=2 mL/h

V.2.2.2. Determination of the level of polydispersity of droplet volumes within a particular channel and across all channels

Droplets size distribution is a crucial parameter in description of an emulsion. It is of even greater importance to provide droplets of uniform volume across whole chip when they are to be applied to pharmaceutical purposes (as *e.g.* carriers of active substances). For this reason I directed much attention to the droplets size distribution considering both i)

combination of droplets produced within particular T-junctions and ii) droplets coming out of all parallel streams. Implemented procedure allowed me to verify the influence of applied rates of flow, as well as slight differences in microchannels geometry resulting from milling, on the comparability of produced droplets.

I characterized the droplet size distribution in particular channels by calculating the standard deviation σ ($\sigma = \left[\left(\frac{1}{n}\right)\sum_{i=1}^{n}(L_i - \overline{L})^2\right]^{\frac{1}{2}}$) around the mean value $\overline{L}$ ($\overline{L} = \left(\frac{1}{n}\right)\sum_{i=1}^{n} L_i$) of the lengths L_i of the droplets within certain channel. My measurements show that σ values are always lower than 5% of $\overline{L}$ he mean value what indicates highly monodisperse populations of droplets within each channel. In the **Figure 34** I demonstrate mean values of L with standard deviation bars as a function of particular microchannel for different sets of flow rates.

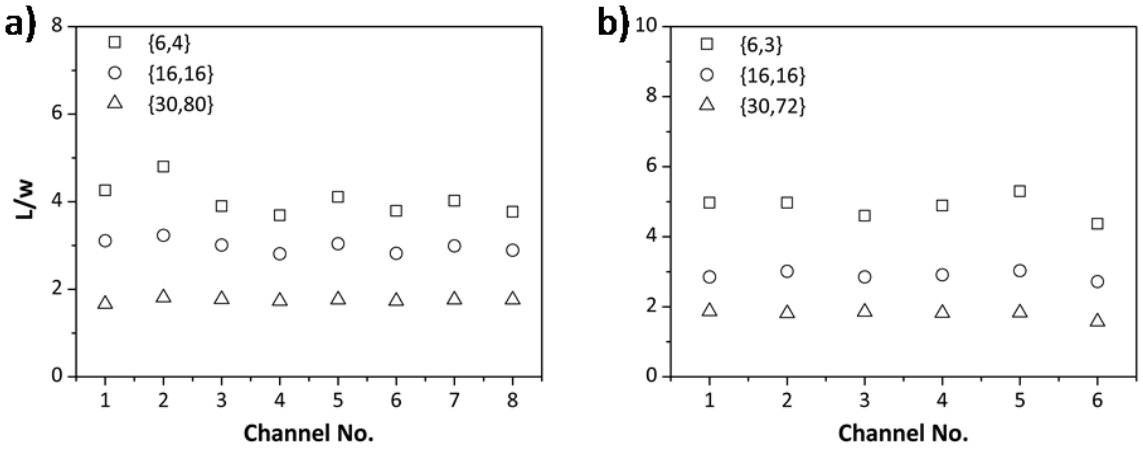

Figure 34 The dependence of normalized length of droplets obtained using various flow rates in respective microchannels for linear (a) and logarithmic (b) chips. Symbols on the plot (circles, triangles and squares) refer to different sets of rates of flow that are given in wavy brackets {Q_D, Q_C}.

In order to determine the droplet size distribution across the parallel channels, I used the same formula and calculated the standard deviation (σ*) around the mean $\overline{L}$ *. On the basis of determined values of σ* and $\overline{L}$ * I calculated relative standard deviation, defined as σ*/ $\overline{L}$ *.

The results of my observations indicate that at higher flow rates the emulsions consist of fairly uniform droplets (sigma/L < 5%), whereas with the decrease in the flow rates the variation coefficient increases to approximately 10%, with occasional higher spikes (**Figure 35**). The difference observed between the droplet variations of the individual channels and when they are considered together results most probably from imperfections of the fabrication process, especially the milling step.

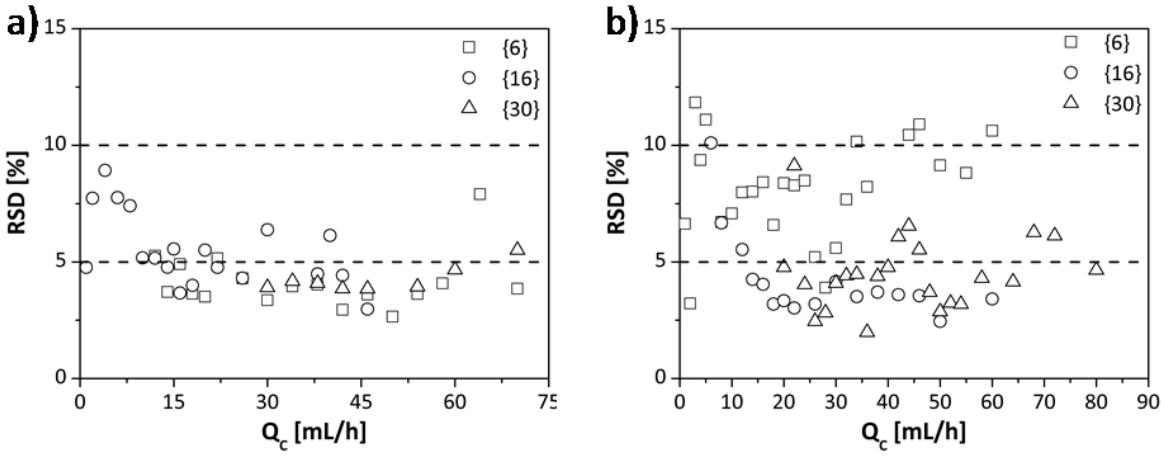

Figure 35 The relative standard deviation of the droplet lengths across the microchannels for the linear (a) and logarithmic (b) devices. The symbols correspond to respective flow rates {Q_D} [mL/h].

V.2.2.3. Determination of the profile of concentrations

I performed image analysis in order to determine the concentration of the dye inside the droplets observed in the parallel outlet streams. The analysis employed the Lambert-Beer law $I = I_0 e^{-\alpha C l}$ where I_0 and I are the intensities of the incident and transmitted light, respectively, α is the molar absorptivity coefficient of the dye, l – the length of the optical path through the droplet, and C the concentration of the dye. As I_0, l and α are constant, I assumed the proportionality of C to –ln I. To facilitate the interpretation of the results I normalized the determined concentrations to the 0-1 non-dimensional scale, where 1 corresponds to the maximal concentration of the dye, and 0 deionized water. **Figure 36** presents a high level of consistency of the recorded concentration gradient in the case of both linear and logarithmic chips over a wide range of flow rates.

Additionally, I calculated the coefficient of determination (R^2) in order to assess the reliability of designed and experimental gradient profiles for applied rates of flow. To achieve this I employed the expression $R^2 = 1 - \left(\frac{SSE}{SST}\right)$, where *SSE* (error sum of squares) is defined as $SSE = \sum_{i=1}^{N} \left(C_i - \hat{C}_i\right)^2$ and *SST* (total sum of squares) $SST = \left(\sum_{i=1}^{N} C_i^2\right) - \left(\frac{1}{N}\right)\left(\sum_{i=1}^{N} C_i\right)^2$ where N is the number of channels, whereas C_i and $\hat{C}_i$ are the empirical and theoretical values of the concentration, respectively. In **Figure 36** I show that in all cases R^2 is close to unity what suggests that designed gradation of concentrations is achieved in a wide range of flow rates.

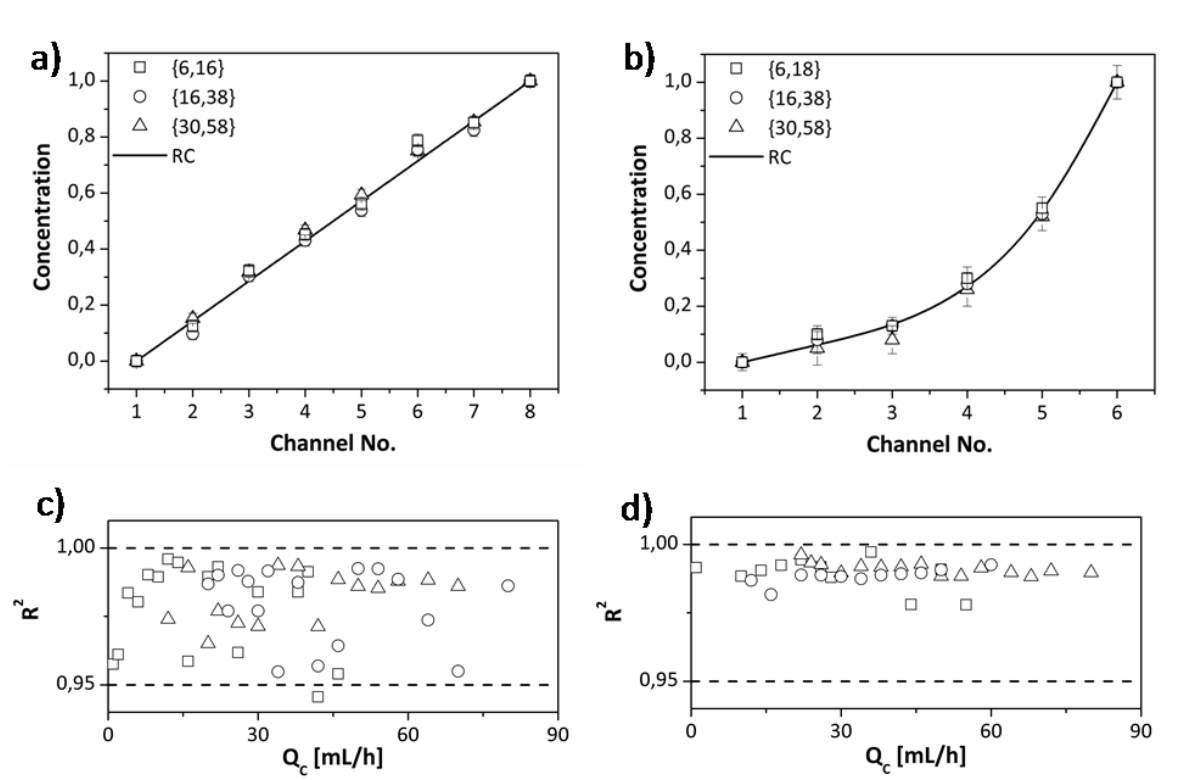

Figure 36 The plots show the agreement of the designed gradient (solid line) with the experimentally obtained profiles for linear (**a**) and logarithmic (**b**) devices. The symbols correspond to the applied flow rates given in wavy brackets {Q_D, Q_C}, [mL/h]. The influence of the continuous phase flow rate on the correlation coefficient (R^2) from the flow rate of the continuous phase for the linear (**c**), and logarithmic (**d**) gradient generator. The symbols correspond to the flow rate of the droplet phase Q_D values are given on the plots (**a**) and (**b**).

V.2.3. Microfluidic device supplied with fluids of different viscosities

Handling fluids of dissimilar viscosities is challenging when designing systems for parallel gradients of concentration. The difficulty consists in the effective mixing of fluids, considering that the diffusion is a relatively slow process

The architecture of my chip almost completely eliminates the contact of applied fluids differing with viscosity before formation of droplets. There is only short section of the channel, where both streams flow in laminar manner. The system enforces the active mixing immediately after combining the fluids into one droplet[118].

The idea of minimization of contact of two components of droplet phase required providing of minor changes in the architecture of my system used in the previously described devices. The changes involved milling two separate microchannels for sub-streams of droplet phase introduced to the droplet generator. This resulted in shifting the confluent point to the junction itself and changing its geometry from T-junction to K-junction (**Figure 37**).

In my experiments I used 62% (w/w) solution of glycerol in water ($\mu=10.11\cdot10^{-3}$ Pa·s) as the more viscous fluid and a solution of dye in deionized water ($\mu=0.89\cdot10^{-3}$ Pa·s) as the less viscous one. To provide stable conditions and repetitive results I kept the containers and resistive capillaries in a water bath at 25 ^{o}C.

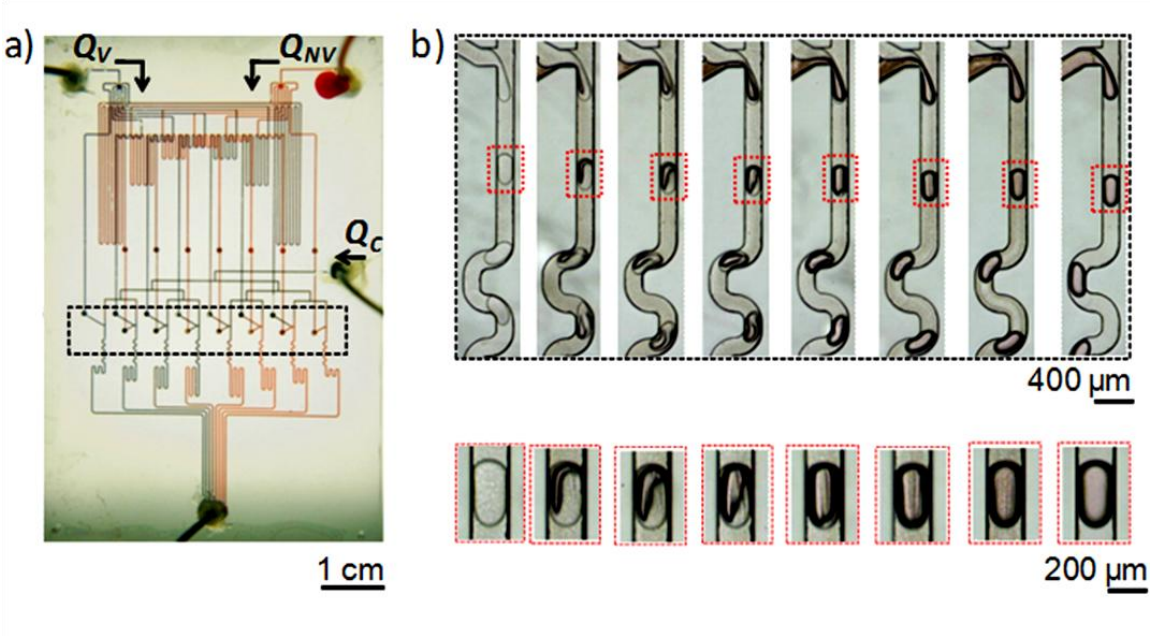

Figure 37. a) Photograph of the microfluidic device applied to generate a linear concentration gradient from fluids of dissimilar viscosities. I pumped solutions of color ink to visualize the network of microchannels responsible for transport of the fluids. I applied red ink into the inlet for liquid A (65 % solution of glycerol in deionized water with red dye), blue ink into the inlet for liquid B (deionized water with blue dye), and green ink into the inlet for the continuous phase (hexadecane with SPAN80 and green dye). Insets (**b**) illustrate the way of delivery of fluids to particular K-junctions and formation of the droplets.

V.2.3.1. Characterization of throughput

I assessed the dependence of droplets volume on the flow rates in similar way as I previously did for the single T-junction and both linear and logarithmic gradient generators. Figure 38 demonstrates examined dependency and shows slight deviations from the trend observed in gradients obtained using same viscosity liquids. Nevertheless, in spite of high differences in viscosity of implemented fluids, the observed difference is not as significant as it could be expected.

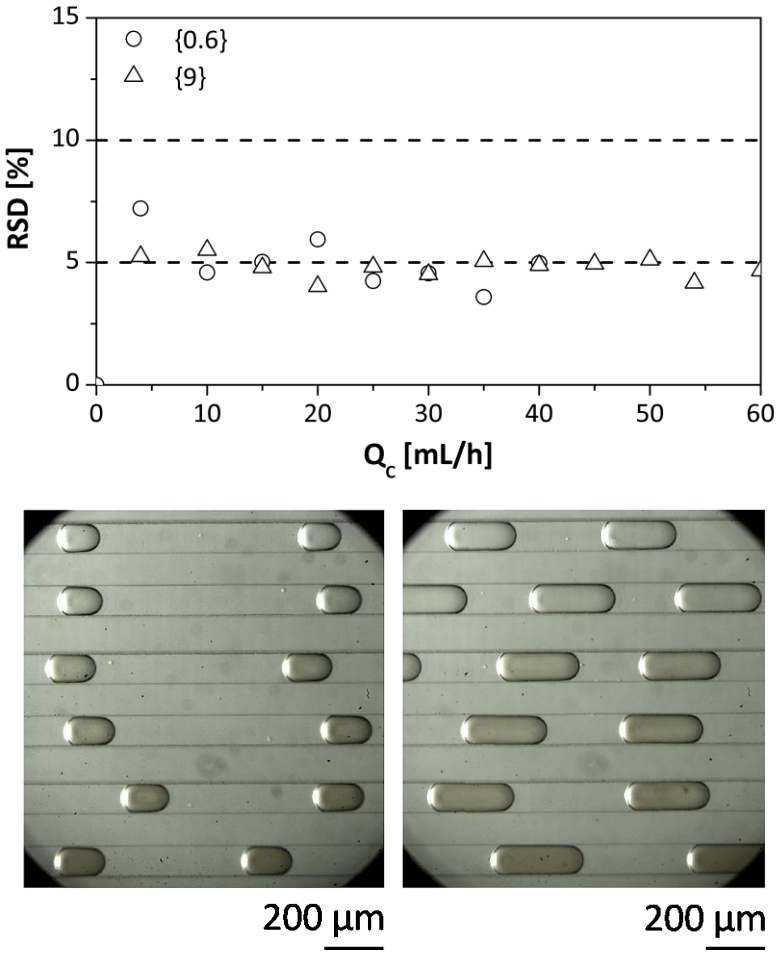

Figure 38. The dependence of the size of the microdroplets on the ratio of the droplet and the continuous phases. The numbers in wavy brackets denote the flow rate of droplet phase (Q_D). Photographs illustrate microdroplets of different sizes, depending on the applied flow rates (left micrograph: Q_D=4 mL/h, Q_C=16 mL/h, right micrograph: Q_D=4 mL/h, Q_C=9 mL/h).

V.2.3.2. Influence of the surface modification on the working range

According to the literature the higher is the viscosity of the droplet phase the sooner the transition from dripping to jetting regime occurs[4, 126, 134-137]. This observation is related, among other factors, to the significant intensification of interactions of the droplet phase with the microchannel's surface (wetting effects). In order to extend the working range I decided to perform the surface modification with dodecylamine (DDA). Application of DDA increases contact angle from 84° for water on unmodified PC to 130° when the measurement is performed in the air – and from 105.3° to 139.7° when measured in the 2% solution of SPAN80 in hexadecane. In the **Figure 39** I present the results obtained for the single junction. The plot

indicates that the modification promotes considerable expansion of the operating range. This observation encouraged me to perform surface modification prior to the experiments.

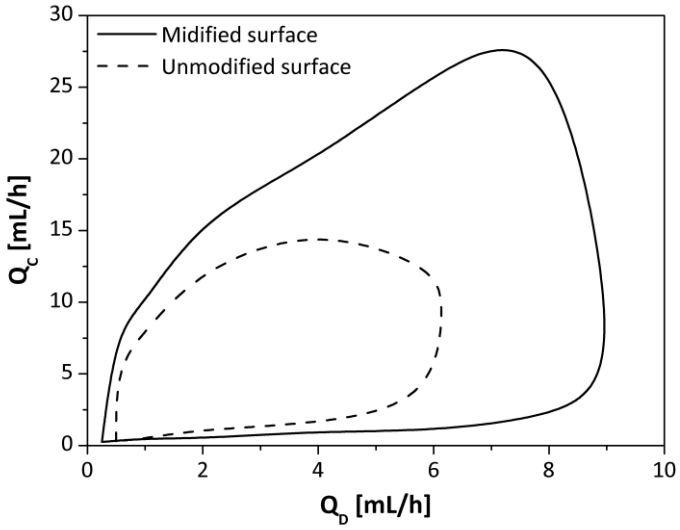

Figure 39. The plot presents operating range of a single T-junction before (solid line) and after (spotted line) chemical modification of the surface of microchannels for water as a droplet phase and 2% solution of SPAN80 in hexadecane as a continuous phase.

V.2.3.3. Influence of the order of liquids delivery on the operation range

I observed that the order of delivered fluids is significant when it comes the operating range of my microfluidic system. I used a single K-junction in order to determine the range in which the systems operate in dripping regime with respect to different configurations of delivery of fluids. In the **Figure 40** I demonstrate two possible ways of introducing the fluids to the K-junction. In the first configuration NV_V (**Figure 40a**) the less viscous fluid (NV, deionized water) is the first one to have contact with the walls of microchannel and more viscous fluid (V, 62.5% water solution of glycerol) is supplied from under the less viscous liquid. **Figure 40b** presents the inverse configuration V_NV.

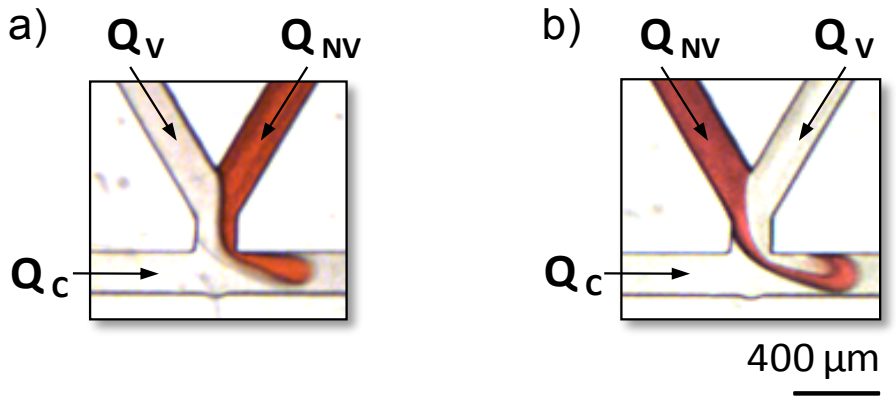

Figure 40. Photographs illustrating two configurations of fluids delivery: (a) NV_V , where the less viscous fluid (deionized water) marked as NV enters the main channel first and (b) V_NV, where more viscous fluid marked as V (62.5% water solution of glycerol), enters the main channel first. QV, QNV and QC describe flow rates of the viscous fluid, the low viscosity fluid, and the continuous phase, respectively.

To assess the influence of the order of fluids delivery on the working range I tested two different ratios of less viscous to viscous fluids (Q_{NV} / Q_V): i) 6/1 and ii) 1/6. As the results indicate, the working range in dripping regime gets narrower with increasing viscosity (**Figure 41a** and **b**). Additionally, I observed that the use of configuration NV_V shifts the transition from dripping to jetting regime to higher flow rates. Therefore it can be concluded that the operating range is determined by the viscosity of substance adjacent to the wall of microchannel. Having that in mind, a seemingly unimportant parameter such as the order of liquids in the K-junction can considerably influence the system's throughput.

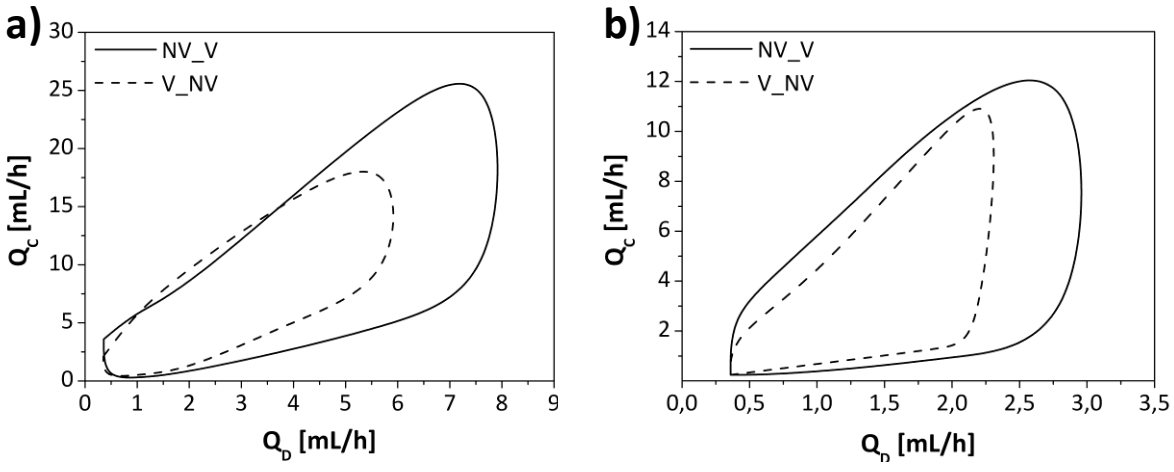

Figure 41. The operating range in dripping regime. The plots illustrate results for different ratios of the low and high viscosity fluids: Q_{NV} / Q_V = 6/1 (**a**) and 1/6 (**b**),. The solid and dashed lines corresponds to the NV_V and V_NV configurations, respectively.

The results in **Figure 41** show that the maximum rate of droplet formation decreases with the increase of fraction of the more viscous liquid. Thus, in the parallel system the throughput is limited to the maximum flow rate that allows forming droplets composed entirely of the more viscous liquid (**Figure 42**).

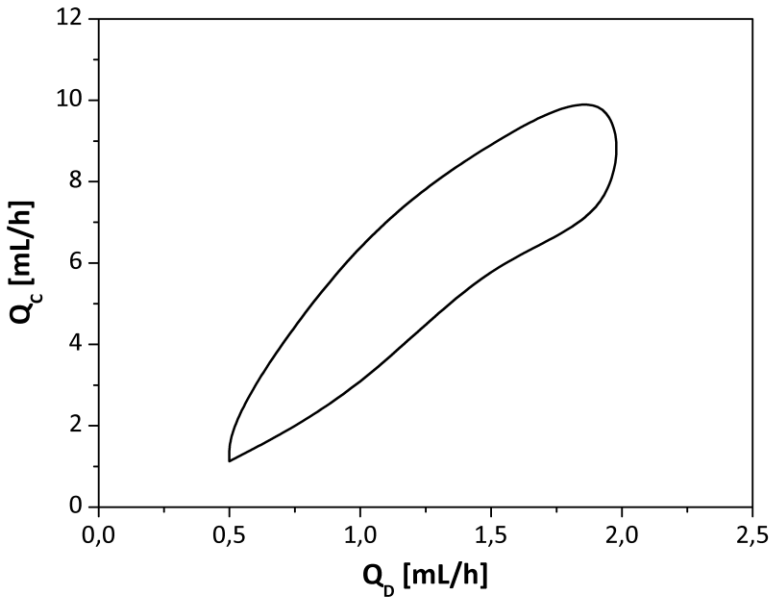

Figure 42. The working range of the gradient generator, which produces droplets composed of fluids of different viscosities, mixed in proportions Q_{NV}/Q_V = {0, 1/7, 2/7, 3/7, 4/7, 5/7, 6/7, ∞}.

V.2.3.4. Distribution of droplets volume within particular channel and across all channels

I calculated the distribution of the droplet size in particular channels in the same way as in subsection **V.2.2.2**. The obtained values of standard deviation were σ < 5% for each channel confirming a narrow distribution of the droplets size. **Figure 43** demonstrates mean values of the droplet length (L) obtained in the particular microchannel for different sets of flow rates.

According to the literature the viscosity of the droplet phase affects both the operational range of droplet generators, and the volume distribution of the droplets[4, 126, 134-137]. My calculations revealed that in spite of the significantly different viscosities and the variable ratio of the input streams, and the fact that each of the junctions was supplied with a different combination of the input streams, the device successfully generated uniform droplets. Furthermore, I observed that the higher the rates of flow, the lower the droplet size variance.

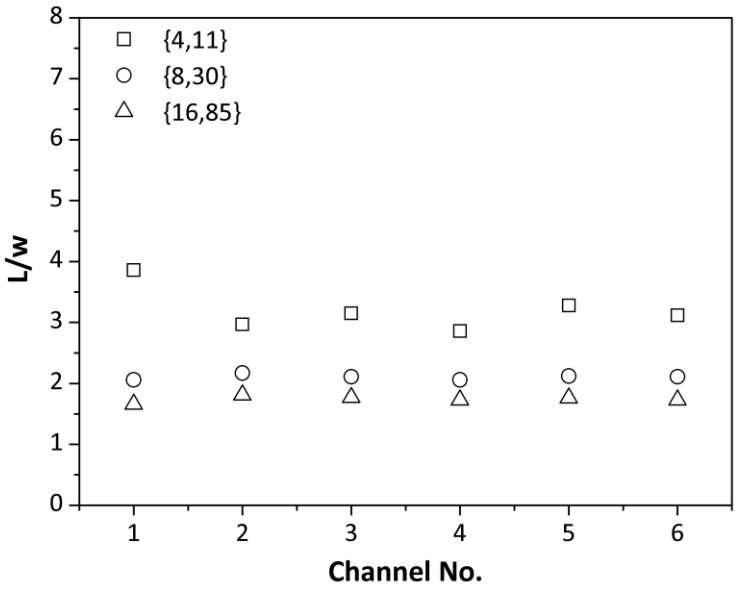

Figure 43. The dependence of normalized length of droplets on various rates of flow in particular microchannels for the system generating gradient of content from fluids of different viscosity. Symbols on the plot (circles, triangles and squares) refer to different settings of droplet and continous phases rates of flow {Q_D, Q_C} [mL/h].

I investigated the level of uniformity of volume of droplets across all microchannels by calculating the relative standard deviation lengths of droplets produced simultaneously. **Figure 44** clearly shows that the size distribution of droplets highly depends on the flow rate. According to collected data, the higher the rates of flow the better the uniformity of droplets. This feature is particularly significant for high throughput systems.

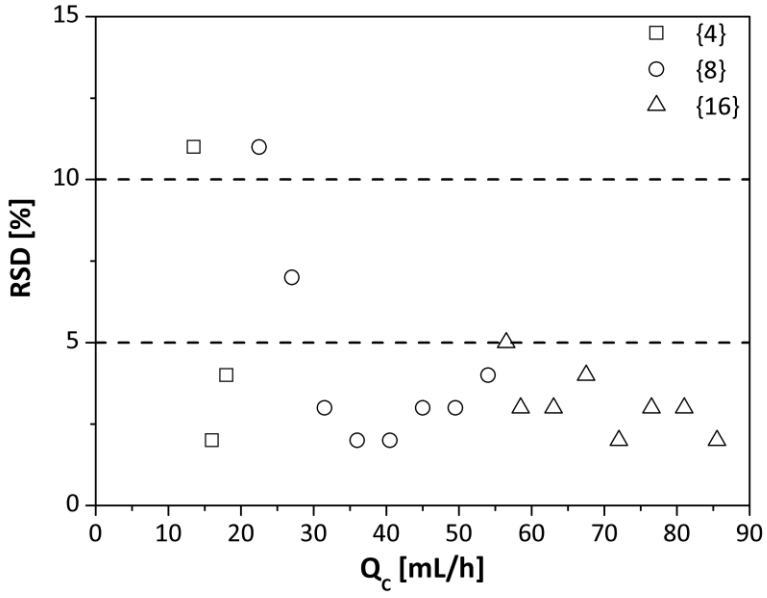

Figure 44. The dependance of the relative standard deviation of the droplet lengths on the flow rates of droplet (Q_D) and continuous (Q_C) phases in a gradient generator using fluids of differing viscosity. The symbols correspond to different flow rates of the droplet phase {Q_D} [mL/h].

V.2.3.5. Determination of the profile of concentrations

In order to experimentally confirm the designed profile of concentrations, I applied the same method of analysis as for the systems supplied with fluids of the same viscosity. **Figure 45** illustrates the reference curve (straight line) and experimentally determined linear gradient in parallel streams of droplets for the lowest and the highest setting of flow rates {Q_D,Q_C} ({4,9} mL/h and {16,85} mL/h). The image analysis revealed negligible differences in the theoretical and the experimental profiles. The correlation coefficients for the experimental and theoretical gradients obtained for wide range of flow rates are above 0.97 (**Figure 46**). This proves that the designed architecture of microchannels is suitable for gradient formation using liquids of differing viscosity.

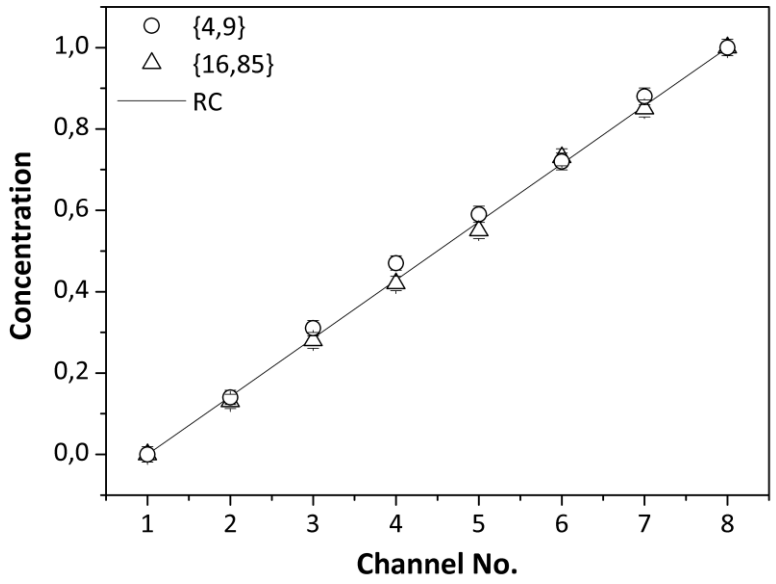

Figure 45. The experimental (symbols) and theoretical (solid line) concentration gradient obtained by mixing liquids of differing viscosity. The numbers in the wavy brackets correspond to the the droplet and continuous phases flow rates {Q_D, Q_C} [mL/h].

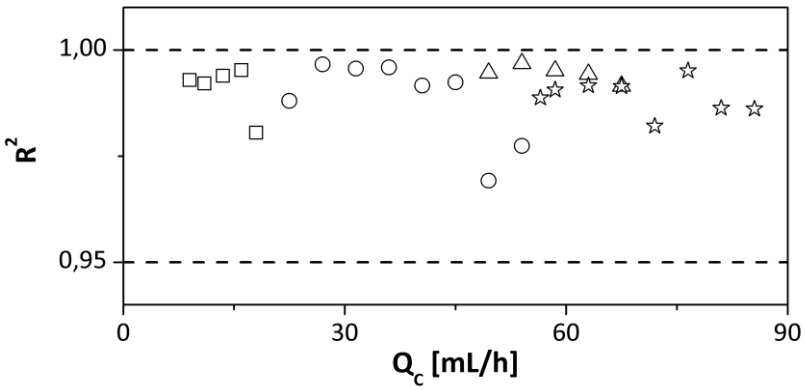

Figure 46. The dependence of R^2 on the flow rate of the continuous phase in gradient generator using fluids of differing viscosity. Symbols on the plot represent different values of the flow rate of the droplet phase Q_D (squares 2, triangles 4, circles 8, and stars 16 [mL/h]).

V.3. Formation of hydrogel blends in a microfluidic gradient generator

In the following subsections I investigated the possible application of the developed gradient generator for using fluids of differing viscosity (see subsection **V.2.3**) in production of hydrogel blends. Particularly, I focus on the working range of exploited microfluidic chip and its ability of maintaining designed profile of concentration as well as low size distribution of the droplets. Additionally, I evaluated the profile of release of model active substance (nanoparticles of gold) in acidic (pH=1.2) and neutral (pH=7.2) environment. Nanoparticles of gold were chosen as a model substance on the basis of their application in similar project[218] and prompt availability thanks to the courtesy of a co-worker from professor Marcin Fiałkowski's Group.

V.3.1. Characterization of the microfluidic system

To simplify and accelerate the characterization of production of emulsions I reduced the number of outlet channels from 8 to 6. Therefore the following ratios of alginate to pectin were available {0, 1/5, 2/5, 3/5, 4/5, 1}. Other procedures concerning fabrication of the system or modification of microchannels with dodecylamine[35], remained unchanged.

I introduced separate output at the end of each outlet channel to provide individual collection of produced hydrogel droplets. As input streams of the droplet phase I used 1 % solution of alginate comprising nanoparticles of gold and 1 % solution pectin (see subsection **IV.2.6**), and as continuous phase I used the rapeseed oil.

V.3.1.1. Working range

I assessed experimentally the maximal and minimal values of flow rate of the droplet ($Q_D = Q_A + Q_B$) and the continuous (Q_C) phases in order to determine the operating range of the system. I selected three values of Q_D, namely {3.6, 5 and 9 mL/h}, and kept them constant while changing the rates of flow of the continuous phase. The working range (**Figure 47**) for droplet regime turned out slightly narrower in comparison to the one investigated in the subsection **V.2.3.3** (**Figure 42**). The phenomenon is associated with the higher viscosities of both input streams of the droplet phase.

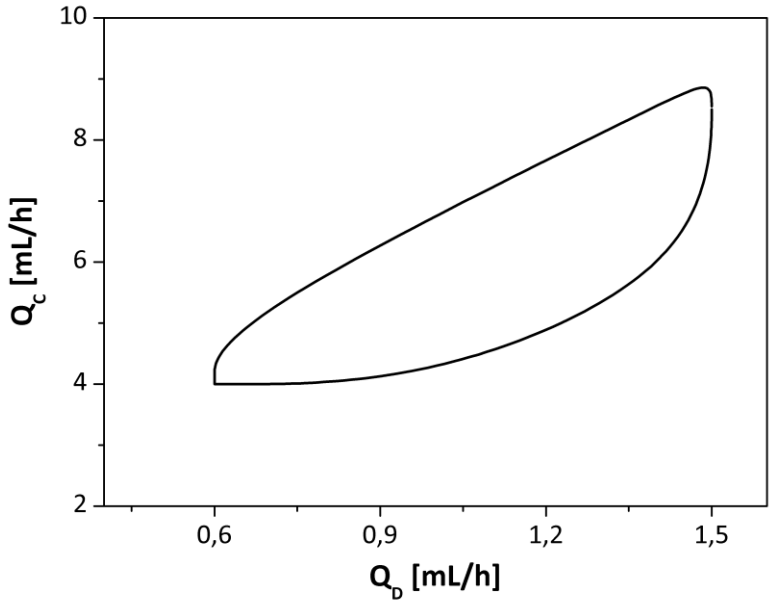

Figure 47. The working range of the gradient generator for fluids of differing viscosity, mixed in proportions Q_{NV}/Q_V = {0, 1/5, 2/5, 3/5, 4/5, ∞}.

V.3.1.2. The level of uniformity of the droplets

The system is characterized by high level of uniformity of volumes of droplets in particular channels (σ < 5 %). As in case of previous systems, the droplets size variance across all channels can be significantly higher. I calculated the RSD of droplet size for all parallel channels for fixed flow rates of droplet and continuous phases as in section **V.2.2.2**.

Figure 48 presents the dependence of the droplet size variance on the flow rates of both phases. According to the results, higher values of Q_D and Q_C promote lower distribution of droplet size. This, in turn, guaranties satisfying level of monodispersity (< 5 %) at higher throughput.

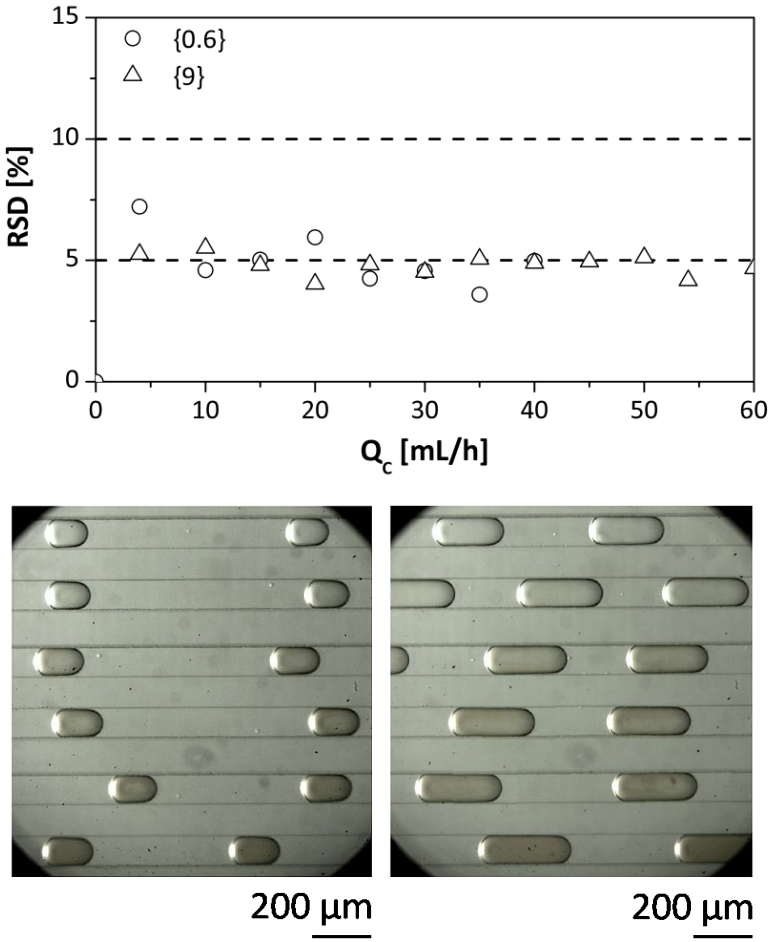

Figure 48. The dependance of the RSD of the droplet size on the flow rates of droplet (Q_D) and continuous (Q_C) phases in gradient generator using fluids of differing viscosity. The symbols correspond to different flow rate of the droplet phase{Q_D} [mL/h]. Two microphotographs illustrate microdroplets of different sizes, depending on the applied flow rate (left micrograph: Q_D=0,6 mL/h, Q_C=20 mL/h, right micrograph: Q_D=0,6 mL/h, Q_C=4 mL/h).

V.3.1.3. Determination of the profile of concentrations

The same procedure as in subsection (**V.2.2.3**) was used in order to assess the correlation between the theoretical and experimental concentration profiles. In order to visualize the differences in content of the droplets I used 1 % water solution of sodium alginate and 1 % water solution of pectin, enriched with gold nanoparticles.

Figure 49 presents the correlation between the reference curve (RC) of the theoretical gradient and experimentally determined linear concentration gradients. The profiles were obtained for parallel streams of droplets at the lowest and the highest flow rates {Q_D,Q_C} ({0.6,4} mL/h and {9,54} mL/h). Calculated values of R^2 are above 0.95, and mostly above 0.97, what confirms a high correlation of experiment with the design (**Figure 50**). The image analysis

reveals also only slight differences between theoretical and the experimental profiles. This proves the usefulness of the developed chip architecture in generation of well defined emulsions produced from substances of different viscosities.

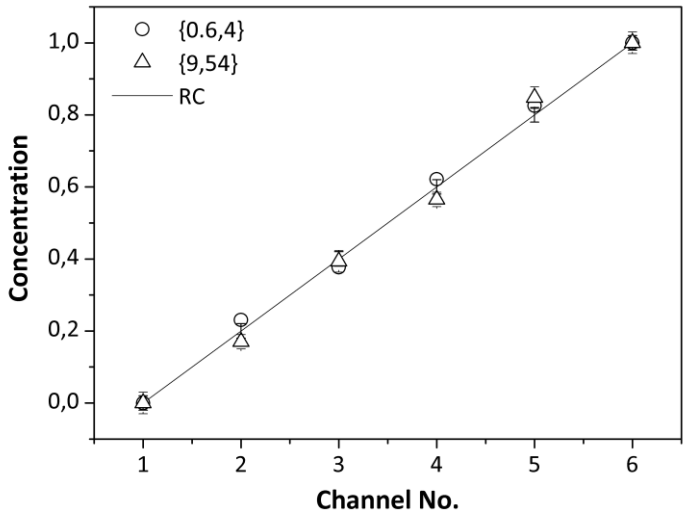

Figure 49. The experimental (symbols) and the designed (solid line) concentration gradients of gold nanoparticles enclosed in the droplets obtained from fluids of differing viscosities. The numbers in the wavy brackets correspond to the flow rates {Q_D, Q_C} [mL/h].

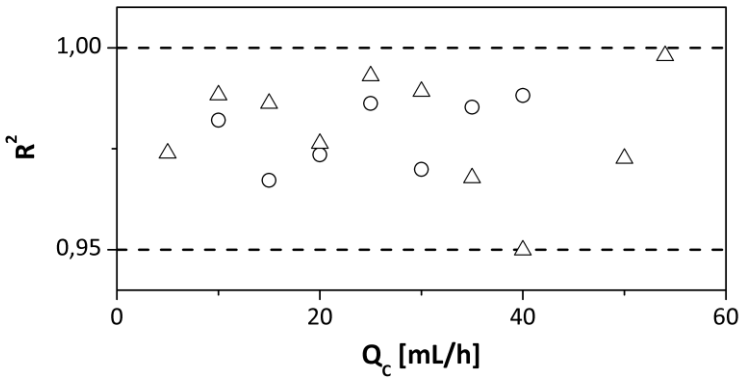

Figure 50. The dependence of R^2 on the flow rate of the continuous phase in a gradient generator using fluids of differing viscosity. Symbols on the plot correspond to the flow rate of the droplet phase Q_D (circles 3.6 and triangles 9 [mL/h]).

V.3.2. Formation of gel particles

In the final stage of the experiment I utilized the developed microfluidic system for high throughput generation of hydrogel particles. I used 1 % aqueous solutions of pectin and sodium alginate prepared accordingly to the description presented in subsection **IV.2.6**. Rapeseed oil was used as the continuous phase.

I produced the hydrogel droplets using the highest possible flow rate (Q_D=9 mL/h; Q_C=54 mL/h) and transferred them via polyethylene tubing directly to biphasic bath containing cross-linking agent (Ca^{2+}). I used separate containers to collect hydrogel droplets of different content (**Figure 51**). Each container was filled with 2 mL of aqueous phase (1 M solution of calcium chloride) forming a layer at the bottom of the container and 5 mL of organic phase (rapeseed oil with suspended calcium ions) forming the top layer.

Hydrogel droplets traveled through the tubings to the container with biphasic bath (see subsection **IV.2.8**). On their way across the organic phase the droplets were initially penetrated by calcium ions suspended in the oil. I observed that the partially solidified entities presented the tendency to gather at the interphase. After several minutes, the droplets precipitated to the bottom of container through the aqueous solution of calcium chloride.

I continued the solidification of produced particles in the presence of calcium ions for an hour. After that period I carried on to the procedure of purification, described in the subsection **IV.2.9**.

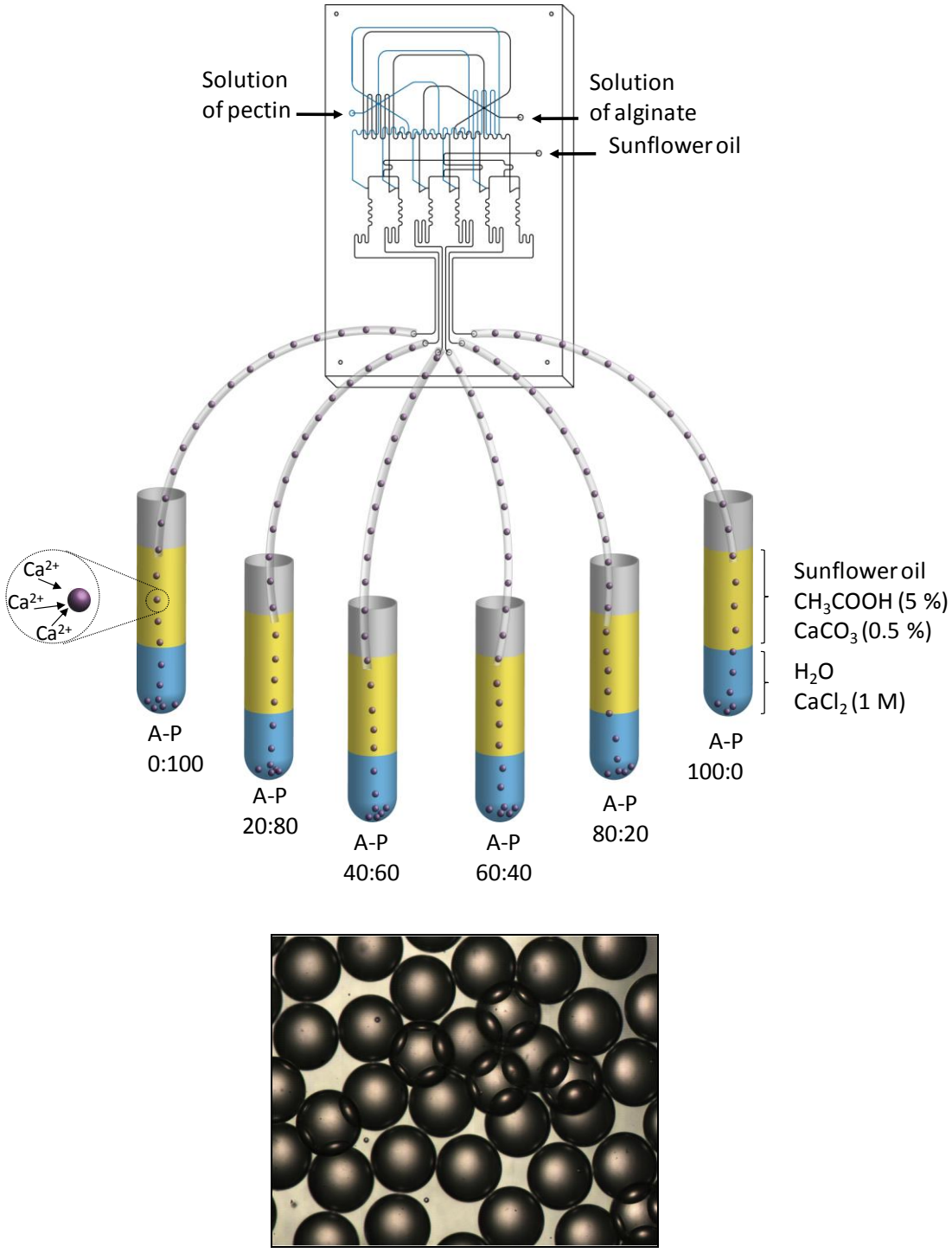

Figure 51. Schematic presentation of a set up for preparation of hydrogel microparticles. Upper part of the scheme presents the microfluidic chip designed for simultaneous generation of emulsions of different proportion of alginate (A) and pectin (P). The system is connected to a set of separate containers with polyethylene tubings that are used for the transport of generated droplets directly into biphasic bath enriched with cross-linking agent (Ca^{2+}). The upper phase of the bath (yellow) contains calcium ions suspended in rapeseed oil, whereas the bottom phase (blue) – dissolved in water. The microphotograph shows microdroplets in the early stage of cross-linking *i.e*. suspended in the oil phase.

V.3.3. Release of model active substance from the microbeads

In order to evaluate the process of slow release of gold nanoparticles entrapped inside hydrogel microparticles firstly I recovered solidified microgels from biphasic bath. Next, I rinsed them with distilled water as described in the subsection **IV.2.8**.

I selected two values of pH for imitation of *in-vivo* environments: i) pH=1.2 and ii) pH=7.2, corresponding to the pH in the stomach and in blood, respectively. I used hydrochloric acid (HCl) to create strongly acidic environment and borate buffer to provide neutral conditions.

At the beginning of the study I weighted 200 mg (wet mass) of each batch of microgels in two series of separate vials. I added 1 mL of HCl to the first set of the vials and 1 mL of the borate buffer to the other. The prepared samples were placed in the Mini Rocker (MR-1, BIOSAN), and agitated gently.

I analyzed the supernatant for the concentration of gold nanoparticles immediately after the initial sedimentation of microgels (t=0) and in the following time points: 0.5, 1, 2, 3, 4, 5 h. After each measurement the solution was returned to the vial. I carried out the measurements spectrophotometrically using Multi-Spec Spec-1501 Shimadzu spectrophotometer (Japan) to measure the absorbance of the solution taken from above the microgels at wave at λ=525 nm (absorbance maximum for the gold nanoparticles).

In both low and neutral pH conditions I observed the release of gold nanoparticles regardless of the microgels composition (**Figure 52** and **53**). The differences in the release for distinct values of pH and alginate to pectin ratio correspond to the results of the study performed by Jaya *et. al*.[226], and the obtained release profiles indicate the following:

- the process is most effective in strongly acidic environment from pectin-rich micorgels
- addition of alginate introduces some resistance of microgels to acidic conditions
- in the neutral pH, the differences in the process are less apparent but the trend of release for all studied compositions of microgels is preserved.

The experiment is a straightforward illustration of screening possibilities of the designed system. The chip clearly allows for simultaneous studies of release profiles from carriers of varied composition. Moreover, the results presented in this subsection as well as in subsection **V.2.3.** demonstrate that providing a well defined network of microchannels (see subsection **V.2.1**) together with elimination of parts of architecture based on laminar flow (typically applied for generation of gradient[75-82]) is sufficient to keep the designed gradient of concentrations.

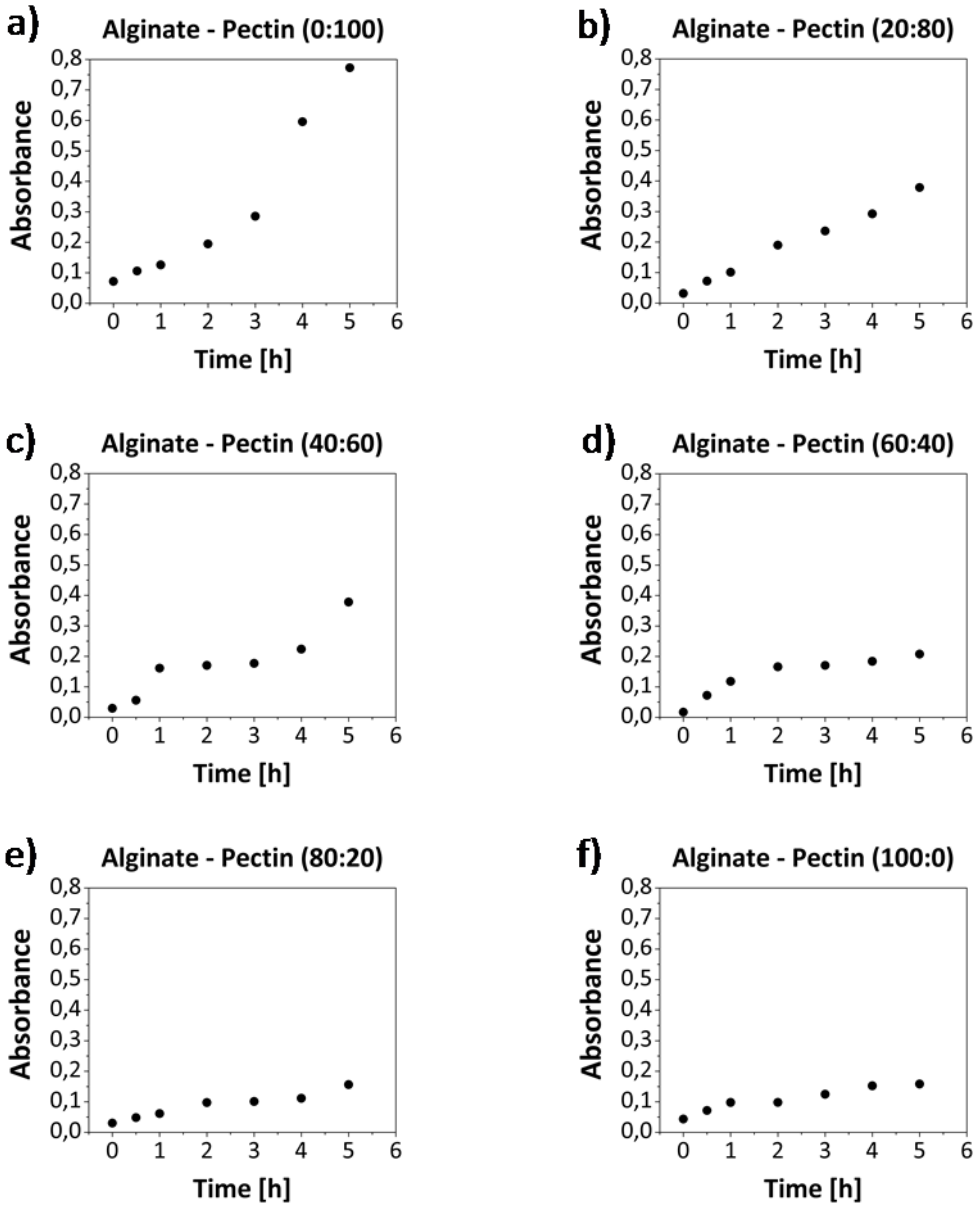

Figure 52. A set of plots illustrating the release profiles of gold nanoparticles from microgels under strongly acidic conditions (pH=1.2). Each plot corresponds to the specific composition of microgels. The absorbance was measured at λ=525 nm.

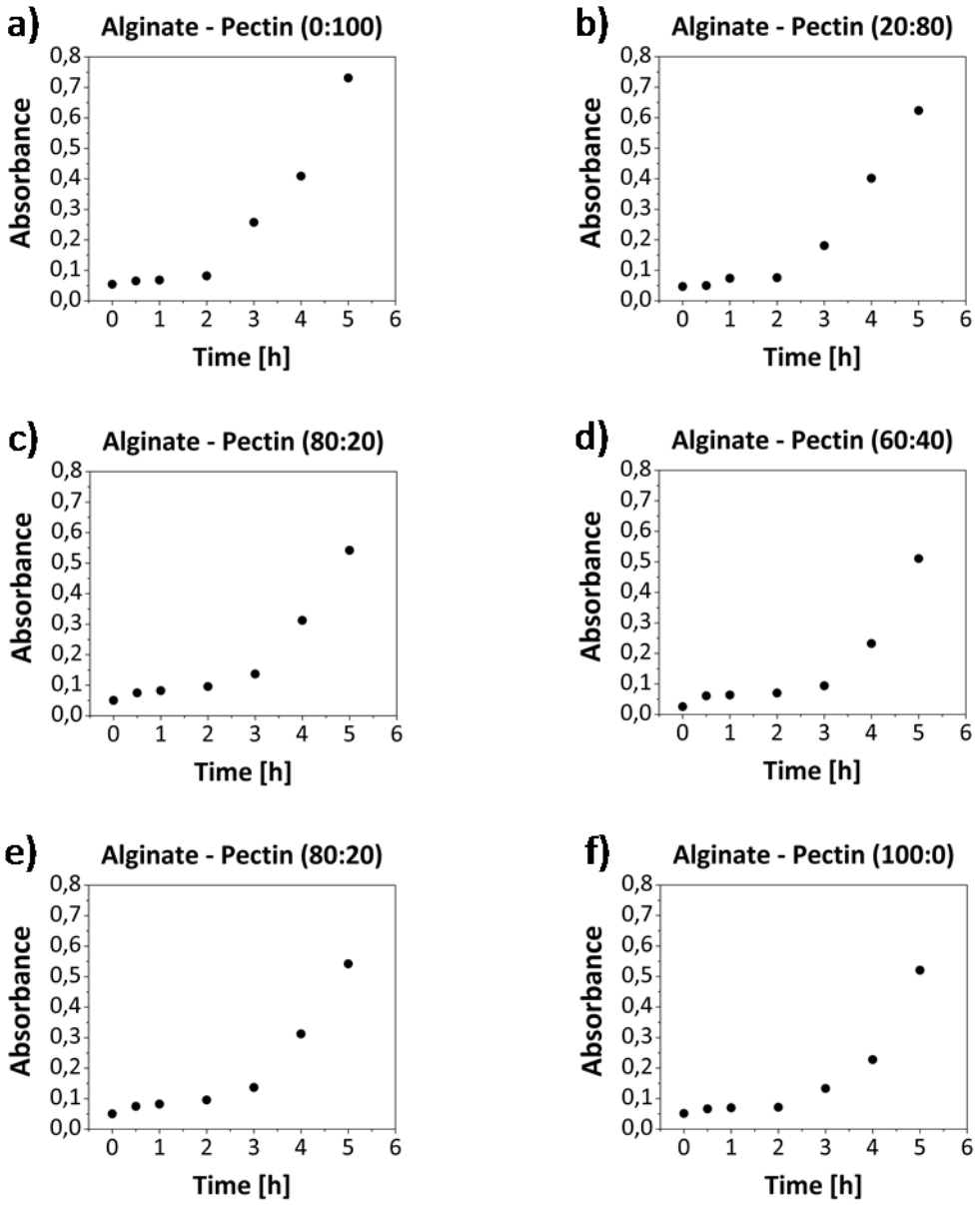

Figure 53. A set of plots illustrating the release profiles of gold nanoparticles from microgels under neutral conditions(pH=7.2). Each plot corresponds to the specific composition of microgels. The absorbance was measured at λ=525 nm .

VI. Discussion and summary

In the thesis I have detailed the design, fabrication and operation of novel microfluidic systems that can be employed in: i) generation of gradient of concentrations in parallel streams of droplets regardless of the values of the shear viscosity coefficients of the used fluids, and for ii) maximization of the throughput of the system. Additionally, as the result of conducted studies, I applied the developed microfluidic device to generation of droplets containing blends of two polysaccharides – alginate and pectin – mixed at different proportions. I investigated the release profiles of a model active substance (gold nanoparticles) from the obtained microparticles.

The bonding is a crucial stage of the procedure dedicated to manufacturing of microfluidic systems. The procedure I developed for bonding polycarbonate substrates guaranties strong and durable seal. The main advantage of the procedure is elimination of its influence on both the properties of the surface and the cross-section of microstructures (*e.g*. microchannels). The method involves application of a custom made set up consisting of a vacuum pump (VAC), a desiccator where PC slabs are placed, a flask with a solvent, and stirrer providing better vapors distribution inside the desiccator (**Figure 18.**). In the experiment the polymeric surfaces were exposed to the vapors of selected substances: dichloromethane (DCM), methylethyl ketone (MEK) or acetone (MKK). The subsequent compression of modified substrates at an elevated temperature (not exceeding the temperature of polycarbonate's glass transition, T_g = 145 ^{o}C) did not affect the surface of microchannels. The developed method presents several advantages in comparison to the traditionally used procedures of (i) thermal[24-28], (ii) chemical[29-33] or (iii) adhesive[36-38] bonding. Although thermal bonding is an easy and inexpensive method for obtaining a durable seal it also is strongly limited as it involves compressing the elements under elevated temperature, close to the temperature of glass transition (T_g)[24-28]. Application of high temperatures together with high pressure often causes deformation of microchannels. The chemical[29-316] and adhesive[36-38] methods usually do not influence the cross-sections of microstructures, however they often affect the properties of the surface. The first one requires application of two different reagents that are capable to react with the used polymer and with each other. The modification of surface with this type of reagent is the first step of chemical bonding procedure. The next step involves a chemical reaction between the modified surfaces. Modification of the surface results in alteration of its chemistry. Different modification of substrates surfaces may also result in uneven wetting properties along the microchannels perimeter. Considering that the developed method exploits

the substances that are only solvents or swelling agents they do not change the chemistry or wetting properties of the surface.

By introducing mild conditions I eliminated the problem of deformation of microchannels' geometry, a common issue of thermal bonding. Since the proposed method does not affect the chemistry of the surface, both wettability and transparency of the native polycarbonate are preserved. Such a durable bonding (undergoing delamination under the pressure higher than 0.4 MPa) can be successfully applied in fabrication of any microfluidic chip made of polycarbonate. However, considering that the composition of PC's may vary from different manufacturers, the method may require reoptimization before application.

The developed methodology allowed me to manufacture a well bonded microfluidic systems, where both the geometry of the channels and their surface properties remained unaffected by the fabrication process. In the following sections of the thesis I introduced the design and the use of microfluidic systems obtained with the optimized bonding procedure. The systems that I demonstrated produce linear and logarithmic concentration gradients in the droplets over a wide range of flow rates. This allowed me to i) tune the volume from 5 to 80 nL and to ii) maximize the throughput of the system up to *ca.* 6 or 2 mL/h per single junction, while applying fluids of the same or different viscosity, respectively .

The generation of gradient of concentrations in the proposed systems relies only on hydrodynamics and does not require any additional active modules such as valves or electronic systems to control [144]. As it is well known, low to moderate values of Reynolds numbers that are typical to microfluidics, result in laminar flow and purely diffusional mixing[41]. In the case of continuous flow gradient generators the concentration is defined and controlled by precisely designed network of microchannels. The typical architecture dedicated to serial dilution is based on a network of channels that take two or more input streams and then iteratively split, combine, and mix their flows to create N outputs of designed combinations[75-82]. The developed architecture of the chips allows for elimination of the reliance solely on the diffusive mixing in the process of gradient generation from input streams. Additionally, by providing active mixing inside the droplets[118] and hydrophobic modification of the microchanels' surface[35] the developed methodology enhanced the throughput of the systems.

Moreover, the architecture enabling the transport of input streams directly to the K-junctions rendered my system independent of the fluids viscosity in contrary to other gradient generators[75-84] that often require additional linearization[99]. This property presents a great potential in numerous biological and pharmaceutical applications. To the best of my knowledge, conducted study for the first time addresses the influence of the order in which fluids of

different viscosities are delivered to the K-junction on the working range of the microfluidic system. The obtained results show that the transition point from the dripping to jetting regime shifts to higher rates of flow when the less viscous fluid enters from the K-junction to the main channel first. This observation proves that the operating range is principally determined by the viscosity of the fluid that flows adjacent to the wall of the microchannel.

A potential drawback of the architecture proposed in the thesis, in comparison to the systems that mix the input streams at different combinations[142-144] is that the maximum ratio of output concentrations in the droplets corresponds to a ratio of resistances of the channels that deliver input streams into the confluent point. Due to this fact in the design that keeps the cross-sections of all the channels similar, production of gradient over many orders of magnitude is significantly hindered. With precise fabrication schemes it is, however, possible to obtain a large span of resistances of the delivery channels by varying their cross-sections.

Finally, the possibility to generate parallel streams of well defined droplets from liquids of different viscosities, made the system noteworthy in preparative applications that frequently involve viscous solutions of polymers to form fully or partially solidified microparticles. Using hydrogels additionally enhances the spectrum of applications as these materials reveal high biocompatibility and biodegradability – properties highly valued in medicine, pharmacy and food industry. Moreover, both alginate and pectins – hydrogels exploited in the thesis – are often recommended as a perfect material for encapsulation of drugs[219], enzymes[211], microorganisms[6] or even cells[7].

In the part dedicated to formation of pectin-alginate capsules I used the well described gradient generating system for high throughput production of hydrogel particles. I used aqueous solutions of sodium alginate and pectin, both enriched with gold nanoparticles, in order to study release profiles of the model active substance (Au nanoparticles) entrapped inside hydrogel microparticles. Similar tests have been conducted by Ogończyk *et al.*, who investigated decomposition of pectin microparticles in the presence of ethylenediaminetetraacetic acid (EDTA) combined with the release of gold nanoparticles. Unlike to these experiments I used acidic (pH=1.2) and neutral (pH=7.2) environment imitating *in-vivo* conditions in order to investigate the release process of gold nanoparticles. In accordance with the literature[226] the decomposition of microparticles depended on the alginate to pectin ratio. The obtained results indicate that the control over composition of microparticles and the ability to create them simultaneously can be particularly useful in screening of release profiles.

The novelty of the PhD thesis includes the following:

- a new method for bonding polycarbonate substrates,

- a new design of a chip that maximizes the throughput of simultaneous droplets generation with gradual changes in their content,

- a study of the influence of viscosity on the working range of a the gradient generator,

- development of a droplet-gradient generator capable of forming droplets using viscous solutions of polymers and their mixtures,

- generation of composite micro-gel particles containing model active substance for the design release profile design and evaluation.

I am convinced that the methods and systems described in this thesis will contribute to the foundation on which new tools for the pharmaceutical and cosmetic industries can be developed.

VII. Acknowledgements

The Project was operated within the Foundation for Polish Science Team Programme and co-financed by the EU within the European Regional Development Fund, through the grant Innovative Economy (POIG.01.01.02-00-008/08).

I would like to express my gratitude to

My Supervisor, Professor Piotr Garstecki, for the opportunity of taking part in described projects as well as his patience and motivation for further work.

Dominika Ogończyk, Ph.D., and Adam Samborski, Ph.D. for the direct cooperation in the projects, their scientific support and assistance.

Ewelina Kalwarczyk, Ph.D from the group of Professor Marcin Fiałkowski, for preparation of gold nanoparticles.

All of my Friends and Colleagues for their support and help.

And last but not least I'm grateful to my Parents for taking care of my education, encouraging me to follow my dreams and trust my choices.

VIII. List of publications and patent applications

VIII.1. Publications

D. Ogonczyk, J. Wegrzyn, P. Jankowski, B. Dabrowski and P. Garstecki, 'Bonding of microfluidic devices fabricated in polycarbonate', *Lab on a Chip*, 2010, 10, 1324–327

J. Wegrzyn, A. Samborski, L. Reissig, P. M. Korczyk, S. Blonski and P. Garstecki, 'Microfluidic architectures for efficient generation of chemistry gradations in droplets' *Microfluidics and Nanofluidics*, 2013, 14, 235–245

VIII.2. Patent applications

Dominika Ogończyk, Judyta Węgrzyn, Paweł Jankowski, Piotr Garsteczki, 'Sposób sklejania płyt poliwęglanowych z zachowaniem ich mikro-struktury powierzchniowej oraz urządzenie do stosowania tego sposobu', (2010)

IX. References

1. S. Jakiela, S. Makulska, P. M. Korczyk and P. Garstecki, *Lab on a Chip*, 2011, **11**, 3603-3608.
2. S. Jakiela, P. M. Korczyk, S. Makulska, O. Cybulski and P. Garstecki, *Physical Review Letters*, 2012, **108**, 134501: 1-5.
3. J. D. Tice, H. Song, A. D. Lyon and R. F. Ismagilov, *Langmuir*, 2003, **19**, 9127-9133.
4. J. D. Tice, A. D. Lyon and R. F. Ismagilov, *Analytica Chimica Acta*, 2004, **507**, 73-77.
5. Z. T. Cygan, J. T. Cabral, K. L. Beers and E. J. Amis, *Langmuir*, 2005, **21**, 3629-3634.
6. W.-P. Voo, P. Ravindra, B.-T. Tey and E.-S. Chan, *Journal of Bioscience and Bioengineering*, 2011, **111**, 294-299.
7. S. Wiedemeier, F. Ehrhart, E. Mettler, G. Gastrock, T. Forst, M. M. Weber, H. Zimmermann and J. Metze, *Engineering in Life Sciences*, 2011, **11**, 165-173.
8. M. Y. He, J. S. Edgar, G. D. M. Jeffries, R. M. Lorenz, J. P. Shelby and D. T. Chiu, *Analytical Chemistry*, 2005, **77**, 1539-1544.
9. Y. C. Tan, K. Hettiarachchi, M. Siu and Y. P. Pan, *Journal of the American Chemical Society*, 2006, **128**, 5656-5658.
10. B. Zheng, C. J. Gerdts and R. F. Ismagilov, *Current Opinion in Structural Biology*, 2005, **15**, 548-555.
11. L. Y. Chu, A. S. Utada, R. K. Shah, J. W. Kim and D. A. Weitz, *Angewandte Chemie-International Edition*, 2007, **46**, 8970-8974.
12. C.-Y. Yu, B.-C. Yin, W. Zhang, S.-X. Cheng, X.-Z. Zhang and R.-X. Zhuo, *Colloids and Surfaces B-Biointerfaces*, 2009, **68**, 245-249.
13. H. Becker, ed. L. E. Locascio, Talanta, 2002, vol. 56, pp. 267–287.
14. J. N. Lee, C. Park and G. M. Whitesides, *Analytical Chemistry*, 2003, **75**, 6544-6554.
15. L. L. Clements, *Engineering Plastics, Engineered Materials Handbook*, Metals Park, ASM International, 1988.
16. M. Stickler and T. Rhein, *Polymethacrylates, Ullmann's Encyclopedia of Industrial Chemistry*, New York, 1992.
17. J. Y. Shin, J. Y. Park, C. Y. Liu, J. S. He and S. C. Kim, *Pure and Applied Chemistry*, 2005, **77**, 801-814.
18. K. Friedrich, H. J. Sue, P. Liu and A. A. Almajid, *Tribology International*, 2011, **44**, 1032-1046.
19. D. A. Scola, *Polyimide Resins, Constituent Materials*, ASM Handbook 21 Composites, 2001.
20. L. Martynova, L. E. Locascio, M. Gaitan, G. W. Kramer, R. G. Christensen and W. A. MacCrehan, *Analytical Chemistry*, 1997, **69**, 4783-4789.
21. R. M. McCormick, R. J. Nelson, M. G. AlonsoAmigo, J. Benvegnu and H. H. Hooper, *Analytical Chemistry*, 1997, **69**, 2626-2630.
22. S. Yang and D. L. Devoe, *Methods in molecular biology (Clifton, N.J.)*, 2013, **949**, 115-123.
23. E. R. G. O. Rodrigues and R. A. S. Lapa, *Analytical Sciences*, 2009, **25**, 443-448.
24. J. N. Yang, Y. J. Liu, C. B. Rauch, R. L. Stevens, R. H. Liu, R. Lenigk and P. Grodzinski, *Lab on a Chip*, 2002, **2**, 179-187.
25. Y. J. Liu, C. B. Rauch, R. L. Stevens, R. Lenigk, J. N. Yang, D. B. Rhine and P. Grodzinski, *Analytical Chemistry*, 2002, **74**, 3063-3070.
26. K.-S. Hong, J. Wang, A. Sharonov, D. Chandra, J. Aizenberg and S. Yang, *Journal of Micromechanics and Microengineering*, 2006, **16**, 1660-1666.
27. M. H. Sorouraddin, M. Amjadi and M. Safi-Shalamzari, *Analytica Chimica Acta*, 2007, **589**, 84-88.
28. H. Shadpour, M. L. Hupert, D. Patterson, C. Liu, M. Galloway, W. Stryjewski, J. Goettert and S. A. Soper, *Analytical Chemistry*, 2007, **79**, 870-878.
29. J. C. McDonald and G. M. Whitesides, *Accounts of Chemical Research*, 2002, **35**, 491-499.
30. W. Zhang, S. Lin, C. Wang, J. Hu, C. Li, Z. Zhuang, Y. Zhou, R. A. Mathies and C. J. Yang, *Lab on a Chip*, 2009, **9**, 3088-3094.
31. J. Kim, M. K. Chaudhury and M. J. Owen, *Journal of Colloid and Interface Science*, 2000, **226**, 231-236.
32. N. Y. Lee and B. H. Chung, *Langmuir*, 2009, **25**, 3861-3866.
33. K. S. Lee and R. J. Ram, *Lab on a Chip*, 2009, **9**, 1618-1624.
34. L. Derzsi, P. Jankowski, W. Lisowski and P. Garstecki, *Lab on a Chip*, 2011, **11**, 1151-1156.
35. P. Jankowski, D. Ogonczyk, A. Kosinski, W. Lisowski and P. Garstecki, *Lab on a Chip*, 2011, **11**, 748-752.
36. A. Gerlach, H. Lambach and D. Seidel, *Microsystem Technologies-Micro-and Nanosystems-Information Storage and Processing Systems*, 1999, **6**, 19-22.
37. D. Maas, B. Bustgens, J. Fahrenberg, W. Keller, P. Ruther, W. K. Schomburg, D. Seidel and Ieee, Fabrication of microcomponents using adhesive bonding techniques, San Diego, Ca, 1996.

38. H.-Y. Chen, A. A. McClelland, Z. Chen and J. Lahann, *Analytical Chemistry*, 2008, **80**, 4119-4124.
39. C. Y. Lee, C. L. Chang, Y. N. Wang and L. M. Fu, *International Journal of Molecular Sciences*, 2011, **12**, 3263-3287.
40. C. M. Karst, B. D. Storey and J. B. Geddes, *Physics of Fluids*, 2013, **25**.
41. P. J. A. Kenis, R. F. Ismagilov and G. M. Whitesides, *Science*, 1999, **285**, 83-85.
42. M. Yamada and M. Seki, *Lab on a Chip*, 2005, **5**, 1233-1239.
43. M. Yamada and M. Seki, *Analytical Chemistry*, 2006, **78**, 1357-1362.
44. S. Yang, A. Undar and J. D. Zahn, *Lab on a Chip*, 2006, **6**, 871-880.
45. R. D. Jaeggi, R. Sandoz and C. S. Effenhauser, *Microfluidics and Nanofluidics*, 2007, **3**, 47-53.
46. L. R. Huang, E. C. Cox, R. H. Austin and J. C. Sturm, *Science*, 2004, **304**, 987-990.
47. D. W. Inglis, J. A. Davis, R. H. Austin and J. C. Sturm, *Lab on a Chip*, 2006, **6**, 655-658.
48. T. A. J. Duke and R. H. Austin, *Physical Review Letters*, 1998, **80**, 1552-1555.
49. C. F. Chou, O. Bakajin, S. W. P. Turner, T. A. J. Duke, S. S. Chan, E. C. Cox, H. G. Craighead and R. H. Austin, *Proceedings of the National Academy of Sciences of the United States of America*, 1999, **96**, 13762-13765.
50. L. R. Huang, J. O. Tegenfeldt, J. J. Kraeft, J. C. Sturm, R. H. Austin and E. C. Cox, *Nature Biotechnology*, 2002, **20**, 1048-1051.
51. J. Fu, R. B. Schoch, A. L. Stevens, S. R. Tannenbaum and J. Han, *Nature Nanotechnology*, 2007, **2**, 121-128.
52. K. Hanning, Journal of Chromatography A, 1978, vol. 159.
53. L. Krivankova and P. Bocek, *Electrophoresis*, 1998, **19**, 1064-1074.
54. H. Kobayashi, K. Shimamura, T. Akaida, K. Sakano, N. Tajima, J. Funazaki, H. Suzuki and E. Shinohara, *Journal of Chromatography A*, 2003, **990**, 169-178.
55. D. Kohlheyer, G. A. J. Besselink, S. Schlautmann and R. B. M. Schasfoort, *Lab on a Chip*, 2006, **6**, 374-380.
56. C. X. Zhang and A. Manz, *Analytical Chemistry*, 2003, **75**, 5759-5766.
57. S. Choi and J. K. Park, *Lab on a Chip*, 2005, **5**, 1161-1167.
58. I. Doh and Y. H. Cho, *Sensors and Actuators a-Physical*, 2005, **121**, 59-65.
59. K. E. McCloskey, L. R. Moore, M. Hoyos, A. Rodriguez, J. J. Chalmers and M. Zborowski, *Biotechnology Progress*, 2003, **19**, 899-907.
60. G. Blankenstein and U. D. Larsen, *Biosensors & Bioelectronics*, 1998, **13**, 427-438.
61. W. T. Coakley, *Trends in Biotechnology*, 1997, **15**, 506-511.
62. T. Laurell, F. Petersson and A. Nilsson, *Chemical Society Reviews*, 2007, **36**, 492-506.
63. M. P. MacDonald, G. C. Spalding and K. Dholakia, *Nature*, 2003, **426**, 421-424.
64. G. Milne, D. Rhodes, M. MacDonald and K. Dholakia, *Optics Letters*, 2007, **32**, 1144-1146.
65. B. Nagel, H. Dellweg and L. M. Gierasch, *Pure and Applied Chemistry*, 1992, **64**, 143-168.
66. V. Barron, E. Lyons, C. Stenson-Cox, P. E. McHugh and A. Pandit, *Annals of Biomedical Engineering*, 2003, **31**, 1017-1030.
67. J. M. Bolivar, J. Wiesbauer and B. Nidetzky, *Trends in Biotechnology*, 2011, **29**, 333-342.
68. M. Miyazaki and H. Maeda, *Trends in Biotechnology*, 2006, **24**, 463-470.
69. R. A. Sheldon, *Advanced Synthesis & Catalysis*, 2007, **349**, 1289-1307.
70. M. D. Busto, K. E. Garcia-Tramontin, N. Ortega and M. Perez-Mateos, *Bioresource Technology*, 2006, **97**, 1477-1483.
71. F. Vaillant, A. Millan, P. Millan, M. Dornier, M. Decloux and M. Reynes, *Process Biochemistry*, 2000, **35**, 989-996.
72. H. K. Wu, B. Huang and R. N. Zare, *Journal of the American Chemical Society*, 2006, **128**, 4194-4195.
73. V. V. Abhyankar, M. A. Lokuta, A. Huttenlocher and D. J. Beebe, *Lab on a Chip*, 2006, **6**, 389-393.
74. S.-Y. Cheng, S. Heilman, M. Wasserman, S. Archer, M. L. Shuler and M. Wu, *Lab on a Chip*, 2007, **7**, 763-769.
75. S. K. W. Dertinger, X. Y. Jiang, Z. Y. Li, V. N. Murthy and G. M. Whitesides, *Proceedings of the National Academy of Sciences of the United States of America*, 2002, **99**, 12542-12547.
76. F. Lin, W. Saadi, S. W. Rhee, S. J. Wang, S. Mittal and N. L. Jeon, *Lab on a Chip*, 2004, **4**, 164-167.
77. C. Neils, Z. Tyree, B. Finlayson and A. Folch, *Lab on a Chip*, 2004, **4**, 342-350.
78. M. Yamada, T. Hirano, M. Yasuda and M. Seki, *Lab on a Chip*, 2006, **6**, 179-184.
79. D. Irimia, S. Y. Liu, W. G. Tharp, A. Samadani, M. Toner and M. C. Poznansky, *Lab on a Chip*, 2006, **6**, 191-198.
80. C. Kim, K. Lee, J. H. Kim, K. S. Shin, K.-J. Lee, T. S. Kim and J. Y. Kang, *Lab on a Chip*, 2008, **8**, 473-479.
81. K. Lee, C. Kim, Y. Kim, K. Jung, B. Ahn, J. Y. Kang and K. W. Oh, *Biomedical Microdevices*, 2010, **12**, 297-309.
82. K. Hattori, S. Sugiura and T. Kanamori, *Lab on a Chip*, 2009, **9**, 1763-1772.

83. S. K. W. Dertinger, D. T. Chiu, N. L. Jeon and G. M. Whitesides, *Analytical Chemistry*, 2001, **73**, 1240-1246.
84. K. Campbell and A. Groisman, *Lab on a Chip*, 2007, **7**, 264-272.
85. B. McDonald, K. Pittman, G. B. Menezes, S. A. Hirota, I. Slaba, C. C. M. Waterhouse, P. L. Beck, D. A. Muruve and P. Kubes, *Science*, 2010, **330**, 362-366.
86. A. Mantovani, M. A. Cassatella, C. Costantini and S. Jaillon, *Nature Reviews Immunology*, 2011, **11**, 519-531.
87. A. Muller, B. Homey, H. Soto, N. F. Ge, D. Catron, M. E. Buchanan, T. McClanahan, E. Murphy, W. Yuan, S. N. Wagner, J. L. Barrera, A. Mohar, E. Verastegui and A. Zlotnik, *Nature*, 2001, **410**, 50-56.
88. M. A. O. Mendonca, F. Q. Cunha, E. F. C. Murta and B. M. Tavares-Murta, *Cancer Chemotherapy and Pharmacology*, 2006, **57**, 663-670.
89. G. E. Carpagnano, G. P. Palladino, D. Lacedonia, A. Koutelou, S. Orlando and M. P. Foschino-Barbaro, *Bmc Cancer*, 2011, **11**, 1-9.
90. S. Boyden, *Journal of Experimental Medicine*, 1962, **115**, 453-466.
91. S. H. Zigmond, *Journal of Cell Biology*, 1977, **75**, 606-616.
92. A. F. Brown, *Journal of Cell Science*, 1982, **58**, 455-467.
93. D. Zicha, G. A. Dunn and A. F. Brown, *Journal of Cell Science*, 1991, **99**, 769-775.
94. D. Kim and C. L. Haynes, *Analytical Chemistry*, 2012, **84**, 6070-6078.
95. G. M. Walker, J. Q. Sai, A. Richmond, M. Stremler, C. Y. Chung and J. P. Wikswo, *Lab on a Chip*, 2005, **5**, 611-618.
96. S. J. Wang, W. Saadi, F. Lin, C. M. C. Nguyen and N. L. Jeon, *Experimental Cell Research*, 2004, **300**, 180-189.
97. W. Saadi, S. J. Wang, F. Lin and N. L. Jeon, *Biomedical Microdevices*, 2006, **8**, 109-118.
98. T. Liu, C. Li, H. Li, S. Zeng, J. Qin and B. Lin, *Electrophoresis*, 2009, **30**, 4285-4291.
99. H. A. Yusuf, S. J. Baldock, P. R. Fielden, N. J. Goddard, S. Mohr and B. J. T. Brown, *Microfluidics and Nanofluidics*, 2010, **8**, 587-598.
100. M.-P. N. Bui, C. A. Li, K. N. Han, J. Choo, E. K. Lee and G. H. Seong, *Analytical Chemistry*, 2011, **83**, 1603-1608.
101. Z. Han, W. Li, Y. Huang and B. Zheng, *Analytical Chemistry*, 2009, **81**, 5840-5845.
102. H. Karbstein and H. Schubert, *Chemical Engineering and Processing*, 1995, **34**, 205-211.
103. I. Kobayashi, Y. Murayama, T. Kuroiwa, K. Uemura and M. Nakajima, *Microfluidics and Nanofluidics*, 2009, **7**, 107-119.
104. T. Nisisako, S. Okushima and T. Torii, *Soft Matter*, 2005, **1**, 23-27.
105. J. H. Xu, S. W. Li, J. Tan, Y. J. Wang and G. S. Luo, *Aiche Journal*, 2006, **52**, 3005-3010.
106. J. H. Xu, S. W. Li, J. Tan, Y. J. Wang and G. S. Luo, *Langmuir*, 2006, **22**, 7943-7946.
107. T. Thorsen, R. W. Roberts, F. H. Arnold and S. R. Quake, *Physical Review Letters*, 2001, **86**, 4163-4166.
108. G. R. Yi, T. Thorsen, V. N. Manoharan, M. J. Hwang, S. J. Jeon, D. J. Pine, S. R. Quake and S. M. Yang, *Advanced Materials*, 2003, **15**, 1300-1304.
109. D. R. Link, S. L. Anna, D. A. Weitz and H. A. Stone, *Physical Review Letters*, 2004, **92**, 054503: 1-4.
110. S. Okushima, T. Nisisako, T. Torii and T. Higuchi, *Langmuir*, 2004, **20**, 9905-9908.
111. T. Nisisako and T. Torii, *Lab on a Chip*, 2008, **8**, 287-293.
112. S. van der Graaf, M. L. J. Steegmans, R. G. M. van der Sman, C. Schroen and R. M. Boom, *Colloids and Surfaces a-Physicochemical and Engineering Aspects*, 2005, **266**, 106-116.
113. P. Garstecki, M. J. Fuerstman, H. A. Stone and G. M. Whitesides, *Lab on a Chip*, 2006, **6**, 437-446.
114. J. H. Xu, S. W. Li, J. Tan and G. S. Luo, *Microfluidics and Nanofluidics*, 2008, **5**, 711-717.
115. M. De Menech, P. Garstecki, F. Jousse and H. A. Stone, *Journal of Fluid Mechanics*, 2008, **595**, 141-161.
116. G. F. Christopher, J. Bergstein, N. B. End, M. Poon, C. Nguyen and S. L. Anna, *Lab on a Chip*, 2009, **9**, 1102-1109.
117. C.-H. Choi, J.-H. Jung, Y. W. Rhee, D.-P. Kim, S.-E. Shim and C.-S. Lee, *Biomedical Microdevices*, 2007, **9**, 855-862.
118. H. Song, J. D. Tice and R. F. Ismagilov, *Angewandte Chemie-International Edition*, 2003, **42**, 768-772.
119. H. Liu and Y. Zhang, *Physics of Fluids*, 2011, **23**, 082101-082112.
120. S. Seiffert, J. Thiele, A. R. Abate and D. A. Weitz, *Journal of the American Chemical Society*, 2010, **132**, 6606-6609.
121. A. R. Abate, M. Kutsovsky, S. Seiffert, M. Windbergs, L. F. V. Pinto, A. Rotem, A. S. Utada and D. A. Weitz, *Advanced Materials*, 2011, **23**, 1757-1760.
122. B. Zheng, J. D. Tice and R. F. Ismagilov, *Analytical Chemistry*, 2004, **76**, 4977-4982.
123. S. L. Anna, N. Bontoux and H. A. Stone, *Applied Physics Letters*, 2003, **82**, 364-366.
124. P. Garstecki, H. A. Stone and G. M. Whitesides, *Physical Review Letters*, 2005, **94**, 164501: 1-4.
125. S. L. Anna and H. C. Mayer, *Physics of Fluids*, 2006, **18**, 121512-121525.

126. M. Seo, Z. H. Nie, S. Q. Xu, M. Mok, P. C. Lewis, R. Graham and E. Kumacheva, *Langmuir*, 2005, **21**, 11614-11622.
127. S. Takeuchi, P. Garstecki, D. B. Weibel and G. M. Whitesides, *Advanced Materials*, 2005, **17**, 1067-1072.
128. J. H. Xu, S. W. Li, C. Tostado, W. J. Lan and G. S. Luo, *Biomedical Microdevices*, 2009, **11**, 243-249.
129. Y. Morimoto, K. Kuribayashi-Shigetomi and S. Takeuchi, *Journal of Micromechanics and Microengineering*, 2011, **21**, 1-6.
130. A. S. Utada, E. Lorenceau, D. R. Link, P. D. Kaplan, H. A. Stone and D. A. Weitz, *Science*, 2005, **308**, 537-541.
131. J.-W. Kim, A. S. Utada, A. Fernandez-Nieves, Z. Hu and D. A. Weitz, *Angewandte Chemie-International Edition*, 2007, **46**, 1819-1822.
132. E. Lorenceau, A. S. Utada, D. R. Link, G. Cristobal, M. Joanicot and D. A. Weitz, *Langmuir*, 2005, **21**, 9183-9186.
133. W. J. Duncanson, T. Lin, A. R. Abate, S. Seiffert, R. K. Shah and D. A. Weitz, *Lab on a Chip*, 2012, **12**, 2135-2145.
134. J. Husny and J. J. Cooper-White, *Journal of Non-Newtonian Fluid Mechanics*, 2006, **137**, 121-136.
135. G. F. Christopher, N. N. Noharuddin, J. A. Taylor and S. L. Anna, *Physical Review E*, 2008, **78**, 1-12.
136. J. Berthier, S. Le Vot, P. Tiquet, N. David, D. Lauro, P. Y. Benhamou and F. Rivera, *Sensors and Actuators a-Physical*, 2010, **158**, 140-148.
137. S. Yeom and S. Y. Lee, *Experimental Thermal and Fluid Science*, 2011, **35**, 387-394.
138. W.-B. Du, M. Sun, S.-Q. Gu, Y. Zhu and Q. Fang, *Analytical Chemistry*, 2010, **82**, 9941-9947.
139. J. S. Edgar, G. Milne, Y. Zhao, C. P. Pabbati, D. S. W. Lim and D. T. Chiu, *Angewandte Chemie-International Edition*, 2009, **48**, 2719-2722.
140. X. Z. Niu, B. Zhang, R. T. Marszalek, O. Ces, J. B. Edel, D. R. Klug and A. J. deMello, *Chemical Communications*, 2009, **41**, 6159-6161.
141. L.-F. Cai, Y. Zhu, G.-S. Du and Q. Fang, *Analytical Chemistry*, 2012, **84**, 446-452.
142. B. Zheng and R. F. Ismagilov, *Angewandte Chemie-International Edition*, 2005, **44**, 2520-2523.
143. H. Song, H.-W. Li, M. S. Munson, T. G. Van Ha and R. F. Ismagilov, *Analytical Chemistry*, 2006, **78**, 4839-4849.
144. K. Churski, P. Korczyk and P. Garstecki, *Lab on a Chip*, 2010, **10**, 816-818.
145. R. M. Lorenz, G. S. Fiorini, G. D. M. Jeffries, D. S. W. Lim, M. He and D. T. Chiu, *Analytica Chimica Acta*, 2008, **630**, 124-130.
146. N. Damean, L. F. Olguin, F. Hollfelder, C. Abell and W. T. S. Huck, *Lab on a Chip*, 2009, **9**, 1707-1713.
147. J. R. Burns and C. Ramshaw, *Chemical Engineering Research & Design*, 1999, **77**, 206-211.
148. J. R. Burns and C. Ramshaw, *Chemical Engineering Communications*, 2002, **189**, 1611-1628.
149. G. Dummann, U. Quittmann, L. Groschel, D. W. Agar, O. Worz and K. Morgenschweis, *Catalysis Today*, 2003, **79**, 433-439.
150. N. de Mas, A. Gunther, M. A. Schmidt and K. F. Jensen, *Industrial & Engineering Chemistry Research*, 2003, **42**, 698-710.
151. P. M. Gunther, F. Moller, T. Henkel, J. M. Kohler and G. A. Gross, *Chemical Engineering & Technology*, 2005, **28**, 520-527.
152. I. Shestopalov, J. D. Tice and R. F. Ismagilov, *Lab on a Chip*, 2004, **4**, 316-321.
153. M. Kumemura and T. Korenaga, *Analytica Chimica Acta*, 2006, **558**, 75-79.
154. P. Kumaresan, C. J. Yang, S. A. Cronier, R. G. Blazej and R. A. Mathies, *Analytical Chemistry*, 2008, **80**, 3522-3529.
155. A. Fallah-Araghi, J.-C. Baret, M. Ryckelynck and A. D. Griffiths, *Lab on a Chip*, 2012, **12**, 882-891.
156. N. Wu, J. Oakeshott, S. Brown, C. Easton and Y. Zhu, *Australian Journal of Chemistry*, 2010, **63**, 1313-1325.
157. H. J. Oh, S. H. Kim, J. Y. Baek, G. H. Seong and S. H. Lee, *Journal of Micromechanics and Microengineering*, 2006, **16**, 285-291.
158. A. E. Sgro, P. B. Allen and D. T. Chiu, *Analytical Chemistry*, 2007, **79**, 4845-4851.
159. J. Clausell-Tormos, D. Lieber, J. C. Baret, A. El-Harrak, O. J. Miller, L. Frenz, J. Blouwolff, K. J. Humphry, S. Koster, H. Duan, C. Holtze, D. A. Weitz, A. D. Griffiths and C. A. Merten, *Chemistry & Biology*, 2008, **15**, 427-437.
160. M. K. Yadav, C. J. Gerdts, R. Sanishvili, W. W. Smith, L. S. Roach, R. F. Ismagilov, P. Kuhn and R. C. Stevens, *Journal of Applied Crystallography*, 2005, **38**, 900-905.
161. D. L. Chen, C. J. Gerdts and R. F. Ismagilov, *Journal of the American Chemical Society*, 2005, **127**, 9672-9673.
162. K. Churski, T. S. Kaminski, S. Jakiela, W. Kamysz, W. Baranska-Rybak, D. B. Weibel and P. Garstecki, *Lab on a Chip*, 2012, **12**, 1629-1637.

163. H. Zhang, X.-J. Ju, R. Xie, C.-J. Cheng, P.-W. Ren and L.-Y. Chu, *Journal of Colloid and Interface Science*, 2009, **336**, 235-243.
164. C. Kim, S. Chung, Y. E. Kim, K. S. Lee, S. H. Lee, K. W. Oh and J. Y. Kang, *Lab on a Chip*, 2011, **11**, 246-252.
165. K. Hettiarachchi and A. P. Lee, *Journal of Colloid and Interface Science*, 2010, **344**, 521-527.
166. S. Seiffert, M. B. Romanowsky and D. A. Weitz, *Langmuir*, 2010, **26**, 14842-14847.
167. Y.-L. Yu, M.-J. Zhang, R. Xie, X.-J. Ju, J.-Y. Wang, S.-W. Pi and L.-Y. Chu, *Journal of Colloid and Interface Science*, 2012, **376**, 97-106.
168. J.-W. Kim, R. J. Larsen and D. A. Weitz, *Advanced Materials*, 2007, **19**, 2005-2009.
169. M. Yoshida, K.-H. Roh and J. Lahann, *Biomaterials*, 2007, **28**, 2446-2456.
170. D. S. T. Hsieh, W. D. Rhine and R. Langer, *Journal of Pharmaceutical Sciences*, 1983, **72**, 17-22.
171. B. L. Goode, D. G. Drubin and G. Barnes, *Current Opinion in Cell Biology*, 2000, **12**, 63-71.
172. S. Q. Xu, Z. H. Nie, M. Seo, P. Lewis, E. Kumacheva, H. A. Stone, P. Garstecki, D. B. Weibel, I. Gitlin and G. M. Whitesides, *Angewandte Chemie-International Edition*, 2005, **44**, 724-728.
173. Z. Nie, W. Li, M. Seo, S. Xu and E. Kumacheva, *Journal of the American Chemical Society*, 2006, **128**, 9408–9412.
174. S. M. Vlaming, R. Augulis, M. C. A. Stuart, J. Knoester and P. H. M. van Loosdrecht, *Journal of Physical Chemistry B*, 2009, **113**, 2273-2283.
175. M. Destribats, B. Faure, M. Birot, O. Babot, V. Schmitt and R. Backov, *Advanced Functional Materials*, 2012, **22**, 2642-2654.
176. A. B. Subramaniam, M. Abkarian and H. A. Stone, *Nature Materials*, 2005, **4**, 553-556.
177. L. A. Fielding and S. P. Armes, *Journal of Materials Chemistry*, 2012, **22**, 11235-11244.
178. O. D. Velev, A. M. Lenhoff and E. W. Kaler, *Science*, 2000, **287**, 2240-2243.
179. W. L. Vos, M. Megens, C. M. vanKats and P. Bosecke, *Journal of Physics-Condensed Matter*, 1996, **8**, 9503-9507.
180. C. Lobato-Calleros, E. Rodriguez, O. Sandoval-Castilla, E. J. Vernon-Carter and J. Alvarez-Ramirez, *Food Research International*, 2006, **39**, 678-685.
181. J. Weiss, I. Scherze and G. Muschiolik, *Food Hydrocolloids*, 2005, **19**, 605-615.
182. G. Muschiolik, *Current Opinion in Colloid & Interface Science*, 2007, **12**, 213-220.
183. K. Yoshida, T. Sekine, F. Matsuzaki, T. Yanaki and M. Yamaguchi, *Journal of the American Oil Chemists Society*, 1999, **76**, 195-200.
184. C. Vilos and L. A. Velasquez, *Journal of Biomedicine and Biotechnology*, 2012, **2012**, 1-9.
185. R. K. Shah, J.-W. Kim, J. J. Agresti, D. A. Weitz and L.-Y. Chu, *Soft Matter*, 2008, **4**, 2303-2309.
186. A. P. Esser-Kahn, S. A. Odom, N. R. Sottos, S. R. White and J. S. Moore, *Macromolecules*, 2011, **44**, 5539-5553.
187. T.-C. Chao and A. Ros, *Journal of the Royal Society Interface*, 2008, **5**, S139-S150.
188. Y.-J. Eun, A. S. Utada, M. F. Copeland, S. Takeuchi and D. B. Weibel, *Acs Chemical Biology*, 2011, **6**, 260-266.
189. T. Mattila-Sandholm, P. Myllarinen, R. Crittenden, G. Mogensen, R. Fonden and M. Saarela, *International Dairy Journal*, 2002, **12**, 173-182.
190. H. Zimmermann, D. Zimmermann, R. Reuss, P. J. Feilen, B. Manz, A. Katsen, M. Weber, F. R. Ihmig, F. Ehrhart, P. Gessner, M. Behringer, A. Steinbach, L. H. Wegner, V. L. Sukhorukov, J. A. Vasquez, S. Schneider, M. M. Weber, F. Volke, R. Wolf and U. Zimmermann, *Journal of Materials Science-Materials in Medicine*, 2005, **16**, 491-501.
191. J. Aleman, A. V. Chadwick, J. He, M. Hess, K. Horie, R. G. Janes, P. Kratochvil, I. Meisel, I. Mita, G. Moad, S. Penczek and R. F. T. Stepto, 2007, **79**, 1801-1829.
192. B. D. Ratner and A. S. Hoffman, *Acs Symposium Series*, 1976, 1-36.
193. S. Van Vlierberghe, P. Dubruel and E. Schacht, *Biomacromolecules*, 2011, **12**, 1387-1408.
194. L. E. Ruff, E. A. Mahmoud, J. Sankaranarayanan, J. M. Morachis, C. D. Katayama, M. Corr, S. M. Hedrick and A. Almutairi, *Integrative Biology*, 2013, **5**, 195-203.
195. X. Chen, X. Li, Y. Zhou, X. Wang, Y. Zhang, Y. Fan, Y. Huang and Y. Liu, *Journal of Biomaterials Applications*, 2012, **27**, 391-402.
196. M.-R. Park, B.-B. Seo and S.-C. Song, *Biomaterials*, 2013, **34**, 1327-1336.
197. Ed. by Robert Y. Ning, Advancing Desalination, InTech, 2012.
198. B. H. Rehm, H. Ertesvag and S. Valla, *Journal of Bacteriology*, 1996, **178**, 5884-5889.
199. B. H. A. Rehm and S. Valla, *Applied Microbiology and Biotechnology*, 1997, **48**, 281-288.

201. O. Smidsrod, ed. K. I. Draget, Carbohydrates in Europe, 1996, **14**, 6-13.
202. S. Valla and G. SkjakBraek, *Agro Food Industry Hi-Tech*, 1996, **7**, 38-41.

203. K. I. Draget, G. SkjakBraek and O. Smidsrod, *International Journal of Biological Macromolecules*, 1997, **21**, 47-55.
204. G. T. Grant, E. R. Morris, D. A. Rees, P. J. C. Smith and D. Thom, *Febs Letters*, 1973, **32**, 195-198.
205. P. Sikorski, F. Mo, G. Skjak-Braek and B. T. Stokke, *Biomacromolecules*, 2007, **8**, 2098-2103.
206. L. Capretto, S. Mazzitelli, C. Balestra, A. Tosi and C. Nastruzzi, *Lab on a Chip*, 2008, **8**, 617-621.
207. Y. Hu, Q. Wang, J. Wang, J. Zhu, H. Wang and Y. Yang, *Biomicrofluidics*, 2012, **6**.
208. H. Zhang, E. Tumarkin, R. M. A. Sullan, G. C. Walker and E. Kumacheva, *Macromolecular Rapid Communications*, 2007, **28**, 527-538.
209. S. Shin, J.-Y. Park, J.-Y. Lee, H. Park, Y.-D. Park, K.-B. Lee, C.-M. Whang and S.-H. Lee, *Langmuir*, 2007, **23**, 9104-9108.
210. W. Plazinski, *Environmental Science and Pollution Research*, 2012, **19**, 3516-3524.
211. A. Asthana, K. H. Lee, S.-J. Shin, J. Perumal, L. Butler, S.-H. Lee and D.-P. Kim, *Biomicrofluidics*, 2011, **5,** 024117: 1-11.
212. A. G. J. Voragen, G.-J. Coenen, R. P. Verhoef and H. A. Schols, *Structural Chemistry*, 2009, **20**, 263-275.
213. Institute of Food Research, *Science+Innovation*, 2009, **1:09**, 1-12.
214. B. L. Ridley, M. A. O'Neill and D. A. Mohnen, *Phytochemistry*, 2001, **57**, 929-967.
215. W. G. T. Willats, P. Knox and J. D. Mikkelsen, *Trends in Food Science & Technology*, 2006, **17**, 97-104.
216. A. Fang and B. Cathala, *Colloids and Surfaces B-Biointerfaces*, 2011, **82**, 81-86.
217. M. Marquis, D. Renard and B. Cathala, *Biomacromolecules*, 2012, **13**, 1197-1203.
218. D. Ogonczyk, M. Siek and P. Garstecki, *Biomicrofluidics*, 2011, **5,** 013405: 1-12.
219. L. S. Liu, M. L. Fishman, J. Kost and K. B. Hicks, *Biomaterials*, 2003, **24**, 3333-3343.
220. P. Opanasopit, A. Apirakaramwong, T. Ngawhirunpat, T. Rojanarata and U. Ruktanonchai, *Aaps Pharmscitech*, 2008, **9**, 67-74.
221. P. Walkenstrom, S. Kidman, A. M. Hermansson, P. B. Rasmussen and L. Hoegh, *Food Hydrocolloids*, 2003, **17**, 593-603.
222. M. V. Perez Lambrech, V. Sorrivas, M. A. Villar and J. E. Lozano, *Icheap-9: 9th International Conference on Chemical and Process Engineering, Pts 1-3*, 2009, **17**, 1765-1770.
223. M. Miles and J, Bassett, D.C., Ed. Elservier Applied Science Publishers Ltd: New York, 1988.
224. O. Sandoval-Castilla, C. Lobato-Calleros, H. S. Garcia-Galindo, J. Alvarez-Ramirez and E. J. Vernon-Carter, *Food Research International*, 2010, **43**, 111-117.
225. V. Pillay and R. Fassihi, *Journal of Controlled Release*, 1999, **59**, 243-256.
226. S. Jaya, T. D. Durance and R. Wang, *Journal of Microencapsulation*, 2009, **26**, 143-153.
227. N. R. Jana and X. G. Peng, *Journal of the American Chemical Society*, 2003, **125**, 14280-14281.
228. D. Ogonczyk, J. Wegrzyn, P. Jankowski, B. Dabrowski and P. Garstecki, *Lab on a Chip*, 2010, **10**, 1324-1327.
229. P. M. Korczyk, O. Cybulski, S. Makulska and P. Garstecki, *Lab on a Chip*, 2011, **11**, 173-175.
230. M. Fialkowski, C. J. Campbell, I. T. Bensemann and B. A. Grzybowski, *Langmuir*, 2004, **20**, 3513-3516.
231. J. S. Kim and F. S. Ligler, *The Microflow Cytometer*, Pan Stanford Publishing Pte. Ltd., 2010.
232. F. M. White, *Fluid Mechanics*, McGraw-Hill, 2002.
233. G. F. Christopher and S. L. Anna, *Journal of Physics D-Applied Physics*, 2007, **40**, R319-R336.
234. V. van Steijn, C. R. Kleijn and M. T. Kreutzer, *Lab on a Chip*, 2010, **10**, 2513-2518.
235. P. Guillot and A. Colin, *Physical Review E*, 2005, **72,** 066301:1-4.
236. P. Guillot, A. Ajdari, J. Goyon, M. Joanicot and A. Colin, *Comptes Rendus Chimie*, 2009, **12**, 247-257.
237. W. Lee, L. M. Walker and S. L. Anna, *Macromolecular Materials and Engineering*, 2011, **296**, 203-213.